Supplemental Material: Identifying and addressing long-term Alphasense OPC-N3 sensor degradation

Tristalee Mangin, Kamaljeet Kaur, Dillon Tang, Dustin Reitstetter, Raven Reitstetter, Aaron Hanson, Yiqing Meng, Alex Mass, Nancy Daher, Kerry E. Kelly

University of Utah Chemical Engineering Department

Correspondence to: Tristalee Mangin (tristalee.mangin@utah.edu)

Table of Contents

S.1: Additional figures 2
Methods figures 2
Correction model scatter plots 5
Humidograms 8
CASTNET total deposition maps 10
Slope bar charts - OPC-N3 MLR and PMS5003T LR 11
Seasonal OPC-N3 PM_{10} scatter plot matrices 12
Seasonal OPC-N3 $PM_{2.5}$ scatter plot matrices 19
Seasonal PMS5003T $PM_{2.5}$ scatter plot matrices 26
Seasonal OPC-N3 PM_{10} Bland-Altman plots 33
Seasonal OPC-N3 $PM_{2.5}$ Bland-Altman plots 40
Seasonal PMS5003T $PM_{2.5}$ Bland-Altman plots 47
OPC-N3 size selectivity after mirror replacement: Monodisperse particle generator results 54
Autocorrelation plots for OPC-N3 $PM_{2.5}$-to-PMS5003T $PM_{2.5}$ ratio 55
S.2: Additional tables 57
Methods tables 57
Correction model summary tables 57
Cross-correlation summary tables 61
Bland-Altman summary tables 62
OPC-N3-to-PMS5003T $PM_{2.5}$ ratio results 63
S.3: Investigate OPC-N3 reject counts to screen high PM_{10} measurements 65
S.4: OPC-N3 sample flow rate and laser status 68
S.5: Laptop/Alphasense software OPC-N3 colocation results & OPC-N3 power analysis 70
Laptop and Alphasense software OPC-N3 colocation 70
Power analysis 71
S.6: Laboratory precision test variability using never-deployed OPC-N3 sensors 74
S.7: OPC-N3 mirror replacement standard operating procedure 77
Introduction 77
Materials needed 77
Mirror change procedure 78
Alignment check procedure 81
S.8: Mirror replacement repeatability tests 82
S.9: Repeated tests for the mirror alignment check after replacing the mirror 85

S.1: Additional figures

Methods figures

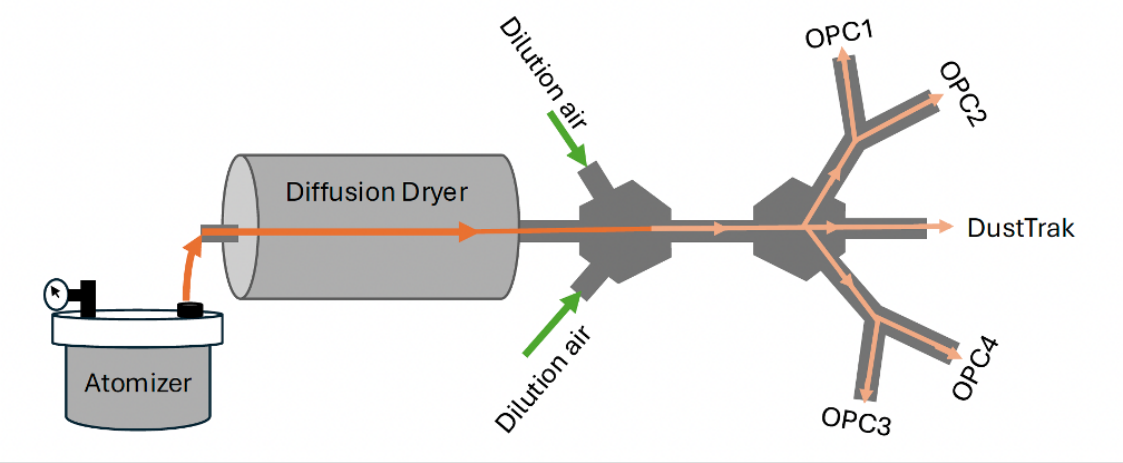


Figure S1: Diagram of the laboratory calibration setup using Arizona road dust particles and comparing the OPC-N3 measurements to the DustTrak measurements.

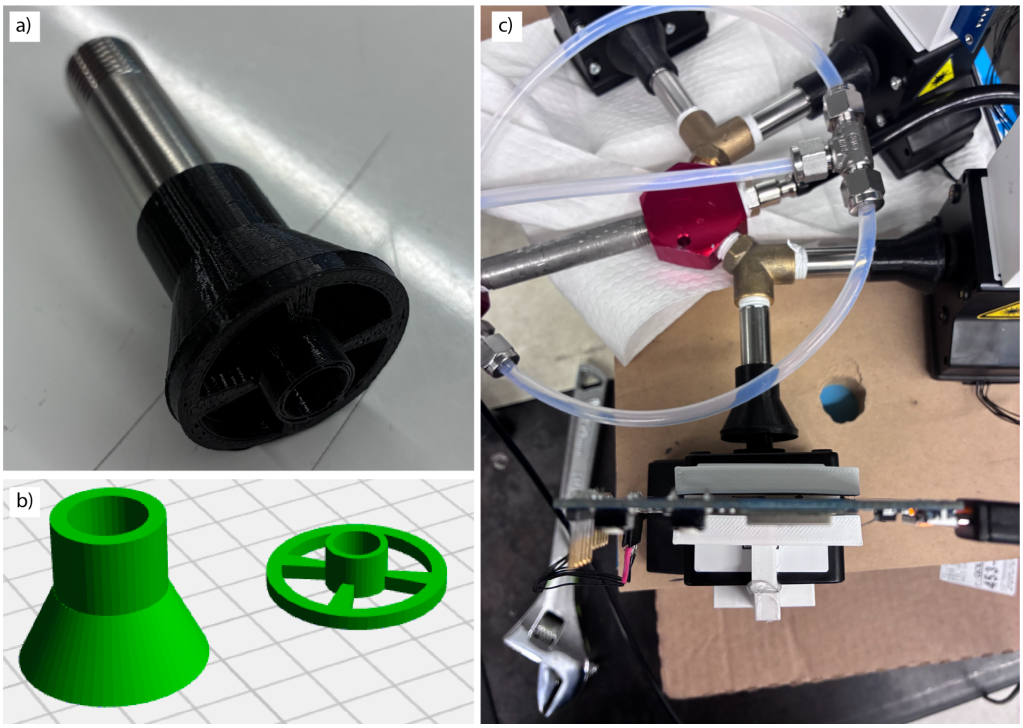


Figure S2: Custom 3D-printed outlet for laboratory calibrations of the OPC-N3 sensor.



Figure S3: a) Google Maps satellite image of the UTTC reference station located on the roof of the Utah Division of Environmental Quality (UDEQ) Technical Support Center, screenshot taken March 10, 2026 (Imagery ©2026 NASA, Map data ©2026 Google). b) Image of the AirU Pro device internals showing the board, Alphasense OPC-N3, and Plantower PMS5003T. c) Image of colocated devices at UTTC.

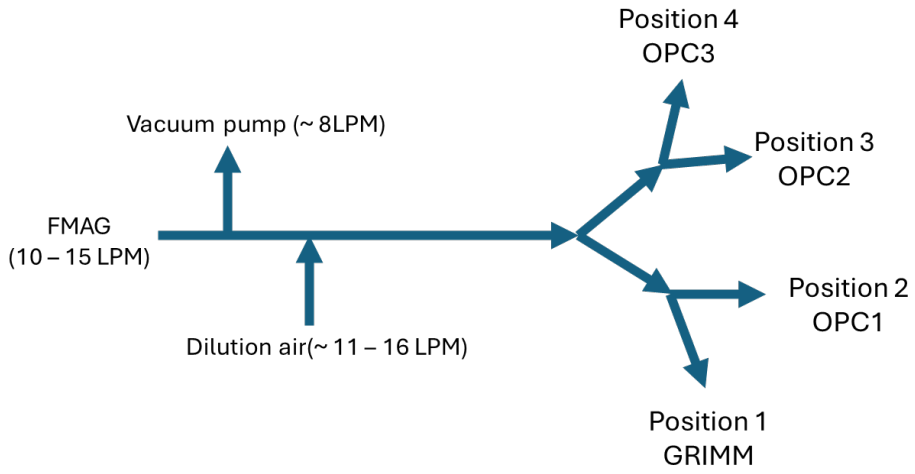


Figure S4: Diagram of the laboratory setup for OPC-N3 size-evaluation using FMAG and GRIMM.

Correction model scatter plots

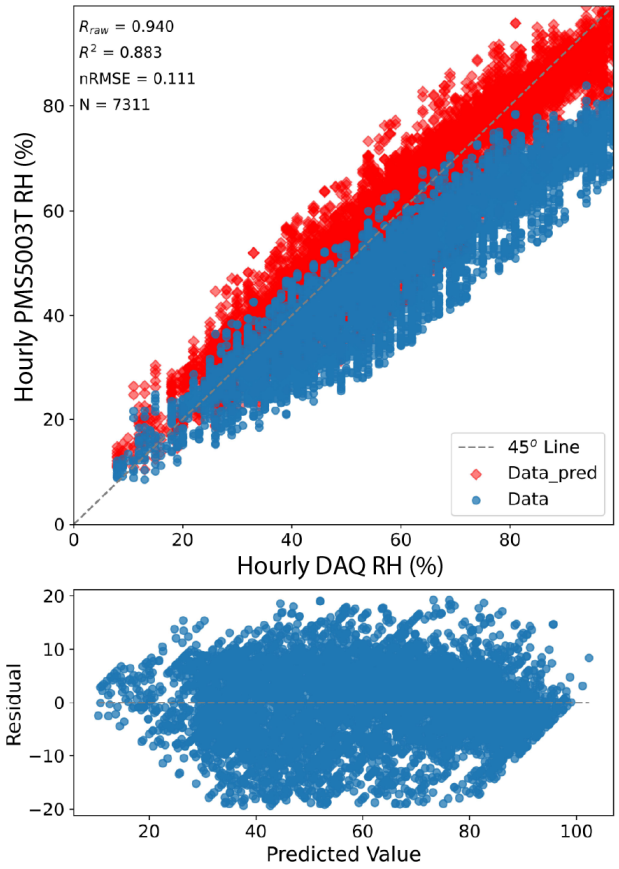


Figure S5: Colocated PMS5003T relative humidity (RH) seasonal regression correction model results for 2024 Winter (November 2024 to February 2025). The blue scatter points are raw PMS5003T RH measurements (Data), and the red diamonds are the corrected RH (Data_pred). DAQ - Utah Division of Air Quality

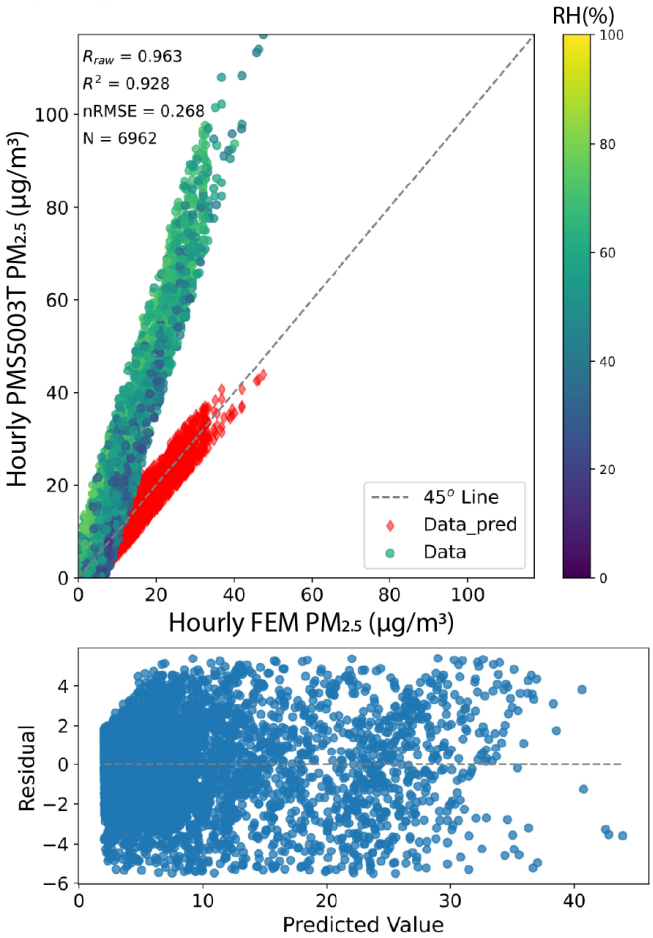


Figure S6: Colocated PMS5003T $PM_{2.5}$ seasonal regression correction model results for 2024 Winter (November 2024 to February 2025). Raw PMS5003T measurements are denoted with circular scatter points colored by RH (Data), and corrected measurements are denoted with red diamonds (Data_pred).

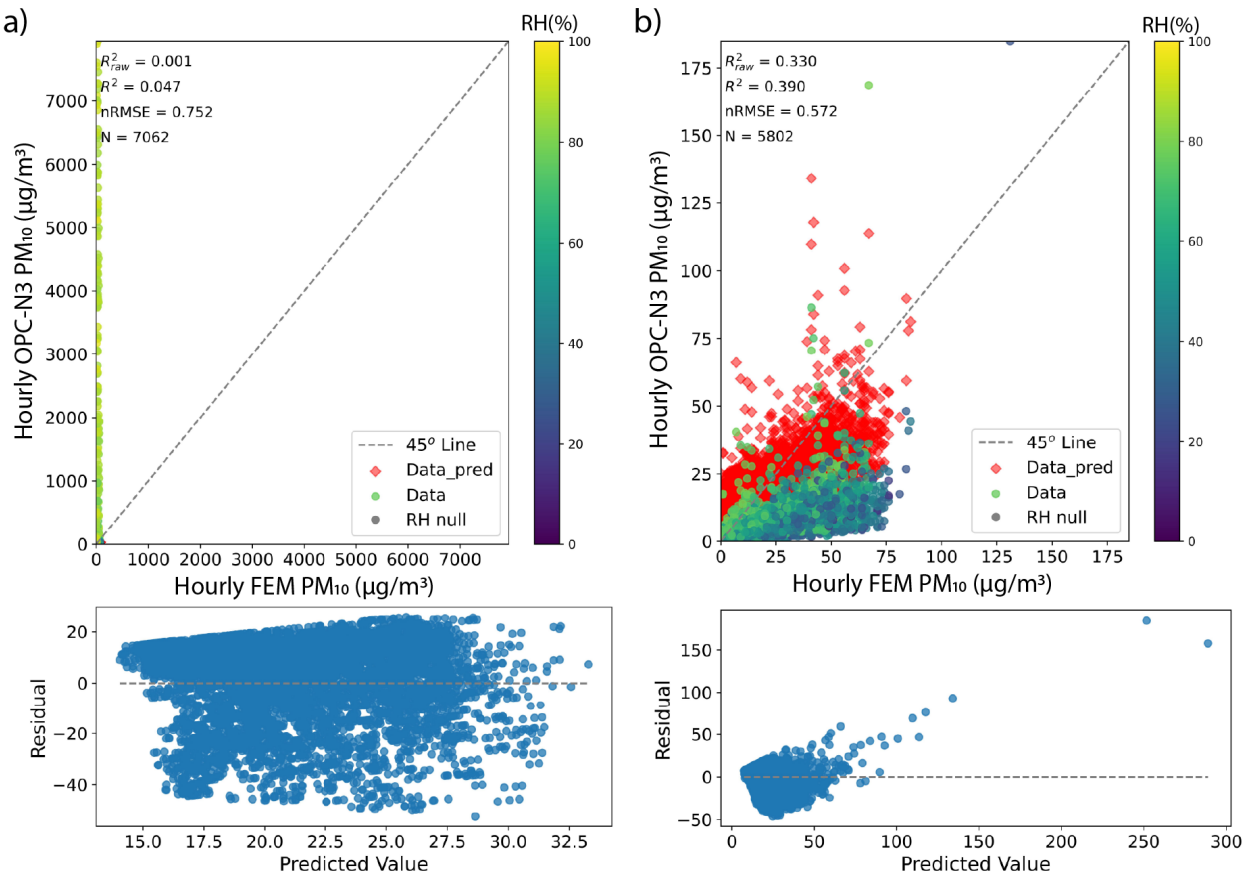


Figure S7: Colocated OPC-N3 PM_{10} seasonal multiple linear regression correction model results for 2024 Winter (November 2024 to February 2025) for hourly measurements (a) and after dropping hourly measurements with relative humidity (RH) > 80% (b). Raw OPC-N3 measurements are denoted with circular scatter points colored by RH (Data), and corrected measurements are denoted with red diamonds (Data_pred). This illustration combines the measurements from the three colocated OPC-N3s.

Humidograms

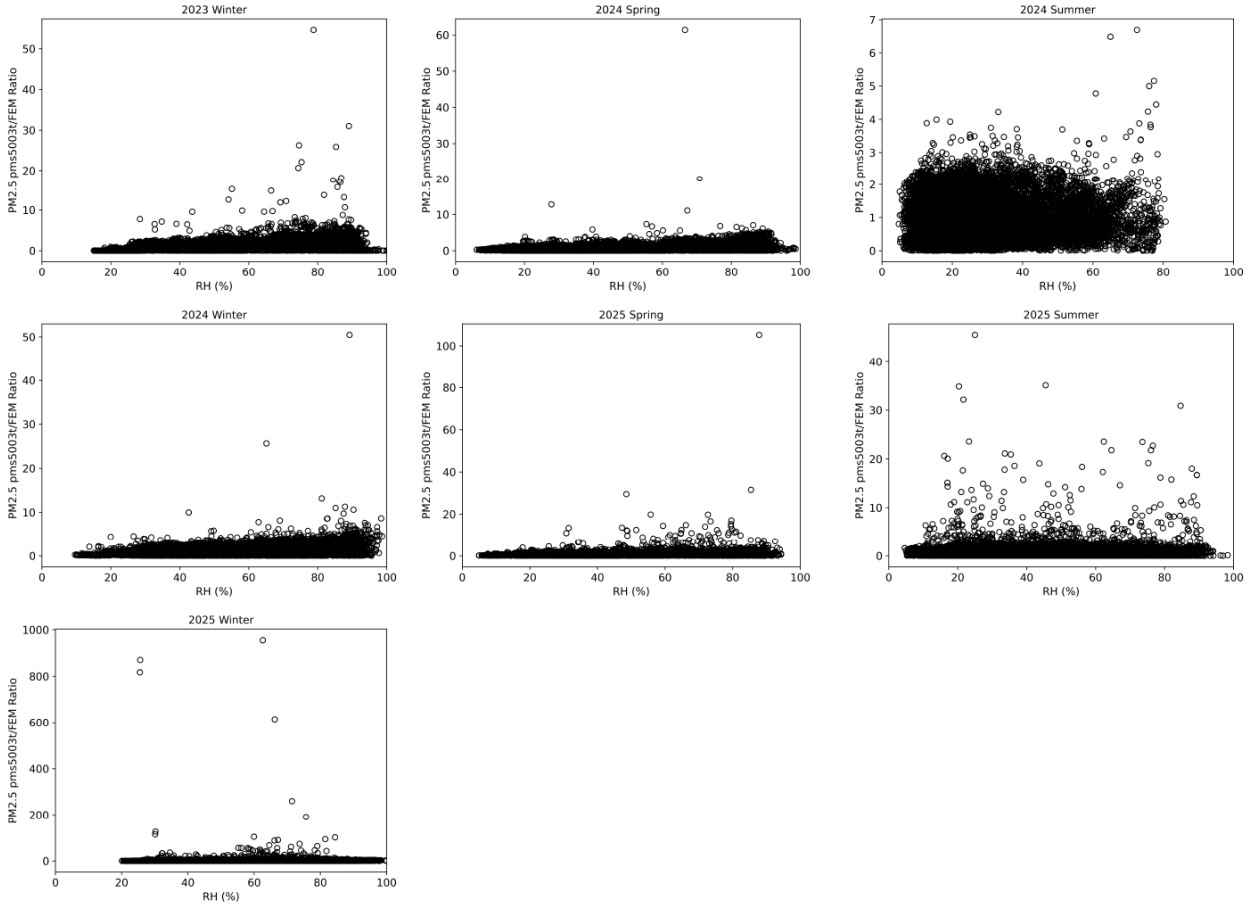


Figure S8: Seasonal colocated PMS5003T sensors $PM_{2.5}$ humidograms. Scatter points show hourly PMS5003T to FEM $PM_{2.5}$ ratio. PMS5003T measurements are raw, hourly-averaged (no correction).

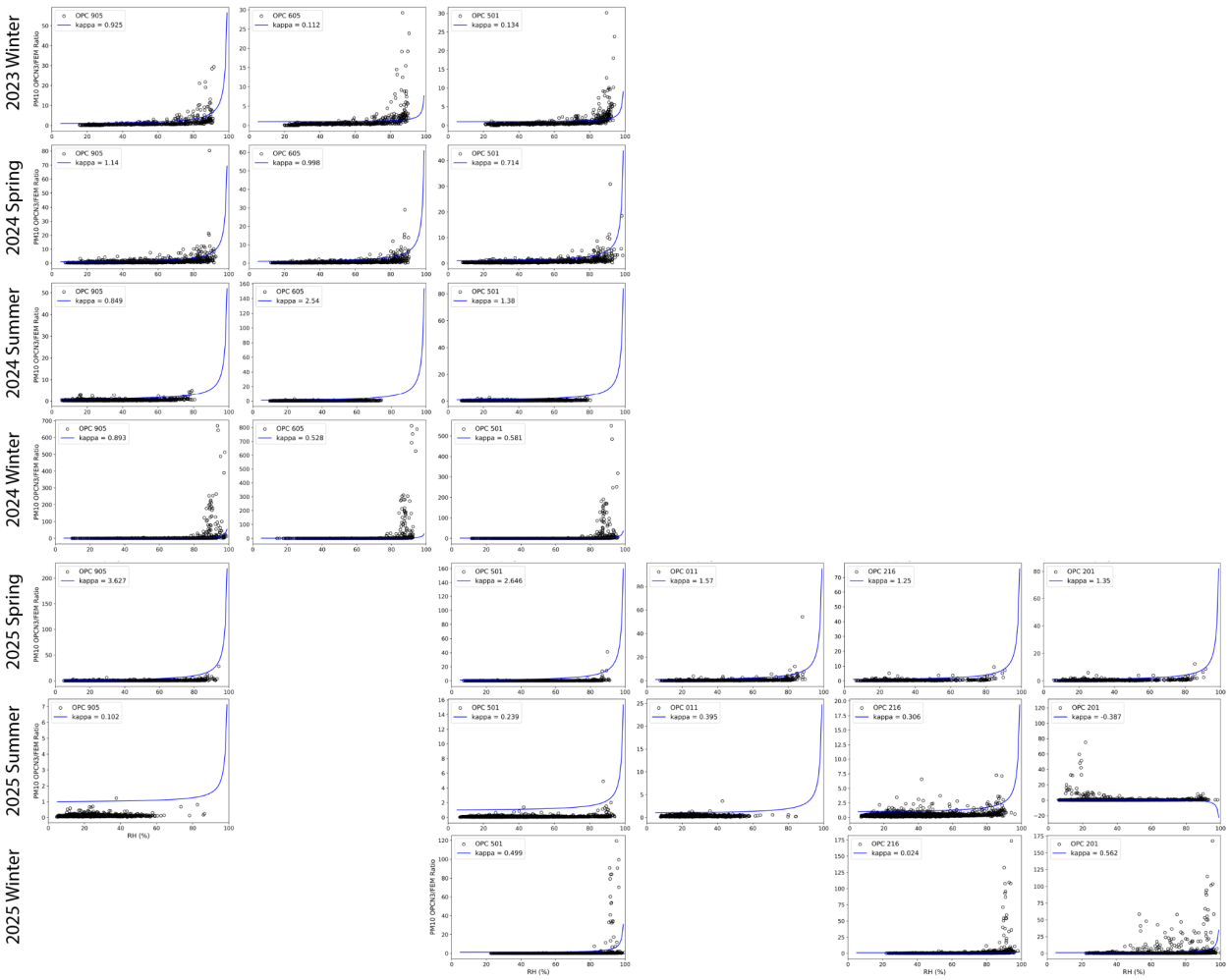


Figure S9: Seasonal colocated OPC-N3 sensor PM_{10} humidograms (individual sensors). Rows represent the different seasons. Columns represent the different OPC-N3 sensors. Scatter points show hourly OPC-N3 to FEM PM_{10} ratio. OPC-N3 measurements are raw, hourly-averaged (no correction). The blue line shows the model fit using the kappa estimated by Eq. (2) after dropping measurements with RH > 80% and removing outliers.

CASTNET total deposition maps

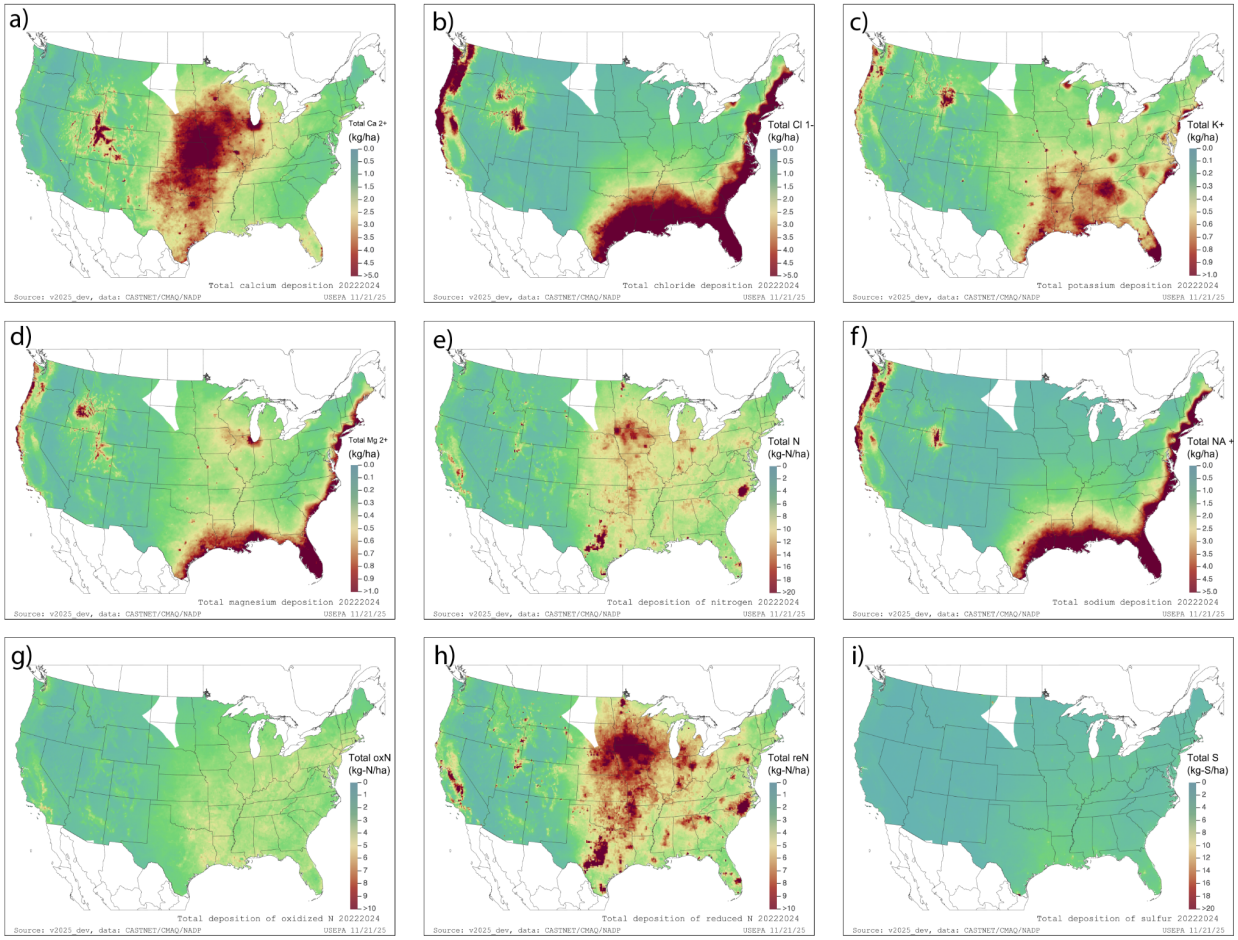


Figure S10: Total deposition maps from CASTNET between 2022 and 2024 for a) calcium, b) chloride, c) potassium, d) magnesium, e) nitrogen, f) sodium, g) oxidized nitrogen, h) reduced nitrogen, and i) sulfur. https://www.epa.gov/castnet/total-deposition-maps

Slope bar charts - OPC-N3 MLR and PMS5003T LR

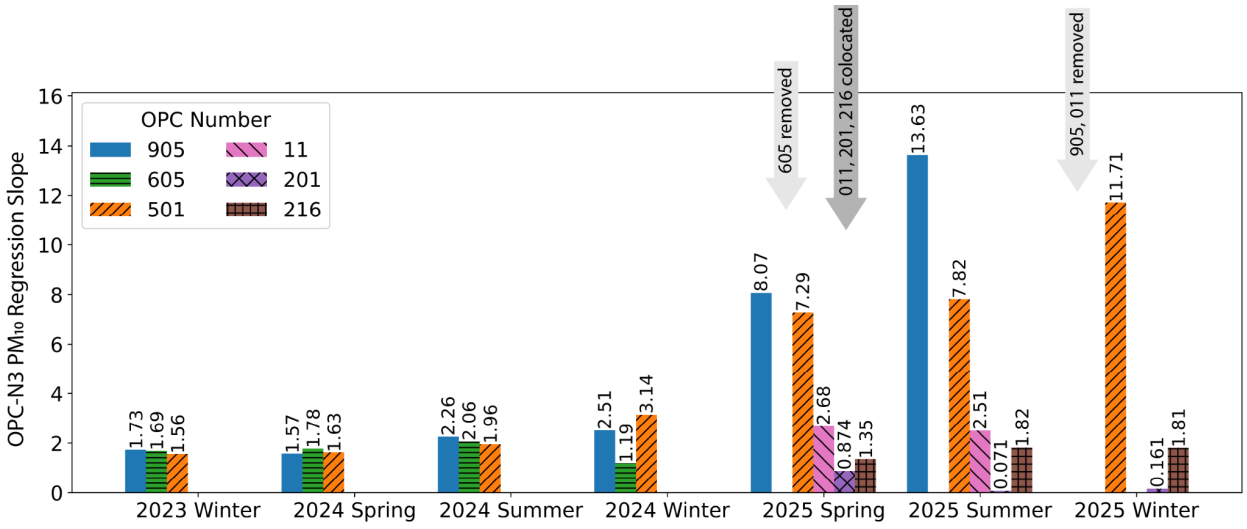


Figure S11: Slopes for colocated OPC-N3 PM_{10} seasonal multiple linear regression correction models with RH > 80% removed.

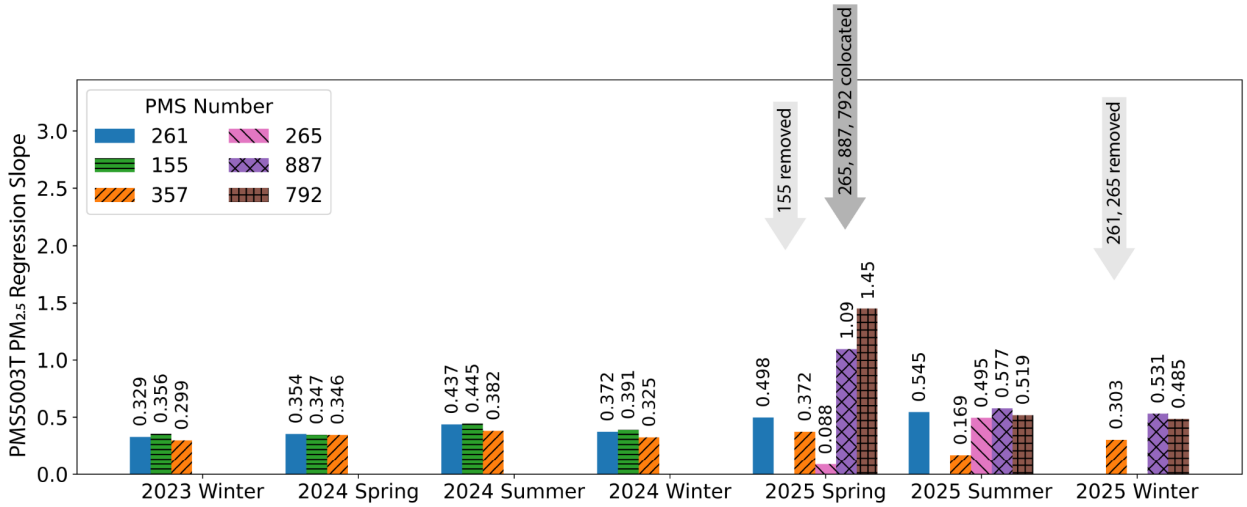


Figure S12: Slopes for colocated PMS5003T $PM_{2.5}$ seasonal regression correction models.

Seasonal OPC-N3 PM_{10} scatter plot matrices

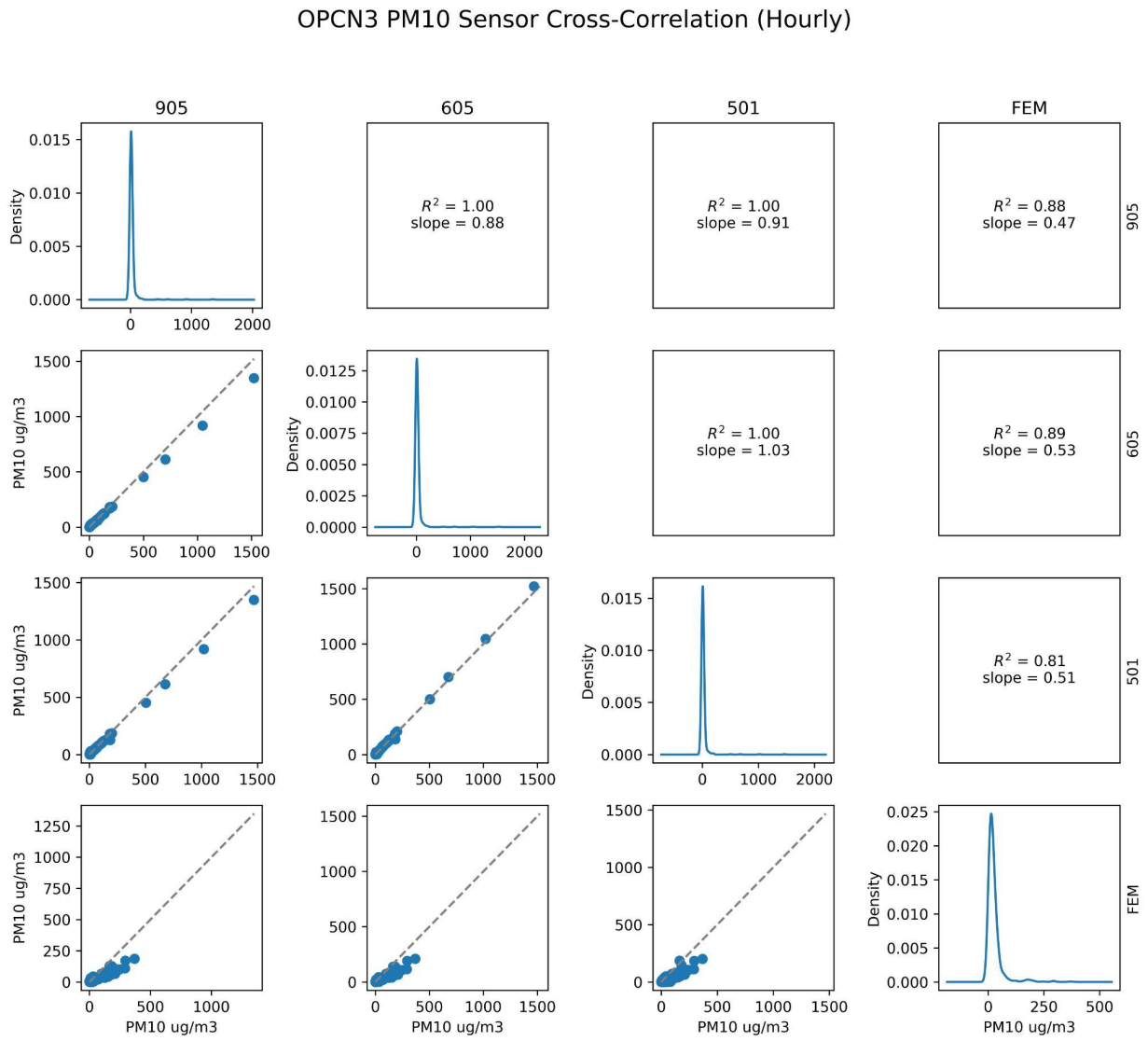


Figure S13: Winter 2023 (January to February 2024) FEM hourly PM_{10} and OPC-N3 raw hourly averaged PM_{10} scatter plot matrix. The dotted gray line is the one-to-one line. Measurements with RH > 80% dropped. x-axis: row sensor number; y-axis: column sensor number.

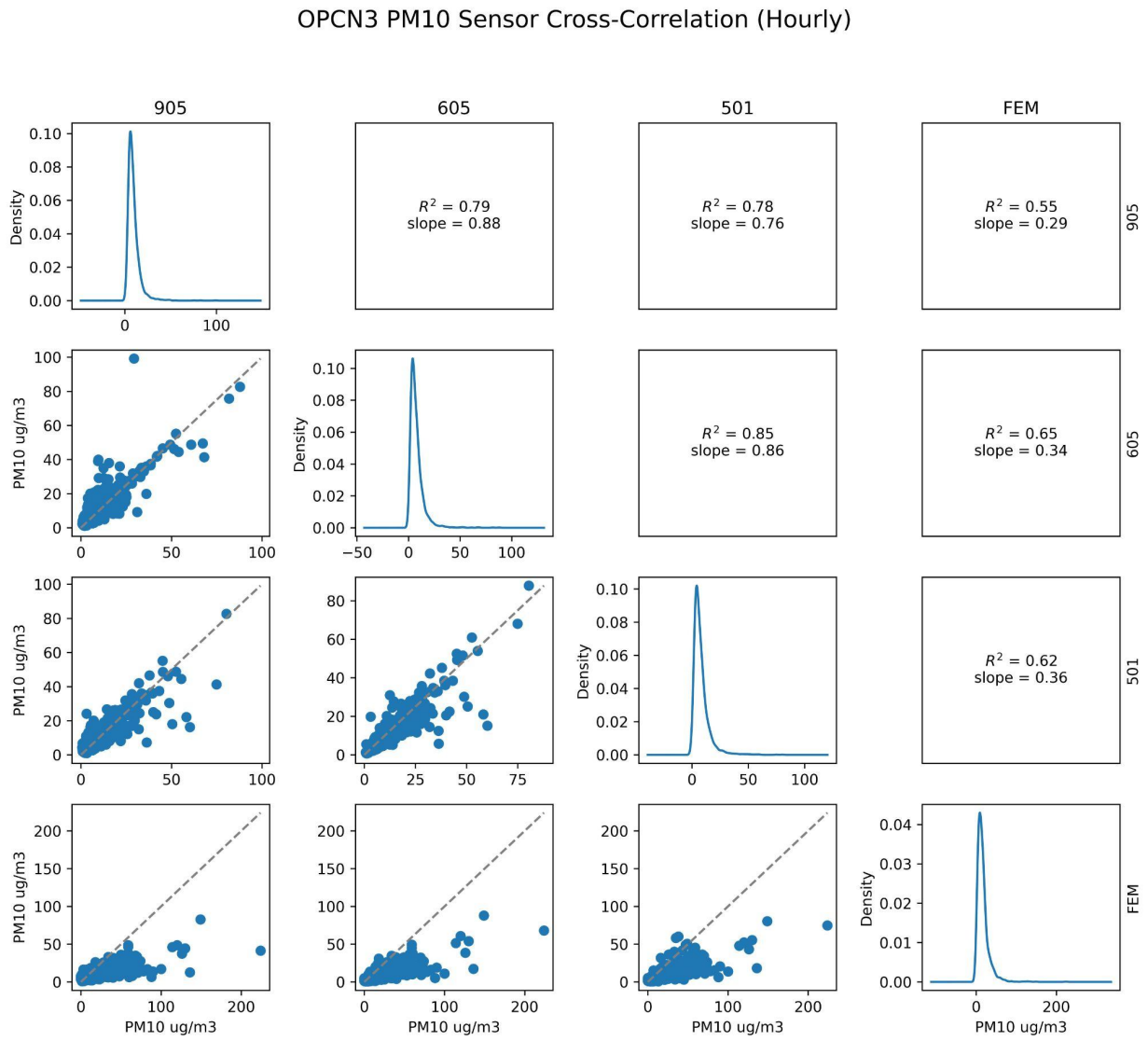


Figure S14: Spring 2024 (March 2024 to May 2024) FEM hourly PM_{10} and OPC-N3 raw hourly averaged PM_{10} scatter plot matrix. The dotted gray line is the one-to-one line. Measurements with RH > 80% dropped. x-axis: row sensor number; y-axis: column sensor number.

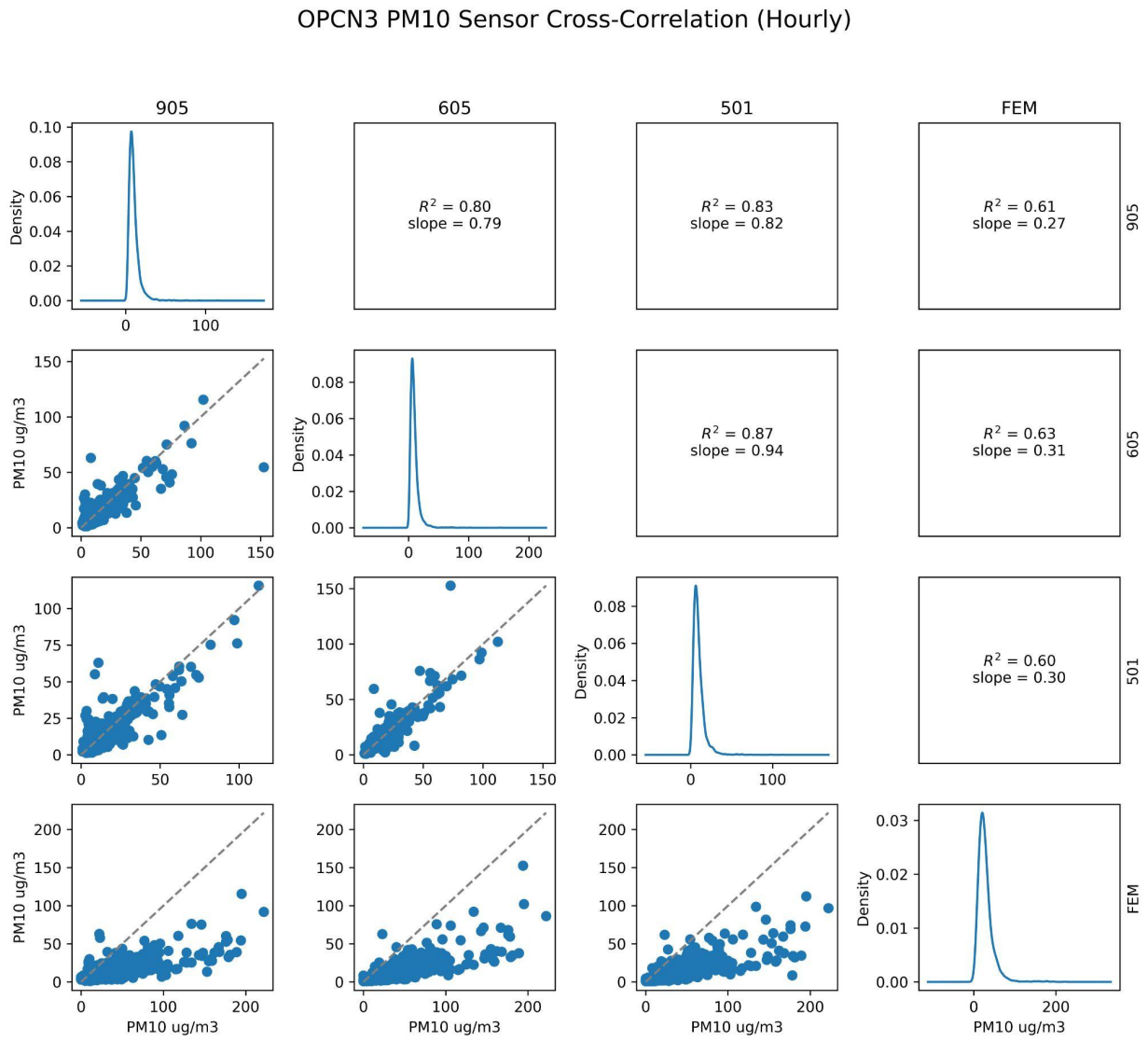


Figure S15: Summer 2024 (June 2024 to October 2024) FEM hourly PM_{10} and OPC-N3 raw hourly averaged PM_{10} scatter plot matrix. The dotted gray line is the one-to-one line. Measurements with RH > 80% dropped. x-axis: row sensor number; y-axis: column sensor number.

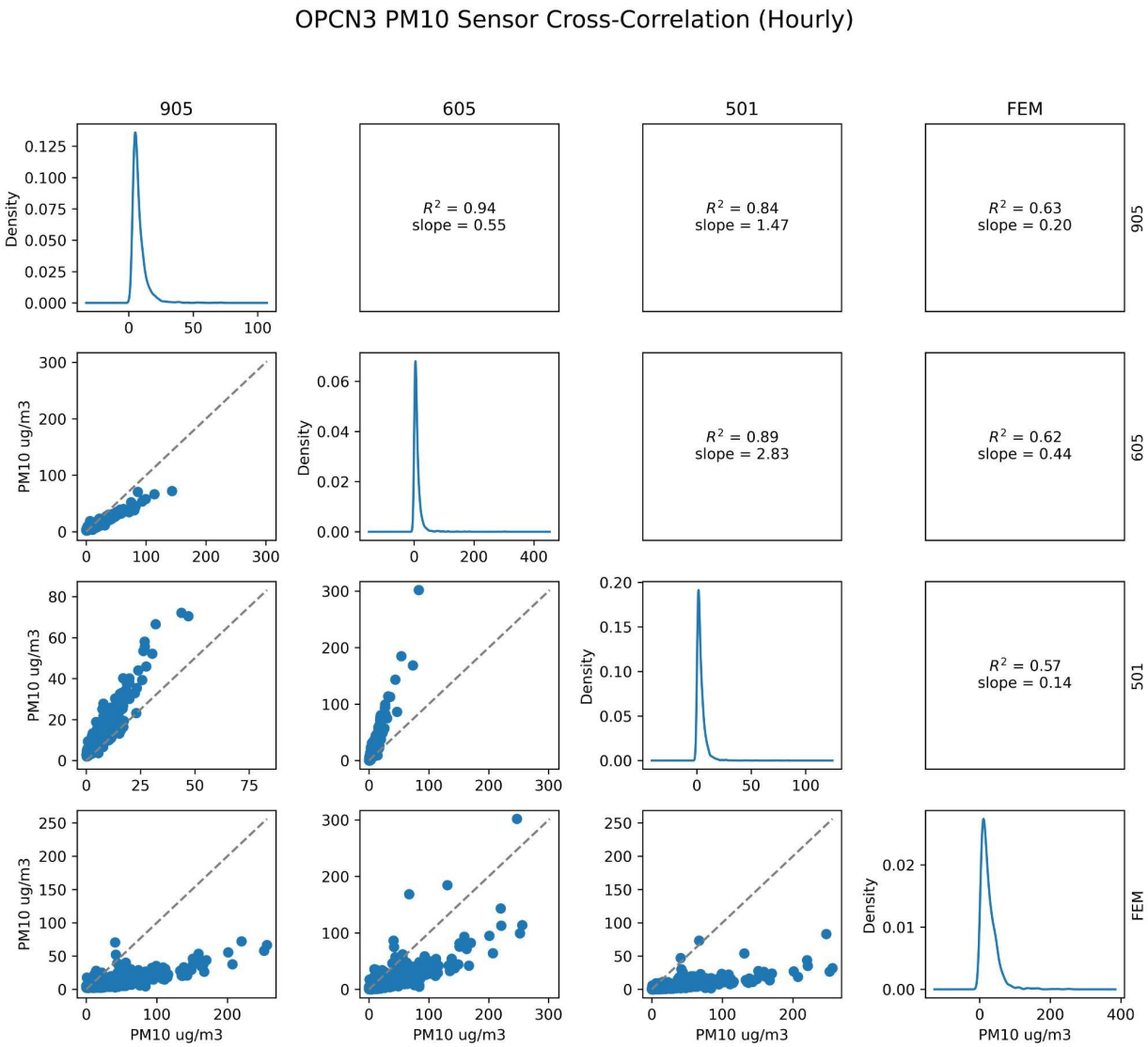


Figure S16: Winter 2024 (November 2024 to February 2025) FEM hourly PM_{10} and OPC-N3 raw hourly averaged PM_{10} scatter plot matrix. The dotted gray line is the one-to-one line. Measurements with RH > 80% dropped. x-axis: row sensor number; y-axis: column sensor number.

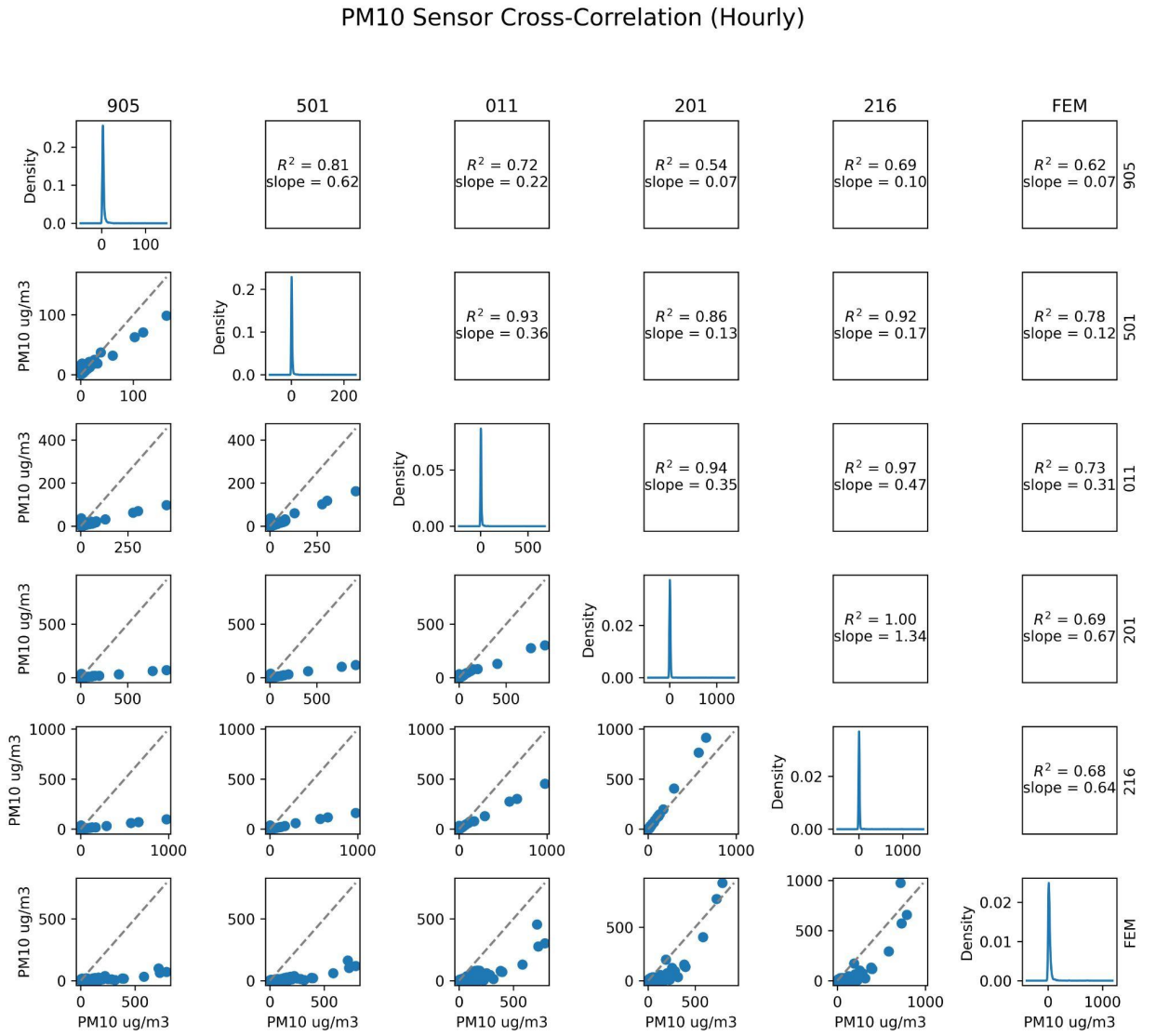


Figure S17: Spring 2025 (March 2025 to May 2025) FEM hourly PM_{10} and OPC-N3 raw hourly averaged PM_{10} scatter plot matrix. The dotted gray line is the one-to-one line. Measurements with RH > 80% dropped. x-axis: row sensor number; y-axis: column sensor number.

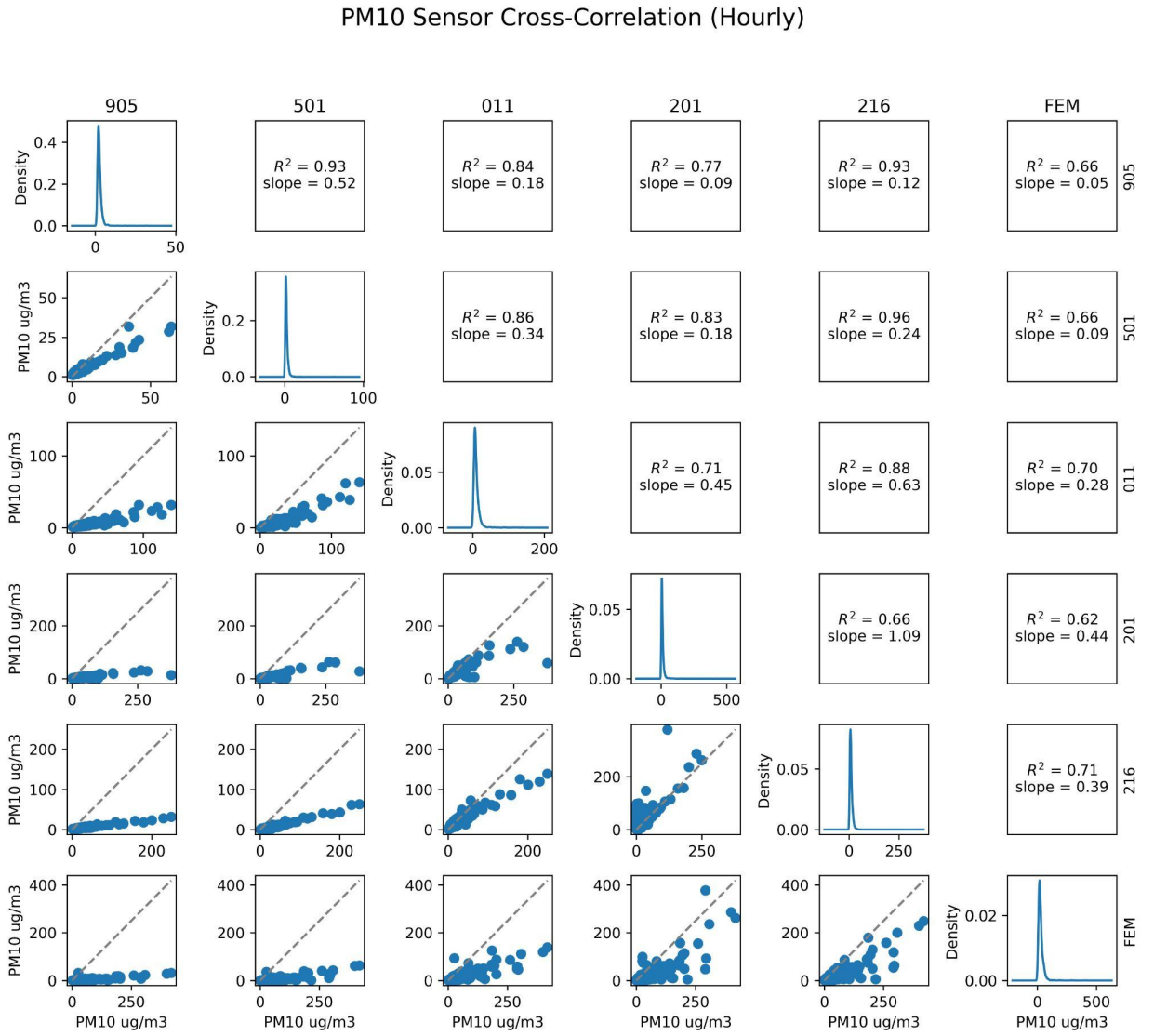


Figure S18: Summer 2025 (June 2025 to October 2025) FEM hourly PM_{10} and OPC-N3 raw hourly averaged PM_{10} scatter plot matrix. The dotted gray line is the one-to-one line. Measurements with RH > 80% dropped. x-axis: row sensor number; y-axis: column sensor number.

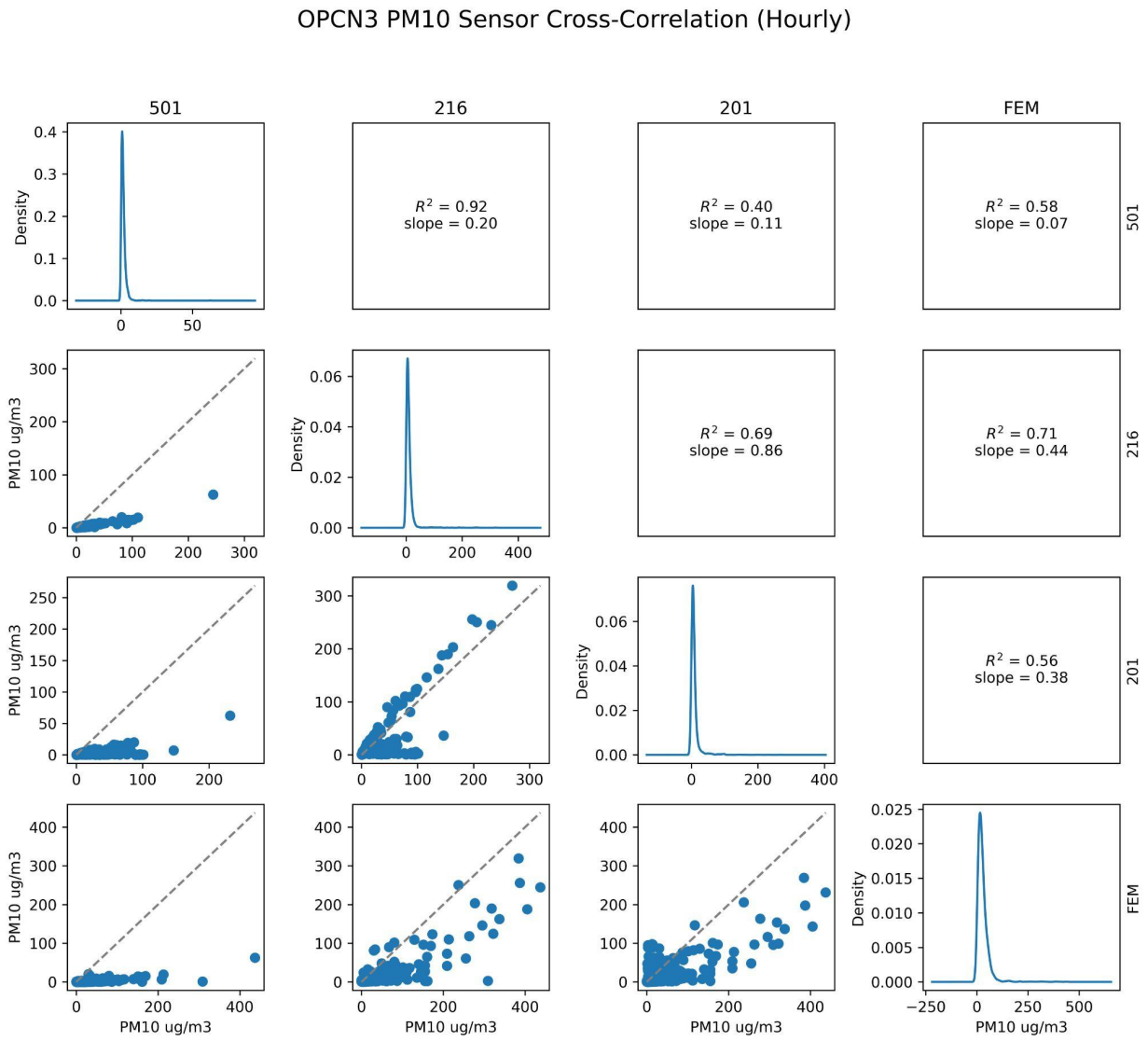


Figure S19: Winter 2025 (November 2025 to February 2026) FEM hourly PM_{10} and OPC-N3 raw hourly averaged PM_{10} scatter plot matrix. The dotted gray line is the one-to-one line. Measurements with RH > 80% dropped. x-axis: row sensor number; y-axis: column sensor number.

Seasonal OPC-N3 $PM_{2.5}$ scatter plot matrices

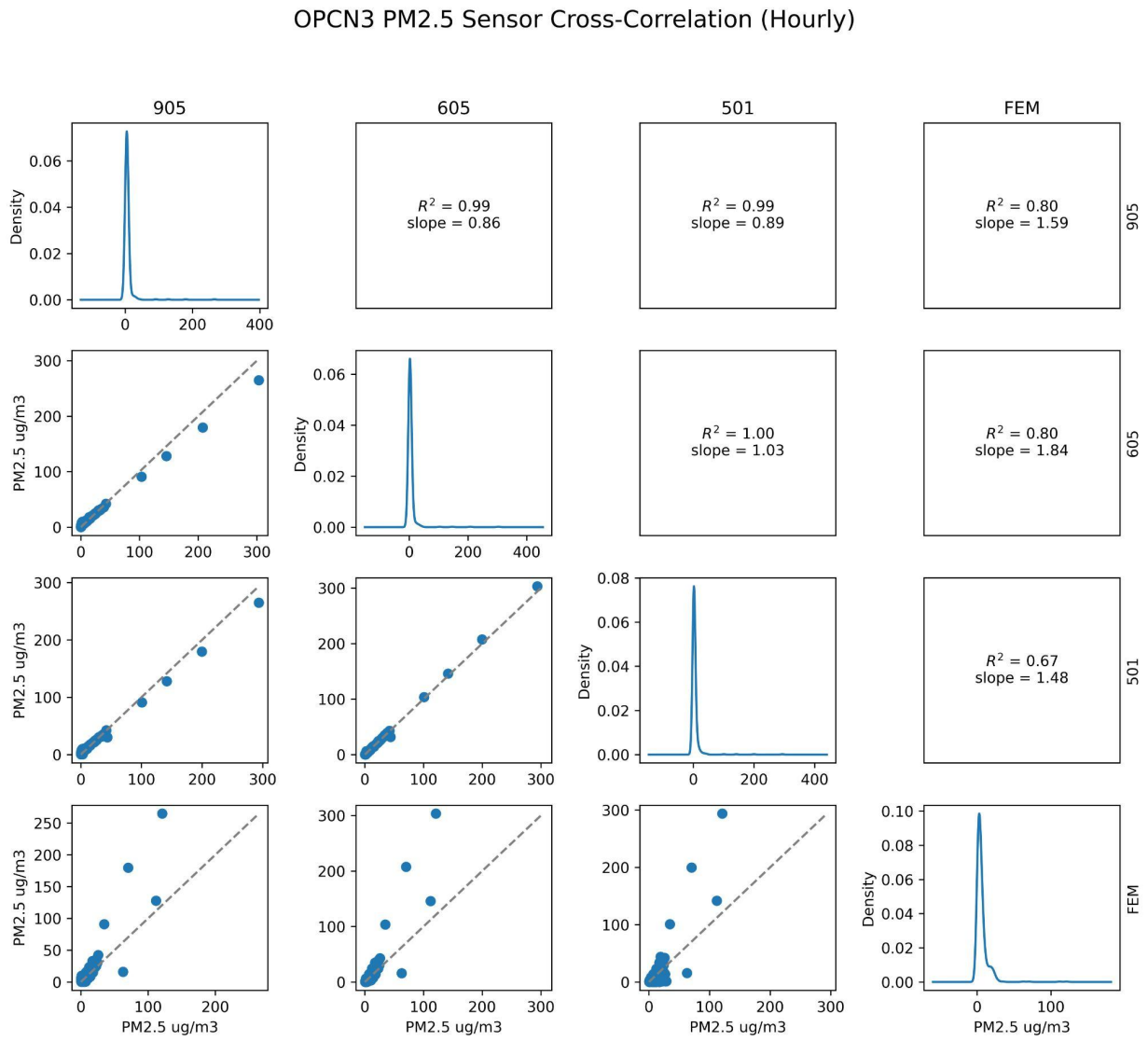


Figure S20: Winter 2023 (January to February 2024) FEM hourly $PM_{2.5}$ and OPC-N3 raw hourly averaged $PM_{2.5}$ scatter plot matrix. The dotted gray line is the one-to-one line. Measurements with RH > 80% dropped. x-axis: row sensor number; y-axis: column sensor number.

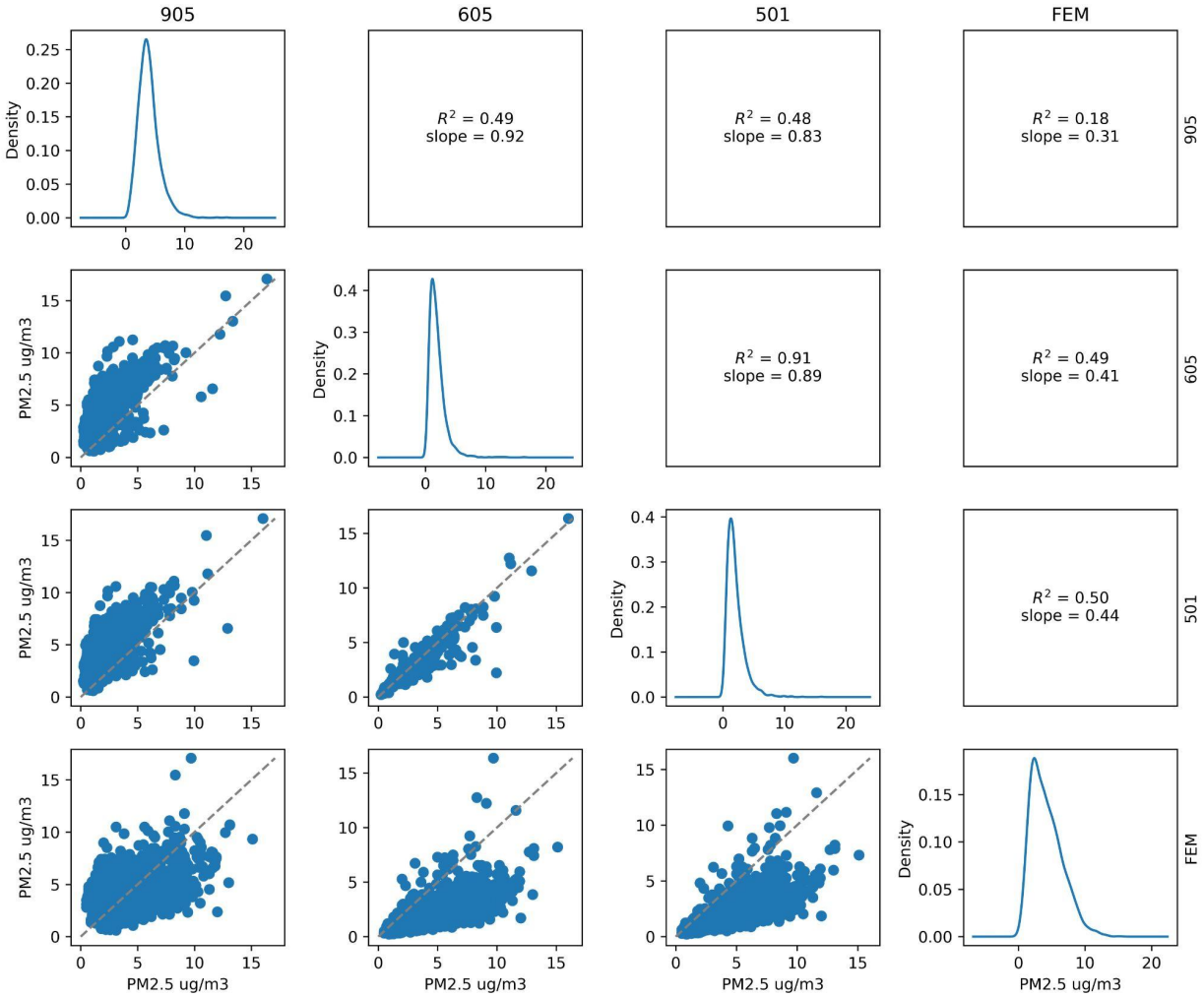


Figure S21: Spring 2024 (March 2024 to May 2024) FEM hourly $PM_{2.5}$ and OPC-N3 raw hourly averaged $PM_{2.5}$ scatter plot matrix. The dotted gray line is the one-to-one line. Measurements with RH > 80% dropped. x-axis: row sensor number; y-axis: column sensor number.

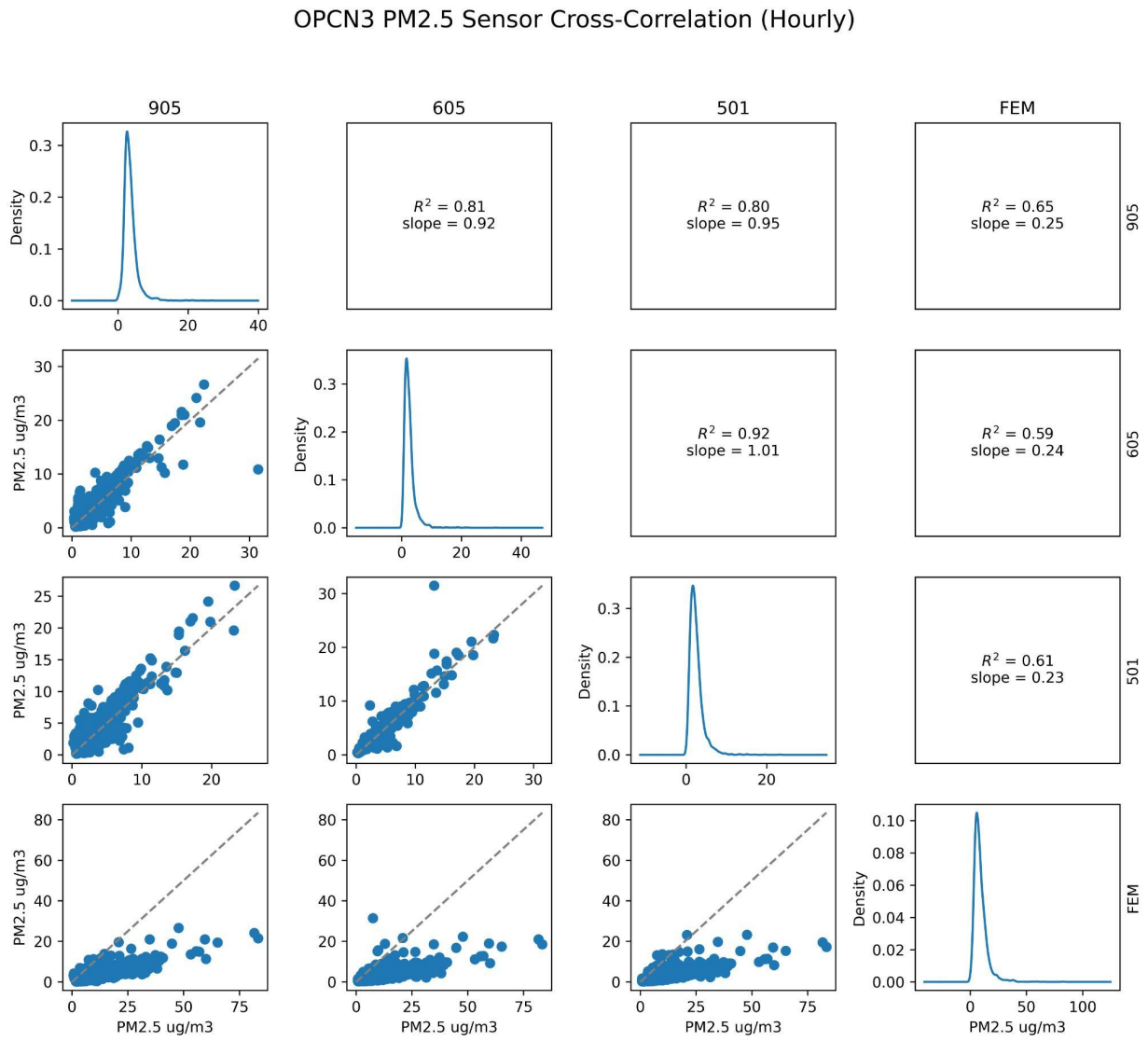


Figure S22: Summer 2024 (June 2024 to October 2024) FEM hourly $PM_{2.5}$ and OPC-N3 raw hourly averaged $PM_{2.5}$ scatter plot matrix. The dotted gray line is the one-to-one line. Measurements with RH > 80% dropped. x-axis: row sensor number; y-axis: column sensor number.

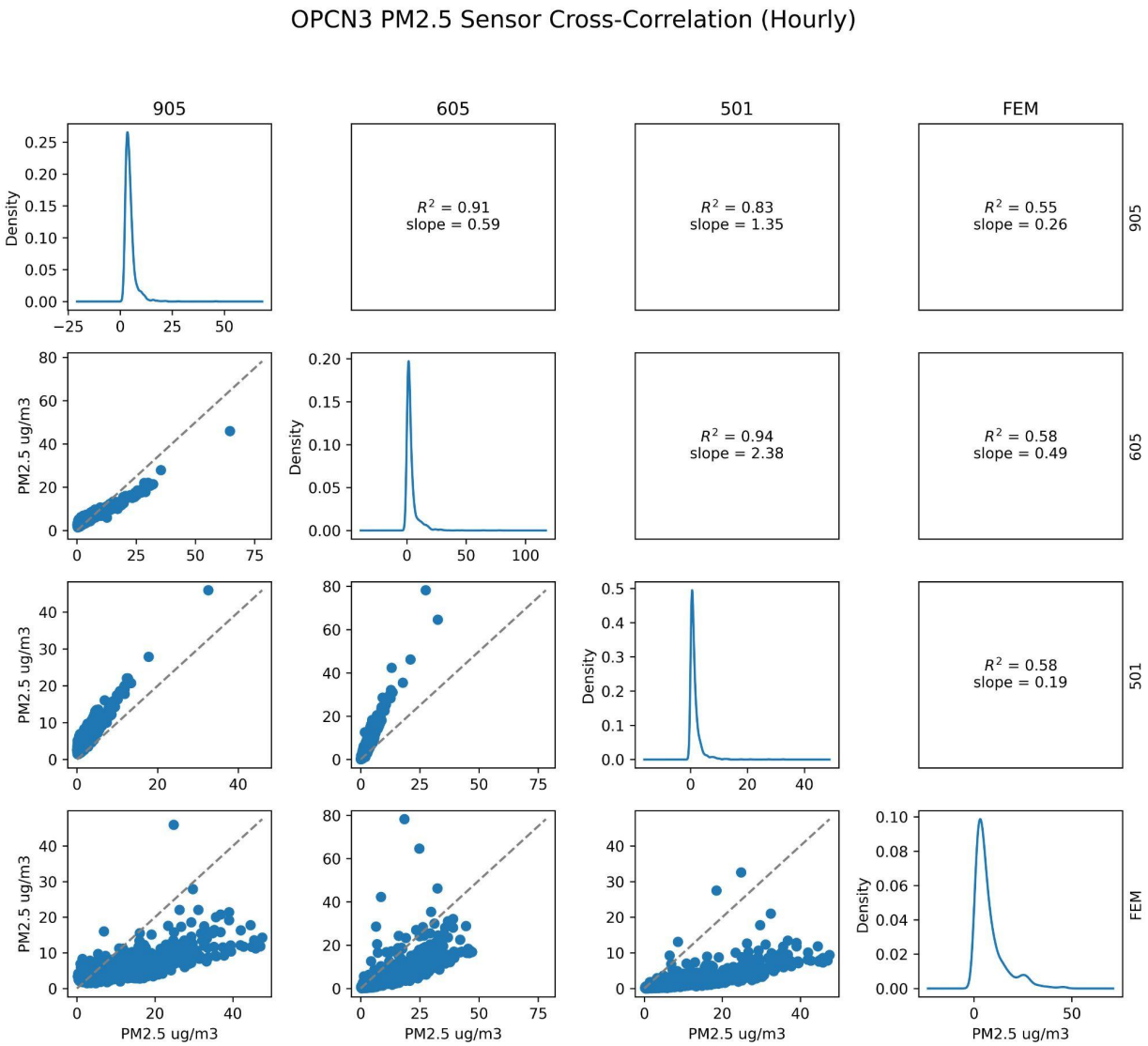


Figure S23: Winter 2024 (November 2024 to February 2025) FEM hourly $PM_{2.5}$ and OPC-N3 raw hourly averaged $PM_{2.5}$ scatter plot matrix. The dotted gray line is the one-to-one line. Measurements with RH > 80% dropped. x-axis: row sensor number; y-axis: column sensor number.

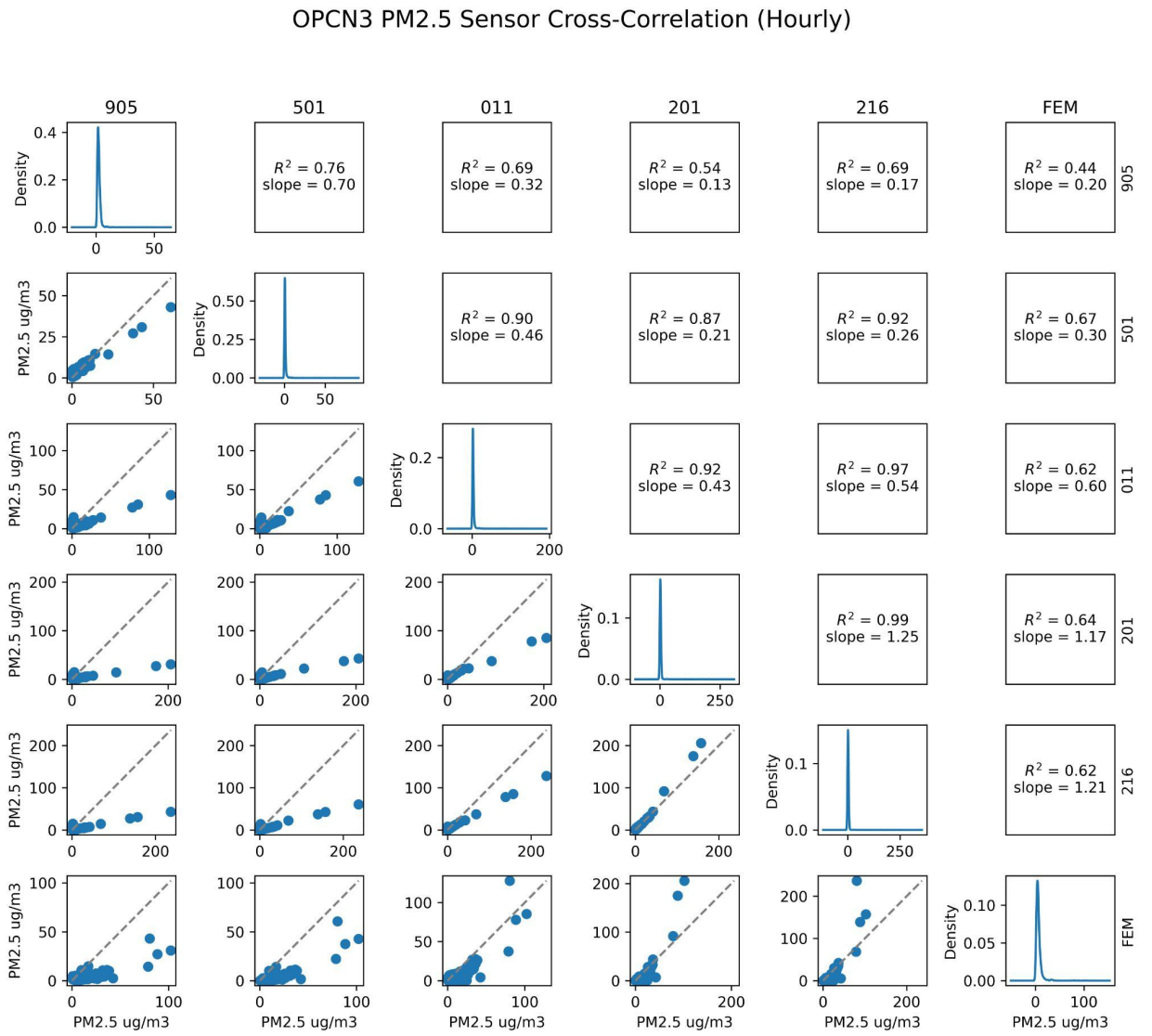


Figure S24: Spring 2025 (March 2025 to May 2025) FEM hourly $PM_{2.5}$ and OPC-N3 raw hourly averaged $PM_{2.5}$ scatter plot matrix. The dotted gray line is the one-to-one line. Measurements with RH > 80% dropped. x-axis: row sensor number; y-axis: column sensor number.

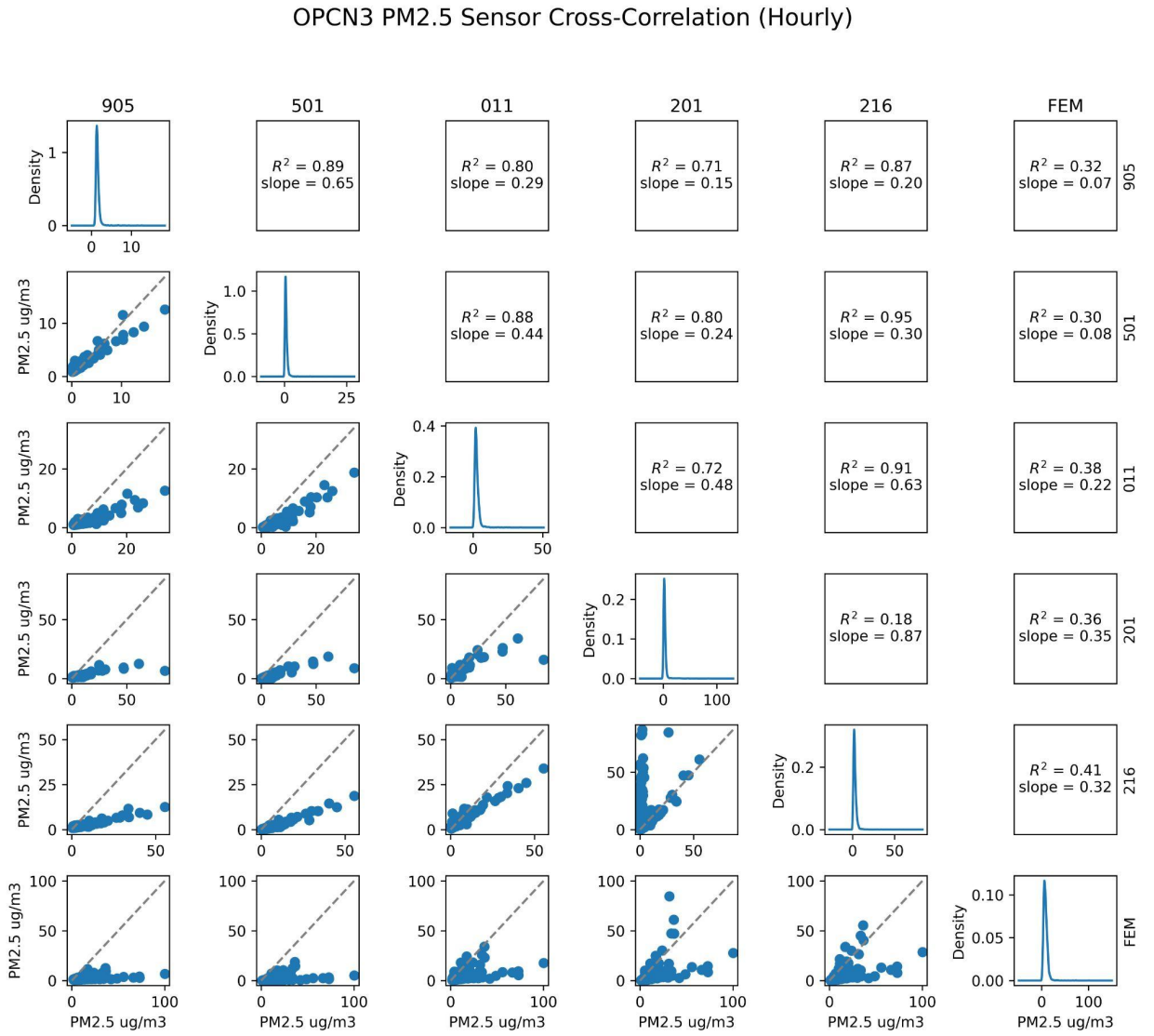


Figure S25: Summer 2025 (June 2025 to October 2025) FEM hourly $PM_{2.5}$ and OPC-N3 raw hourly averaged $PM_{2.5}$ scatter plot matrix. The dotted gray line is the one-to-one line. Measurements with RH > 80% dropped. x-axis: row sensor number; y-axis: column sensor number.

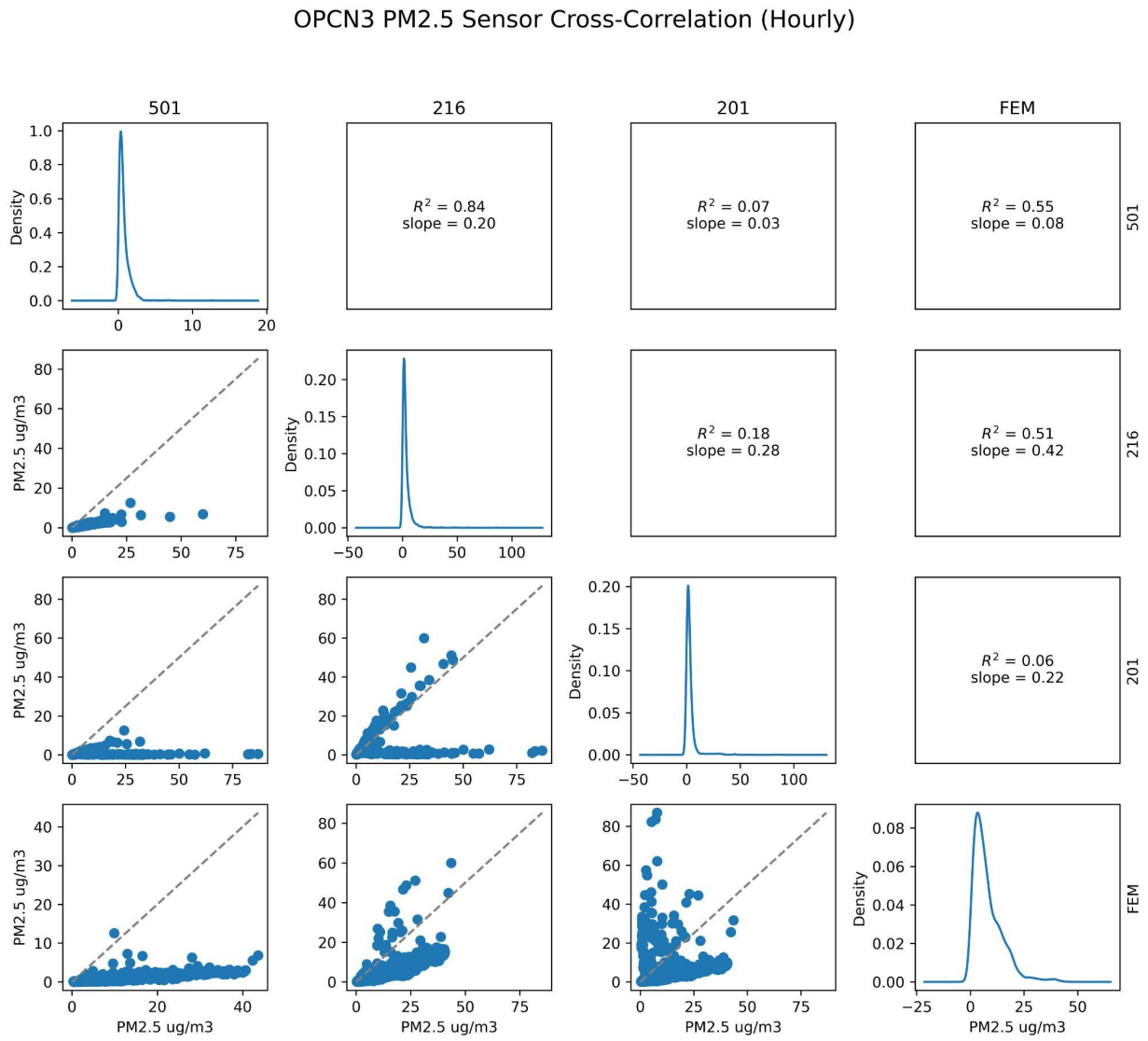


Figure S26: Winter 2025 (November 2025 to February 2026) FEM hourly $PM_{2.5}$ and OPC-N3 raw hourly averaged $PM_{2.5}$ scatter plot matrix. The dotted gray line is the one-to-one line. Measurements with RH > 80% dropped. x-axis: row sensor number; y-axis: column sensor number.

Seasonal PMS5003T $PM_{2.5}$ scatter plot matrices

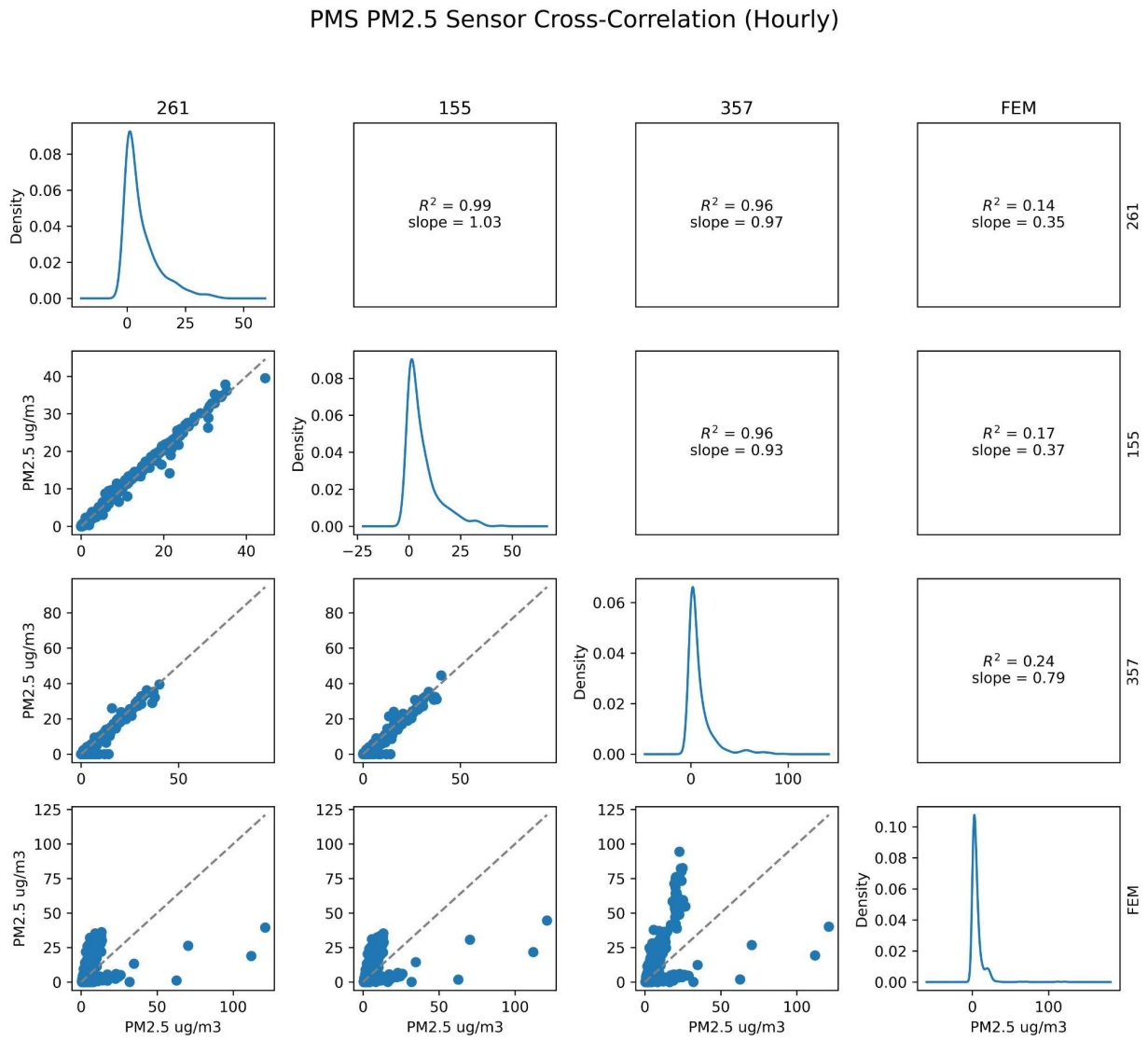


Figure S27: Winter 2023 (January to February 2024) FEM hourly $PM_{2.5}$ and PMS5003T raw hourly averaged $PM_{2.5}$ scatter plot matrix. The dotted gray line is the one-to-one line. Measurements > 100 μg m^{-3} and 3x the FEM dropped. x-axis: row sensor number; y-axis: column sensor number.

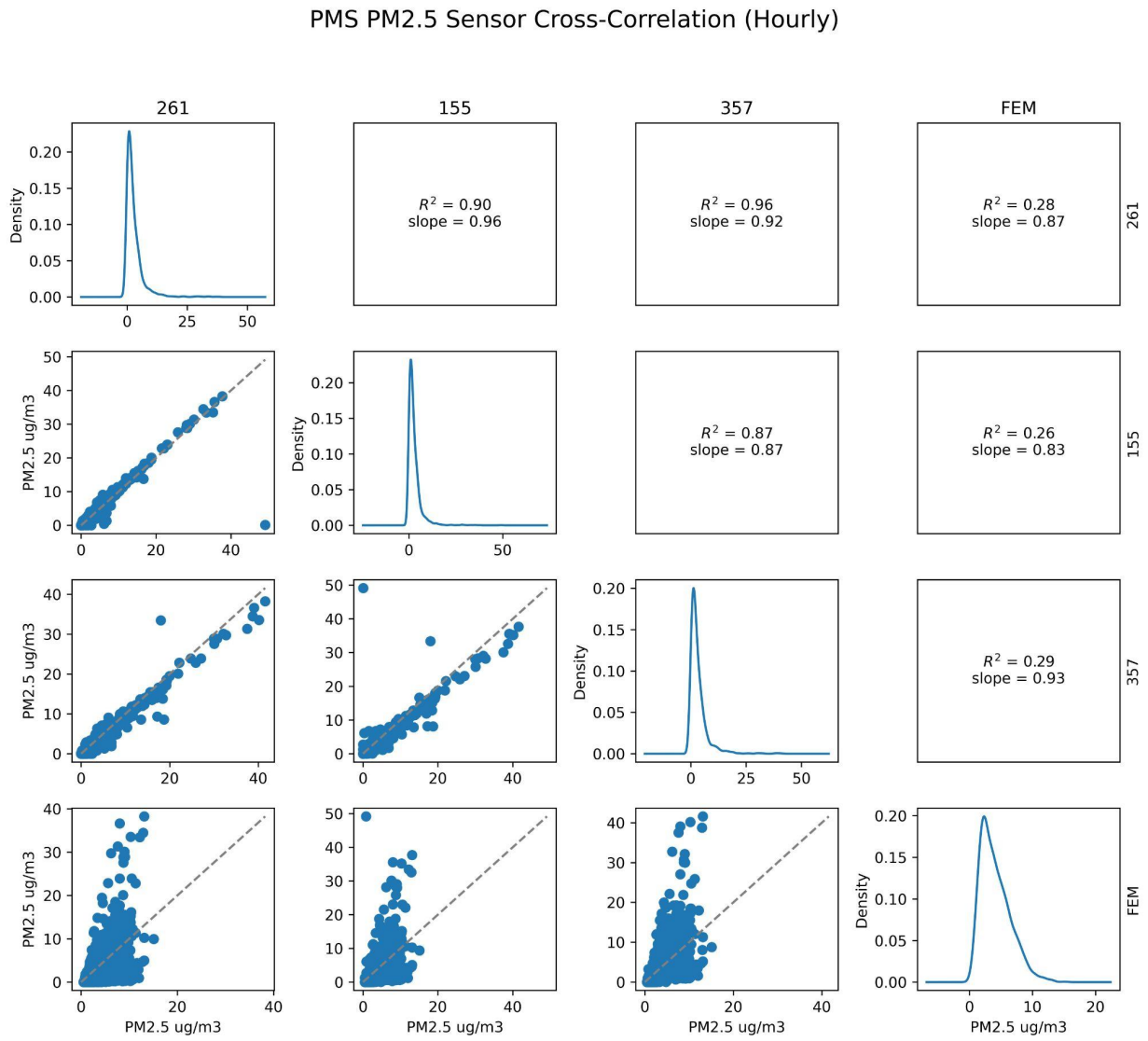


Figure S28: Spring 2024 (March 2024 to May 2024) FEM hourly $PM_{2.5}$ and PMS5003T raw hourly averaged $PM_{2.5}$ scatter plot matrix. The dotted gray line is the one-to-one line. Measurements > 100 μg m^{-3} and 3x the FEM dropped. x-axis: row sensor number; y-axis: column sensor number.

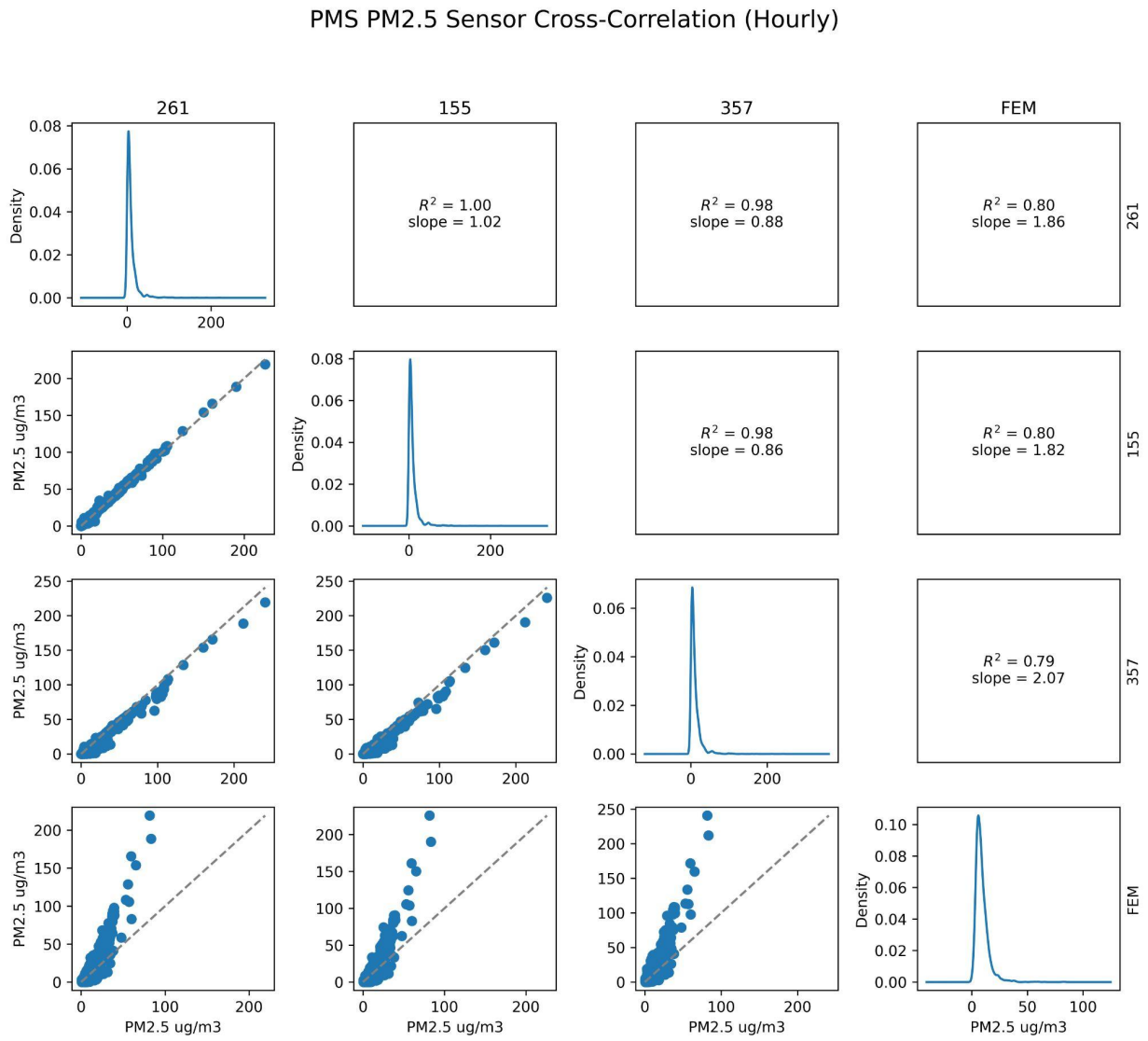


Figure S29: Summer 2024 (June 2024 to October 2024) FEM hourly $PM_{2.5}$ and PMS5003T raw hourly averaged $PM_{2.5}$ scatter plot matrix. The dotted gray line is the one-to-one line. Measurements > 100 μg m^{-3} and 3x the FEM dropped. x-axis: row sensor number; y-axis: column sensor number.

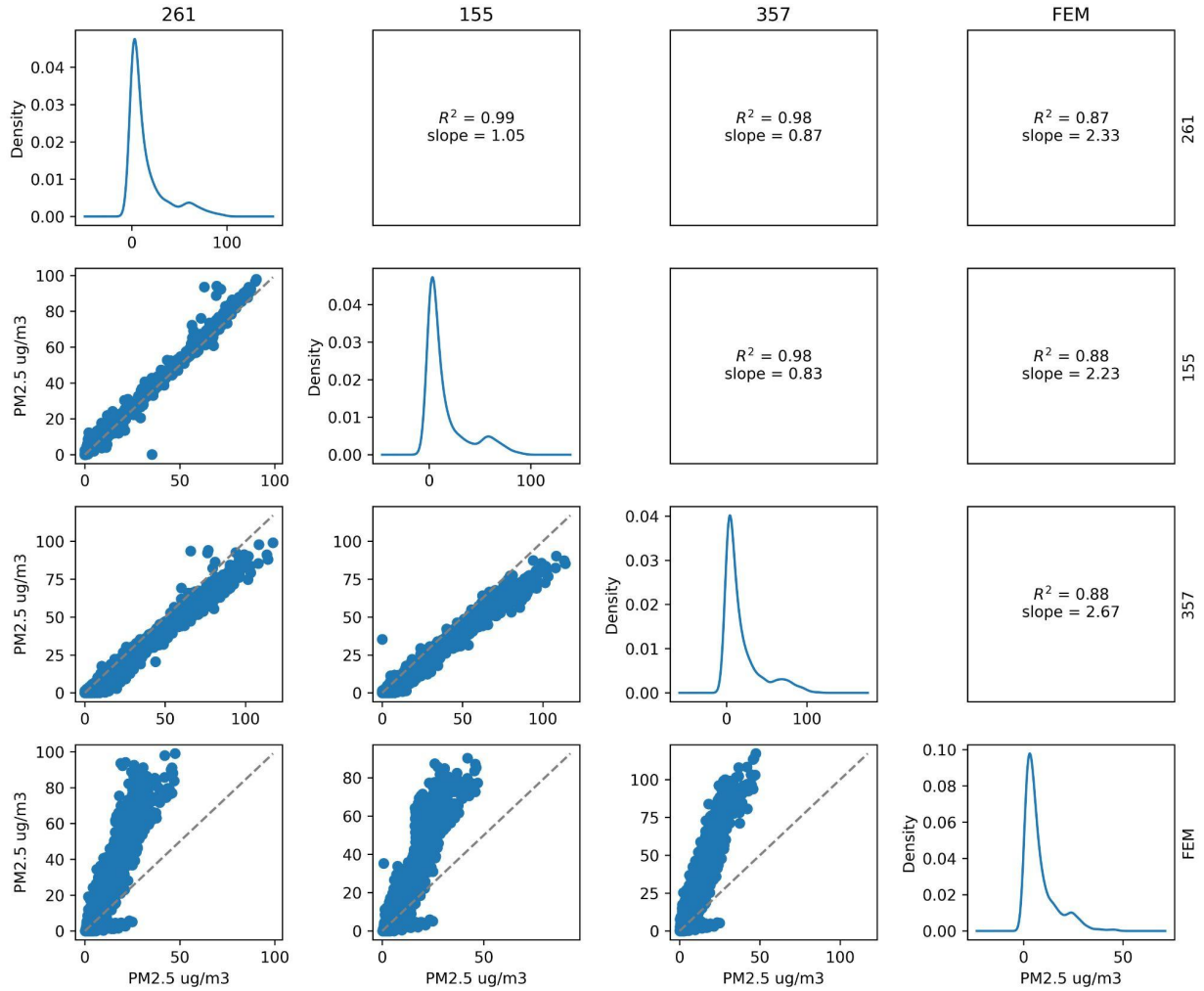


Figure S30: Winter 2024 (November 2024 to February 2025) FEM hourly $PM_{2.5}$ and PMS5003T raw hourly averaged $PM_{2.5}$ scatter plot matrix. The dotted gray line is the one-to-one line. Measurements > 100 μg m^{-3} and 3x the FEM dropped. x-axis: row sensor number; y-axis: column sensor number.

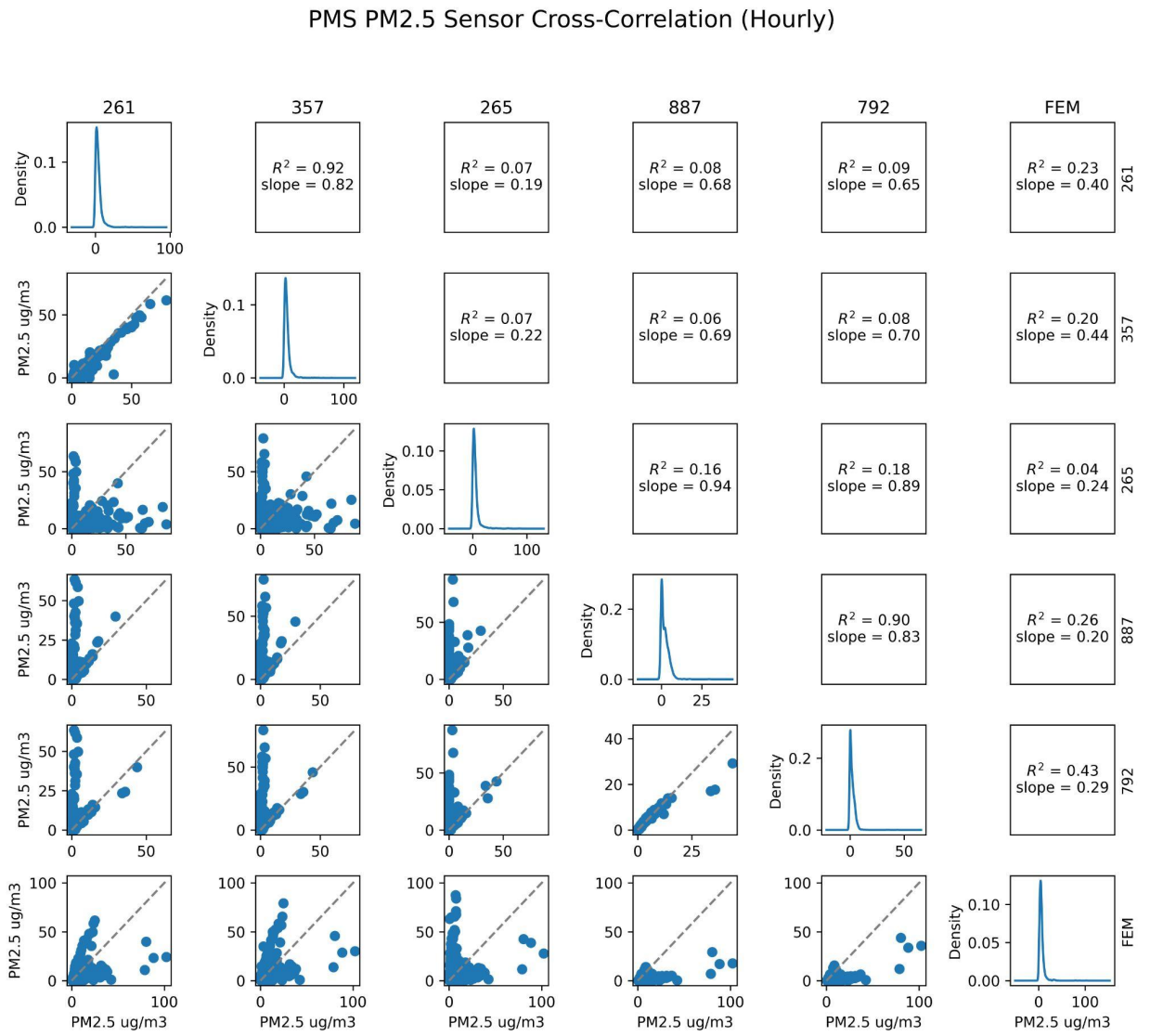


Figure S31: Spring 2025 (March 2025 to May 2025) FEM hourly $PM_{2.5}$ and PMS5003T raw hourly averaged $PM_{2.5}$ scatter plot matrix. The dotted gray line is the one-to-one line. Measurements > 100 μg m^{-3} and 3x the FEM dropped. x-axis: row sensor number; y-axis: column sensor number.

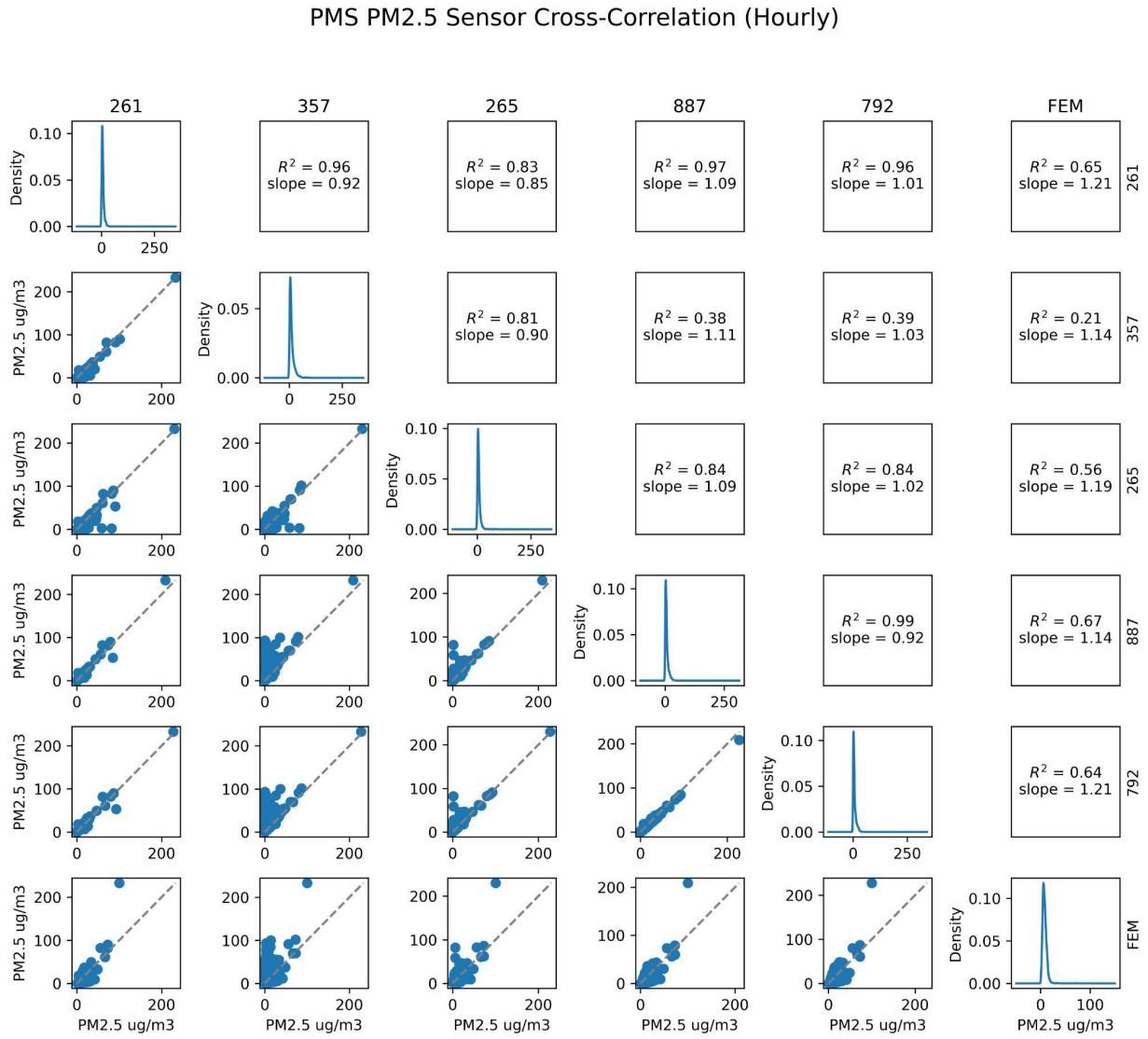


Figure S32: Summer 2025 (June 2025 to October 2025) FEM hourly $PM_{2.5}$ and PMS5003T raw hourly averaged $PM_{2.5}$ scatter plot matrix. The dotted gray line is the one-to-one line. Measurements > 100 μg m^{-3} and 3x the FEM dropped. x-axis: row sensor number; y-axis: column sensor number.

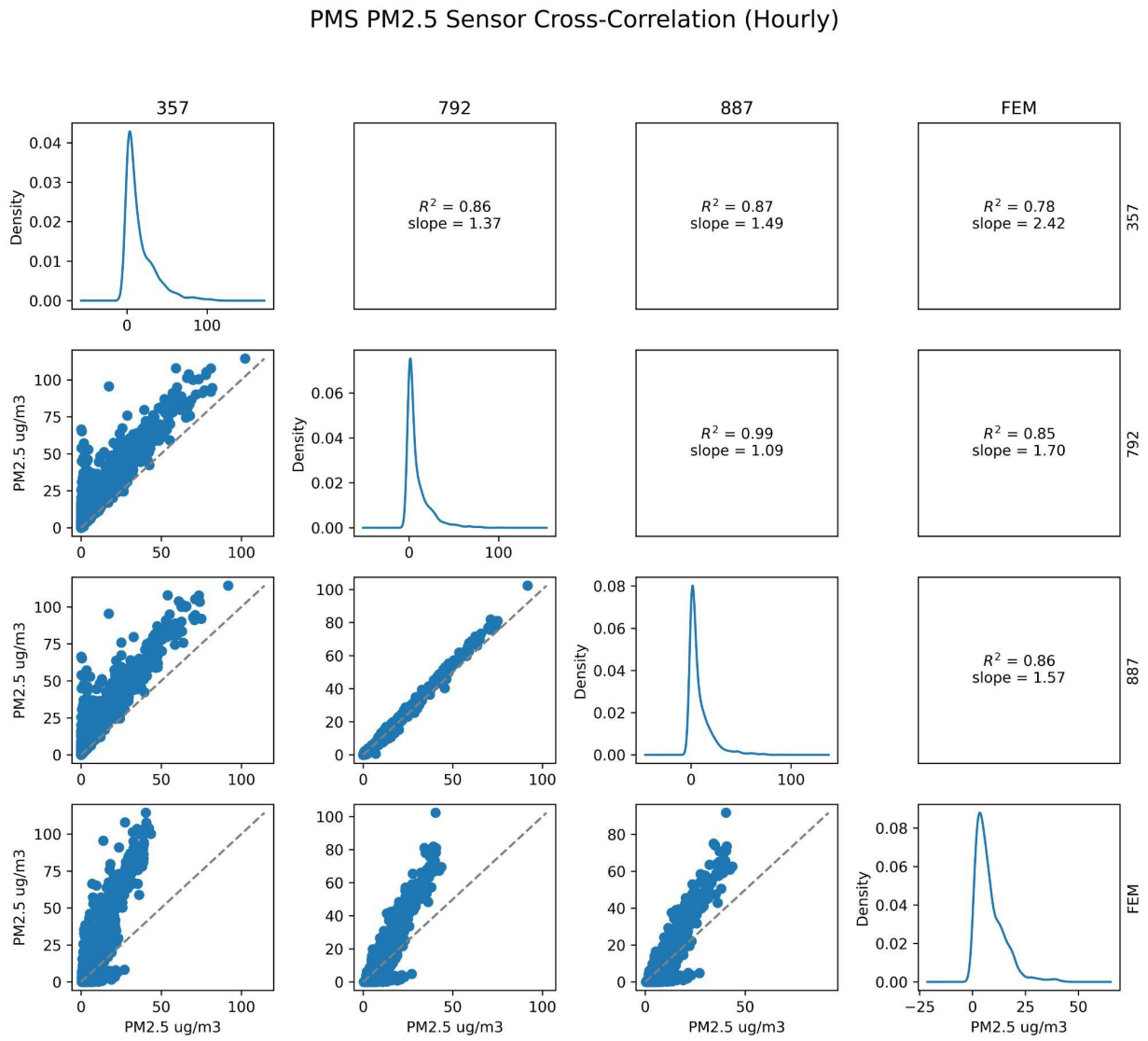


Figure S33: Winter 2025 (November 2025 to February 2026) FEM hourly $PM_{2.5}$ and PMS5003T raw hourly averaged $PM_{2.5}$ scatter plot matrix. The dotted gray line is the one-to-one line. Measurements > 100 μg m^{-3} and 3x the FEM dropped. x-axis: row sensor number; y-axis: column sensor number.

Seasonal OPC-N3 PM_{10} Bland-Altman plots

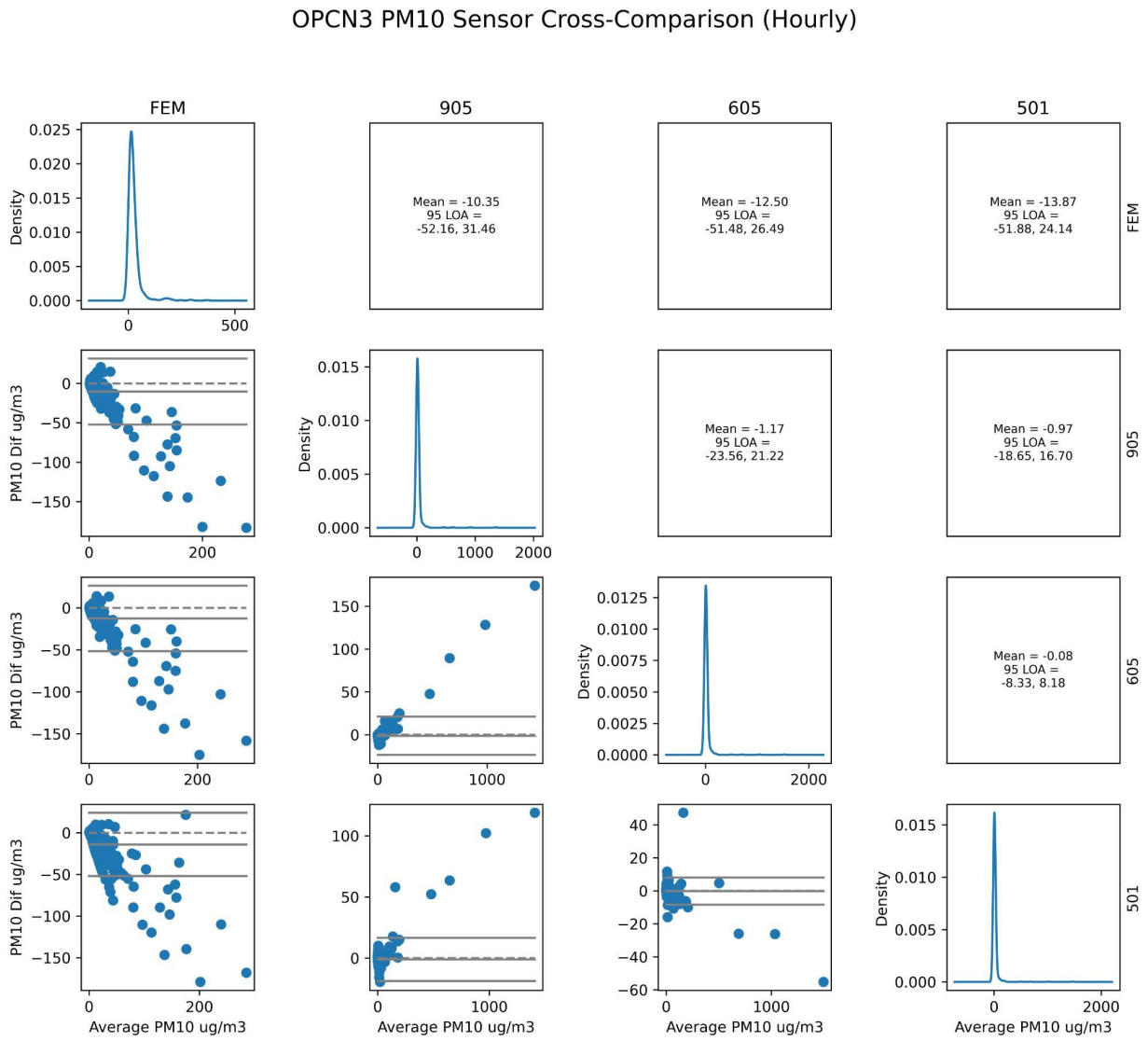


Figure S34: Winter 2023 (January to February 2024) Bland-Altman plots for comparisons of hourly FEM and raw hourly averaged OPC-N3 PM_{10} measurements. The y-axis shows the difference between comparison measurements (column sensor minus row sensor), and the x-axis shows the average. Measurements with RH > 80% dropped. The dotted gray line represents the x-axis (y = 0). The central solid gray line represents the mean difference (bias), and the outer solid gray lines represent the 95% limits of agreement (LOA).

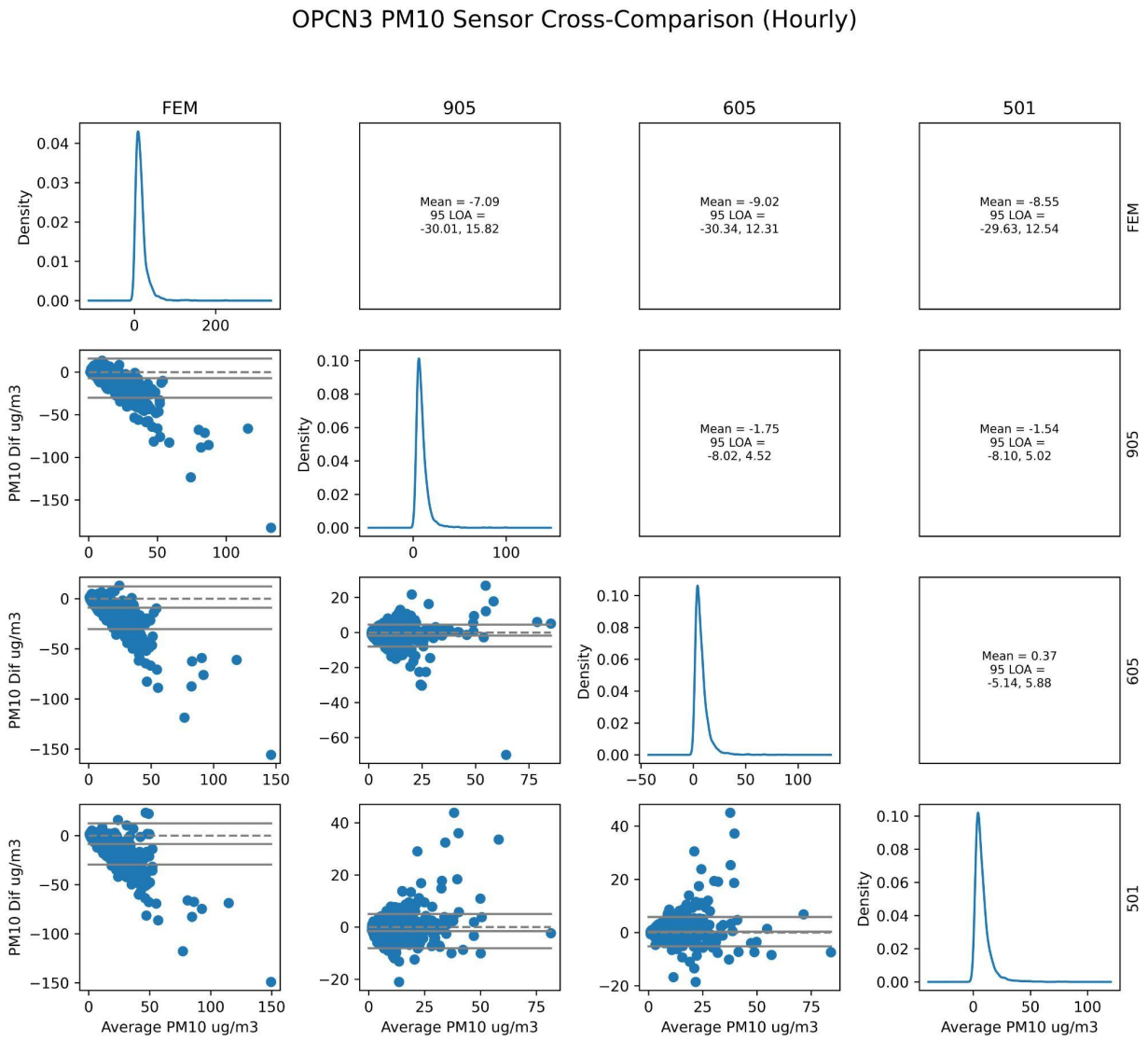


Figure S35: Spring 2024 (March 2024 to May 2024) Bland-Altman plots for comparisons of hourly FEM and raw hourly averaged OPC-N3 PM_{10} measurements. The y-axis shows the difference between comparison measurements (column sensor minus row sensor), and the x-axis shows the average. Measurements with RH > 80% dropped. The dotted gray line represents the x-axis (y = 0). The central solid gray line represents the mean difference (bias), and the outer solid gray lines represent the 95% limits of agreement (LOA).

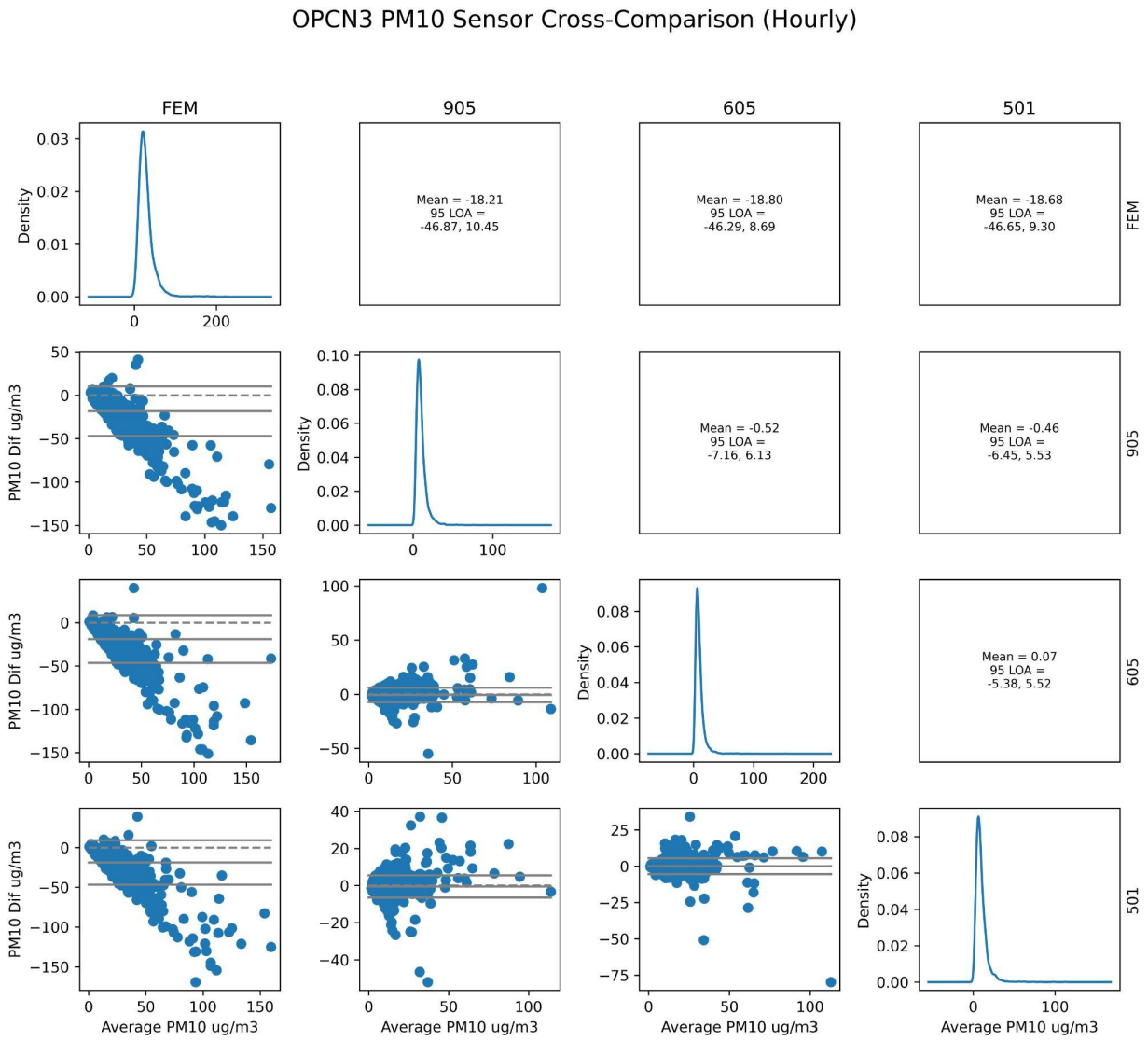


Figure S36: Summer 2024 (June 2024 to October 2024) Bland-Altman plots for comparisons of hourly FEM and raw hourly averaged OPC-N3 PM_{10} measurements. The y-axis shows the difference between comparison measurements (column sensor minus row sensor), and the x-axis shows the average. Measurements with RH > 80% dropped. The dotted gray line represents the x-axis (y = 0). The central solid gray line represents the mean difference (bias), and the outer solid gray lines represent the 95% limits of agreement (LOA).

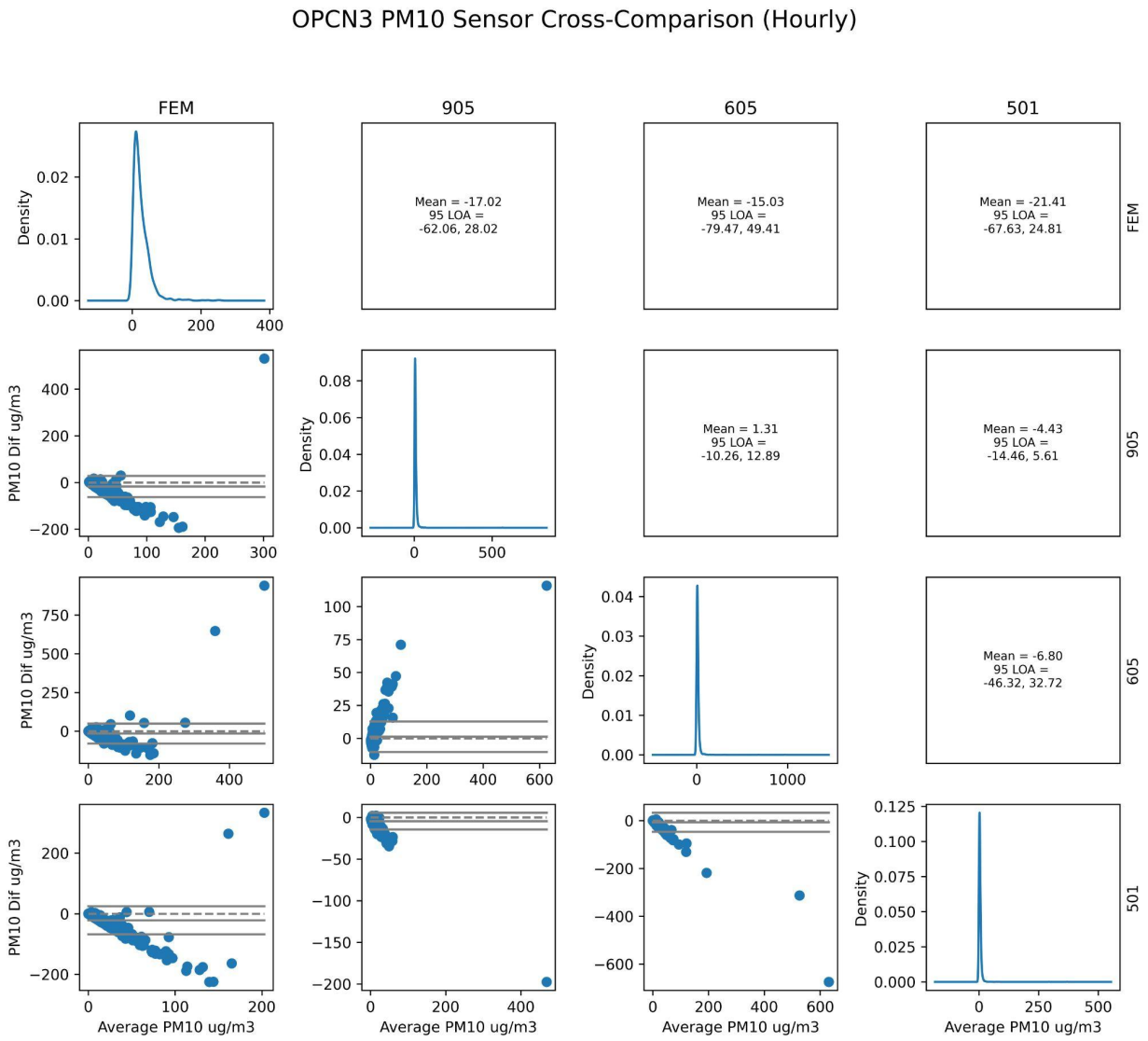


Figure S37: Winter 2024 (November 2024 to February 2025) Bland-Altman plots for comparisons of hourly FEM and raw hourly averaged OPC-N3 PM_{10} measurements. The y-axis shows the difference between comparison measurements (column sensor minus row sensor), and the x-axis shows the average. FEM PM_{10} measurements are hourly. OPC-N3 PM_{10} measurements are hourly averaged (uncorrected). Measurements with RH > 80% dropped. The dotted gray line represents the x-axis (y = 0). The central solid gray line represents the mean difference (bias), and the outer solid gray lines represent the 95% limits of agreement (LOA).

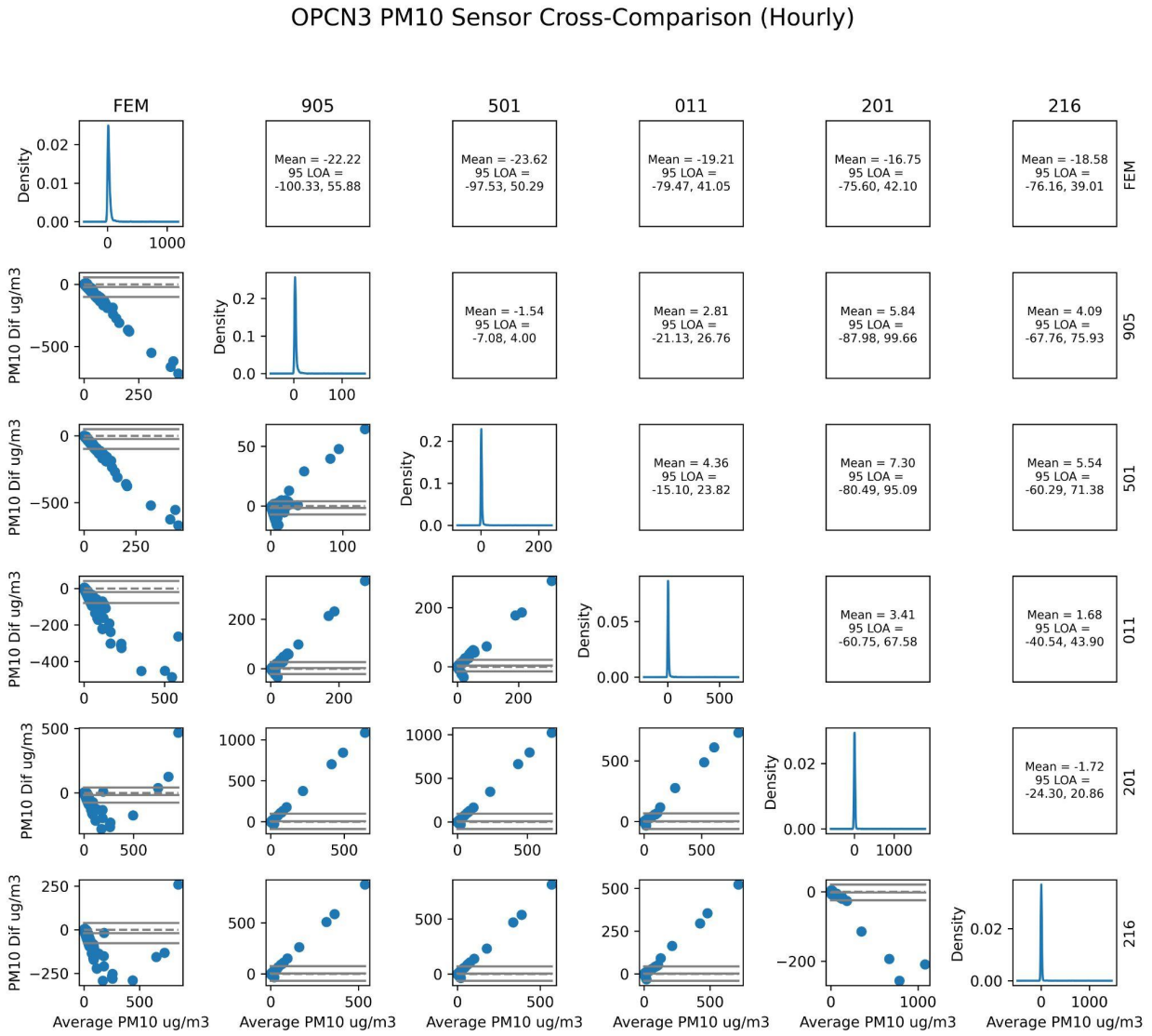


Figure S38: Spring 2025 (March 2025 to May 2025) Bland-Altman plots for comparisons of hourly FEM and raw hourly averaged OPC-N3 PM_{10} measurements. The y-axis shows the difference between comparison measurements (column sensor minus row sensor), and the x-axis shows the average. Measurements with RH > 80% dropped. The dotted gray line represents the x-axis (y = 0). The central solid gray line represents the mean difference (bias), and the outer solid gray lines represent the 95% limits of agreement (LOA).

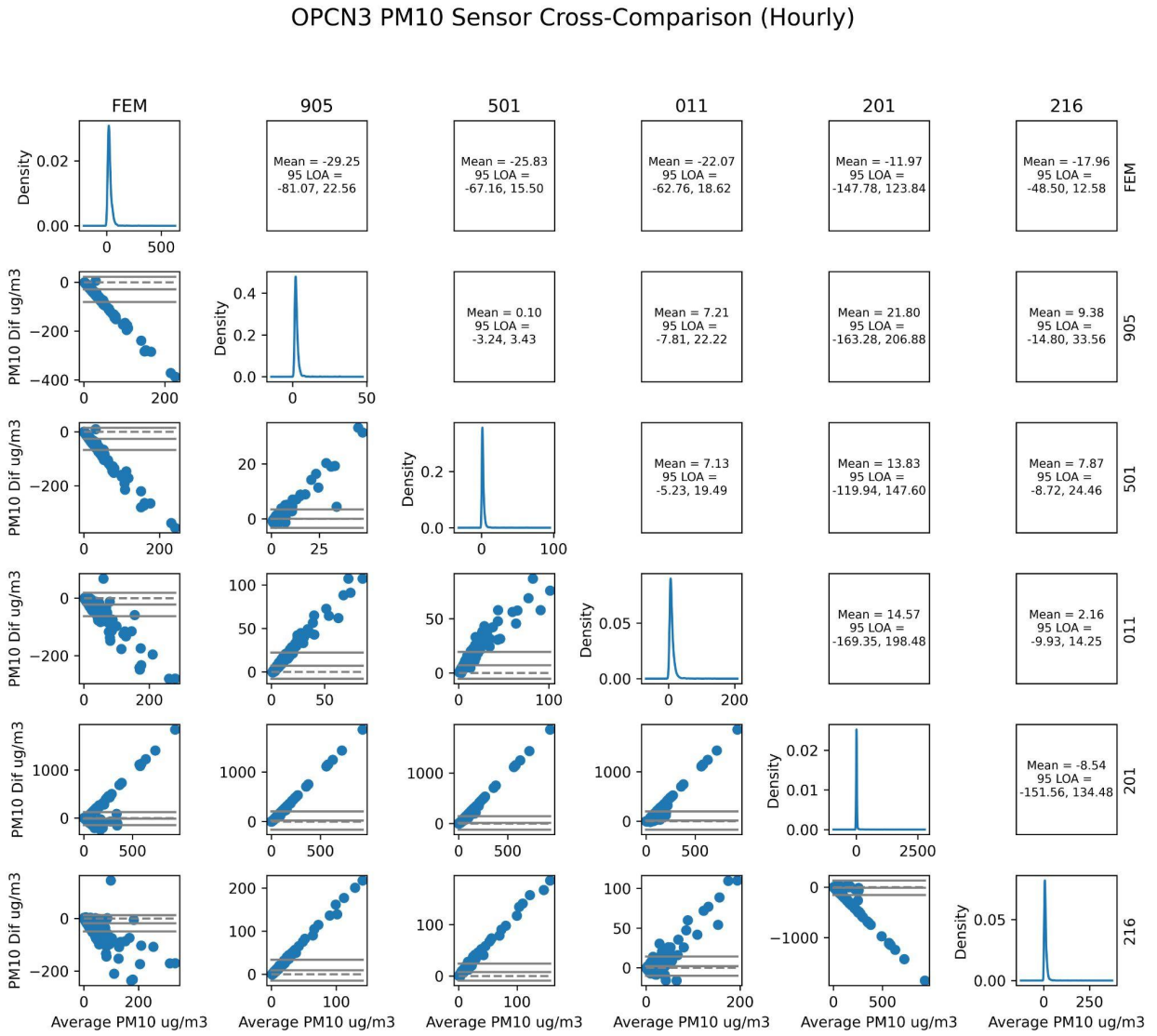


Figure S39: Summer 2025 (June 2025 to October 2025) Bland-Altman plots for comparisons of hourly FEM and raw hourly averaged OPC-N3 PM_{10} measurements. The y-axis shows the difference between comparison measurements (column sensor minus row sensor), and the x-axis shows the average. Measurements with RH > 80% dropped. The dotted gray line represents the x-axis (y = 0). The central solid gray line represents the mean difference (bias), and the outer solid gray lines represent the 95% limits of agreement (LOA).

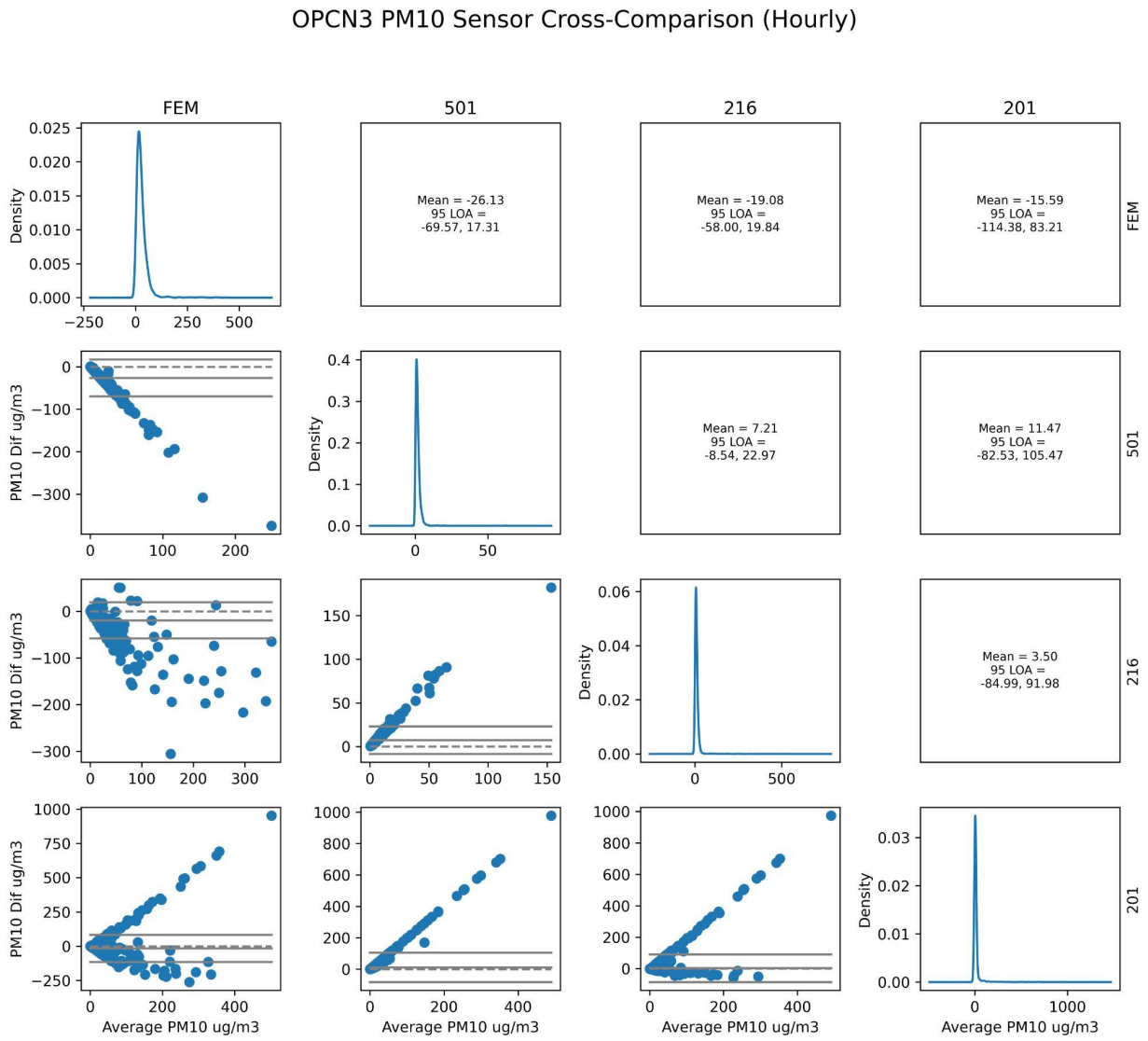


Figure S40: Winter 2025 (November 2025 to February 2026) Bland-Altman plots for comparisons of hourly FEM and raw hourly averaged OPC-N3 PM_{10} measurements. The y-axis shows the difference between comparison measurements (column sensor minus row sensor), and the x-axis shows the average. Measurements with RH > 80% dropped. The dotted gray line represents the x-axis (y = 0). The central solid gray line represents the mean difference (bias), and the outer solid gray lines represent the 95% limits of agreement (LOA).

Seasonal OPC-N3 $PM_{2.5}$ Bland-Altman plots

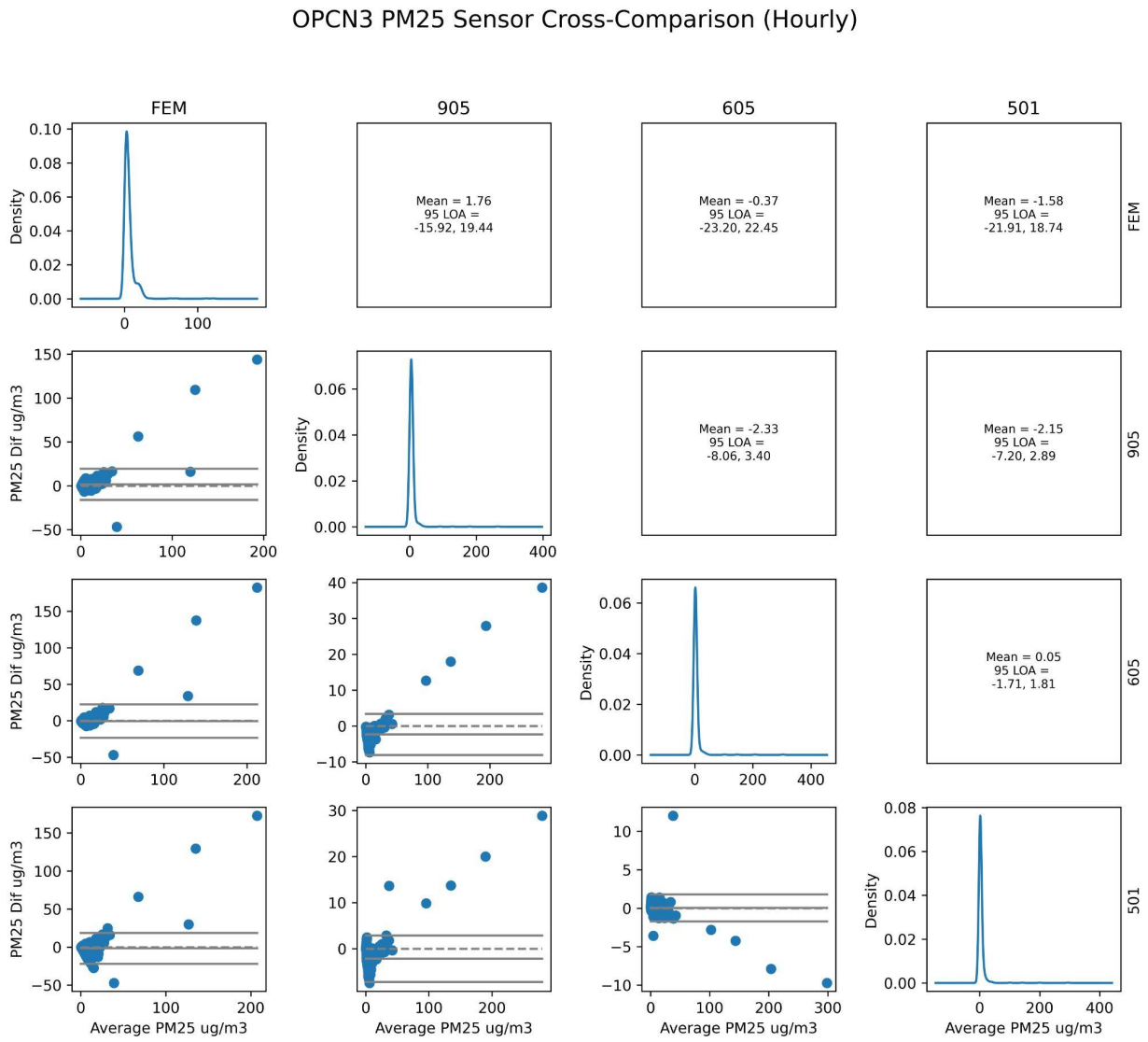


Figure S41: Winter 2023 (January to February 2024) Bland-Altman plots for comparisons of hourly FEM and raw hourly averaged OPC-N3 $PM_{2.5}$ measurements. The y-axis shows the difference between comparison measurements (column sensor minus row sensor), and the x-axis shows the average. Measurements with RH > 80% dropped. The dotted gray line represents the x-axis (y = 0). The central solid gray line represents the mean difference (bias), and the outer solid gray lines represent the 95% limits of agreement (LOA).

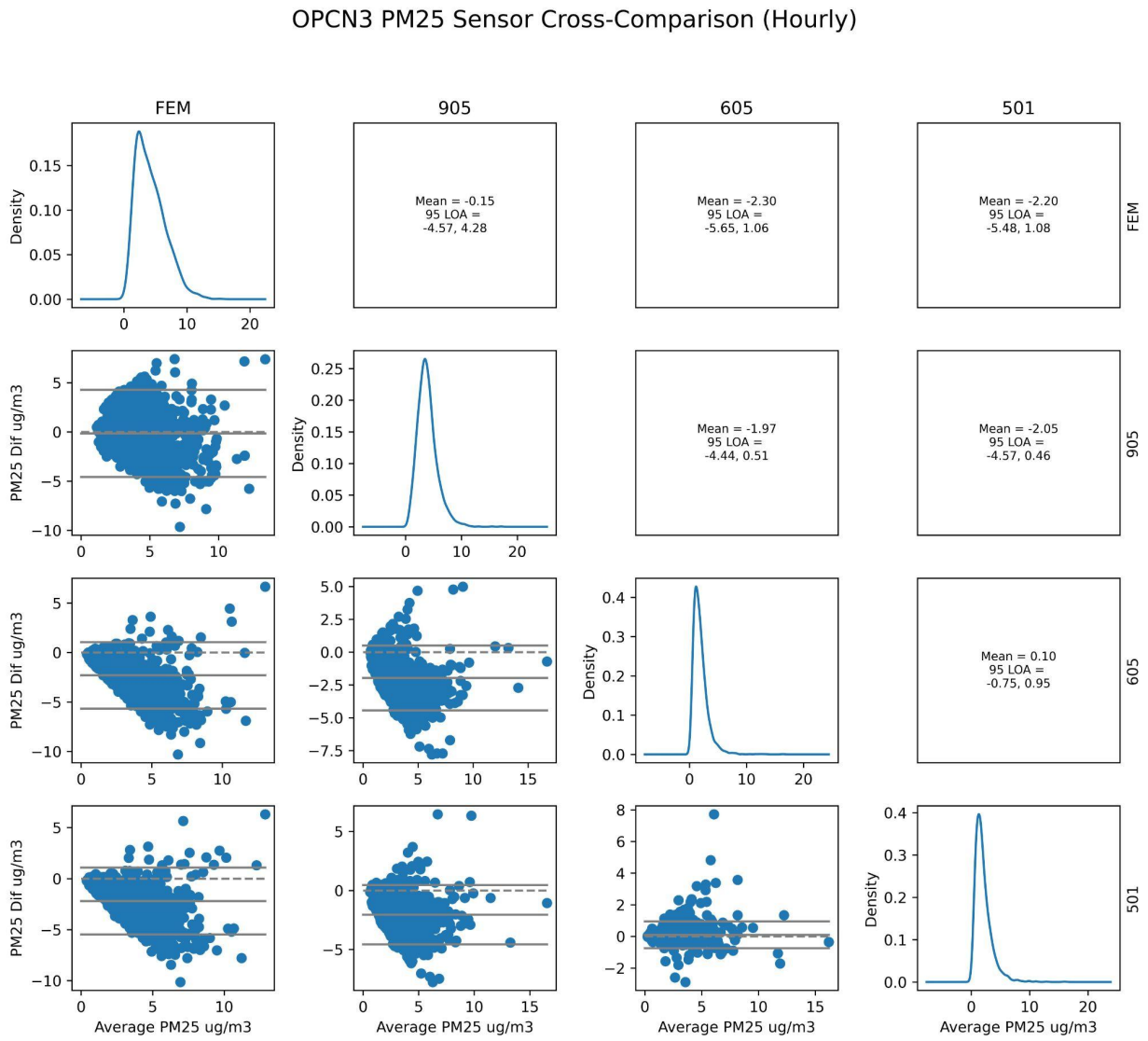


Figure S42: Spring 2024 (March 2024 to May 2024) Bland-Altman plots for comparisons of hourly FEM and raw hourly averaged OPC-N3 $PM_{2.5}$ measurements. The y-axis shows the difference between comparison measurements (column sensor minus row sensor), and the x-axis shows the average. Measurements with RH > 80% dropped. The dotted gray line represents the x-axis (y = 0). The central solid gray line represents the mean difference (bias), and the outer solid gray lines represent the 95% limits of agreement (LOA).

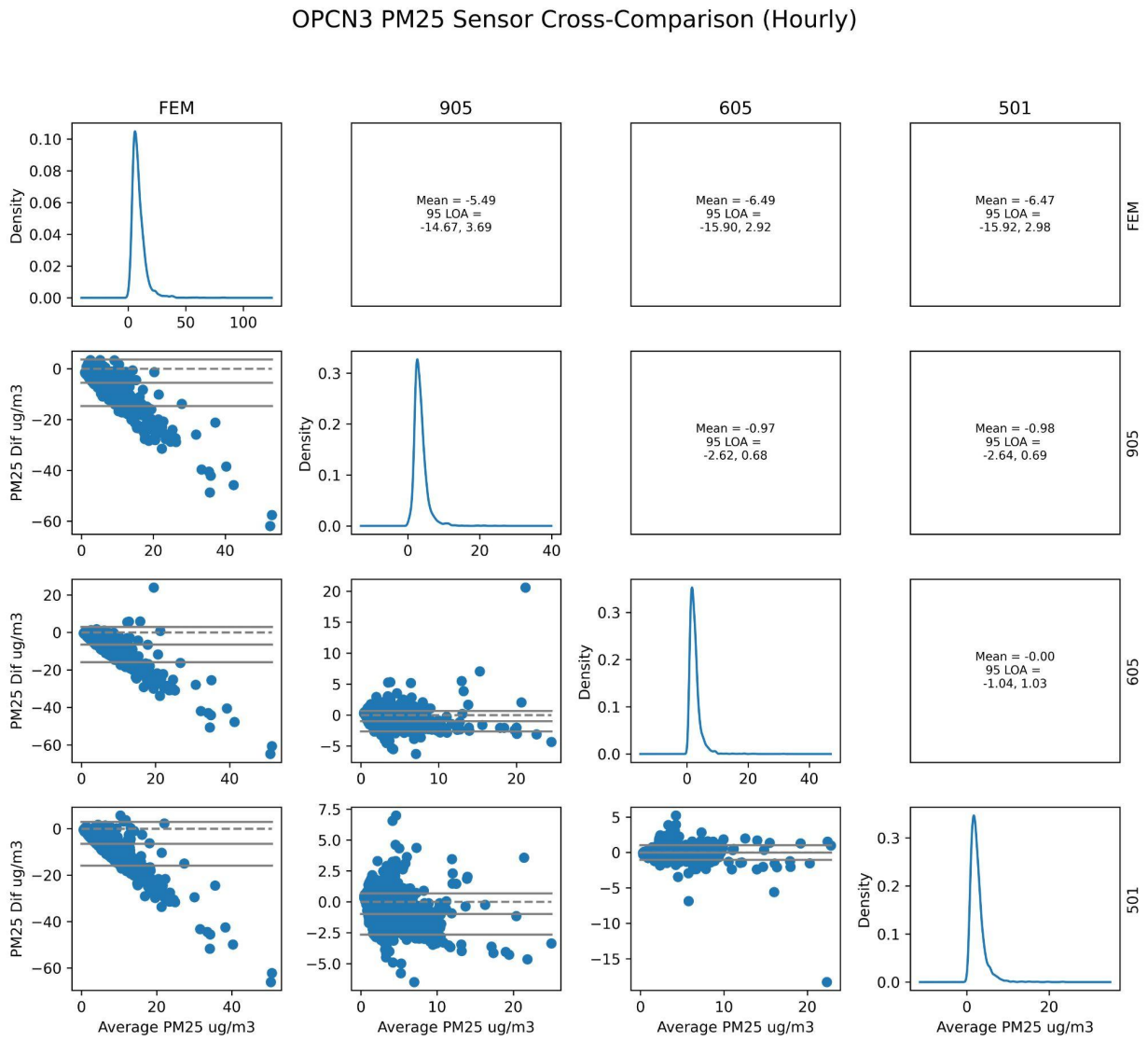


Figure S43: Summer 2024 (June 2024 to October 2024) Bland-Altman plots for comparisons of hourly FEM and raw hourly averaged OPC-N3 $PM_{2.5}$ measurements. The y-axis shows the difference between comparison measurements (column sensor minus row sensor), and the x-axis shows the average. Measurements with RH > 80% dropped. The dotted gray line represents the x-axis (y = 0). The central solid gray line represents the mean difference (bias), and the outer solid gray lines represent the 95% limits of agreement (LOA).

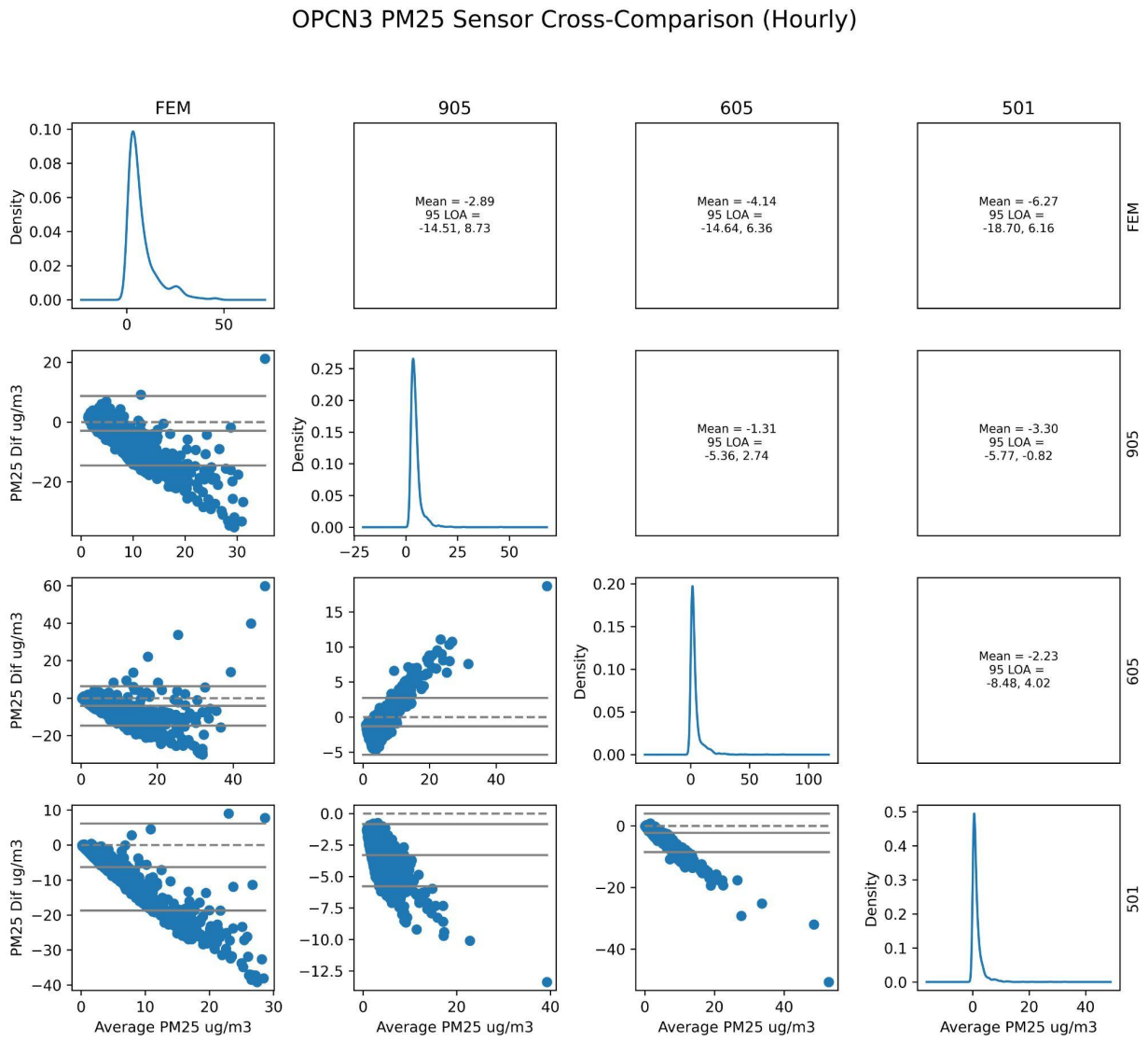


Figure S44: Winter 2024 (November 2024 to February 2025) Bland-Altman plots for comparisons of hourly FEM and raw hourly averaged OPC-N3 $PM_{2.5}$ measurements. The y-axis shows the difference between comparison measurements (column sensor minus row sensor), and the x-axis shows the average. Measurements with RH > 80% dropped. The dotted gray line represents the x-axis (y = 0). The central solid gray line represents the mean difference (bias), and the outer solid gray lines represent the 95% limits of agreement (LOA).

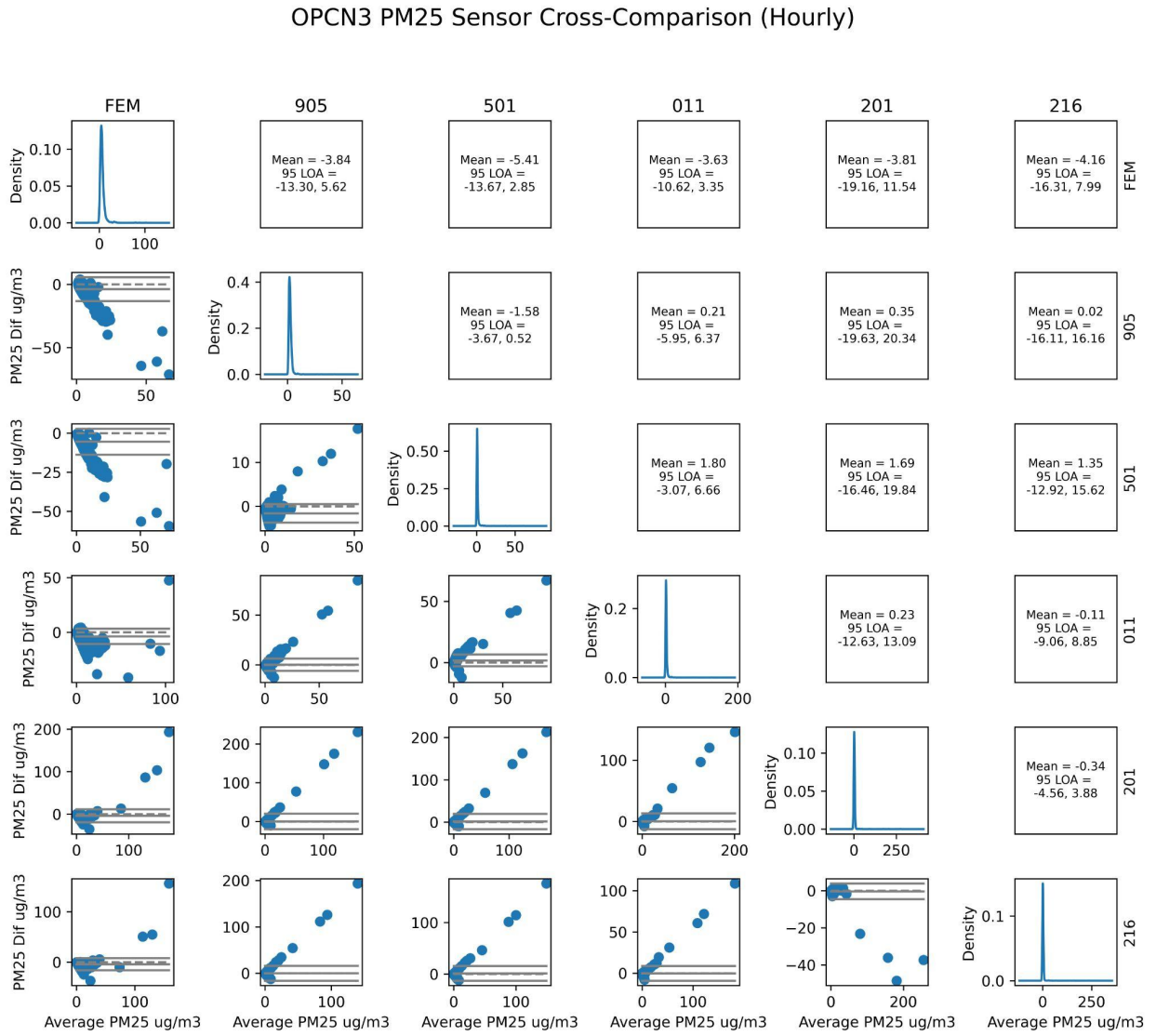


Figure S45: Spring 2025 (March 2025 to May 2025) Bland-Altman plots for comparisons of hourly FEM and raw hourly averaged OPC-N3 $PM_{2.5}$ measurements. The y-axis shows the difference between comparison measurements (column sensor minus row sensor), and the x-axis shows the average. Measurements with RH > 80% dropped. The dotted gray line represents the x-axis (y = 0). The central solid gray line represents the mean difference (bias), and the outer solid gray lines represent the 95% limits of agreement (LOA).

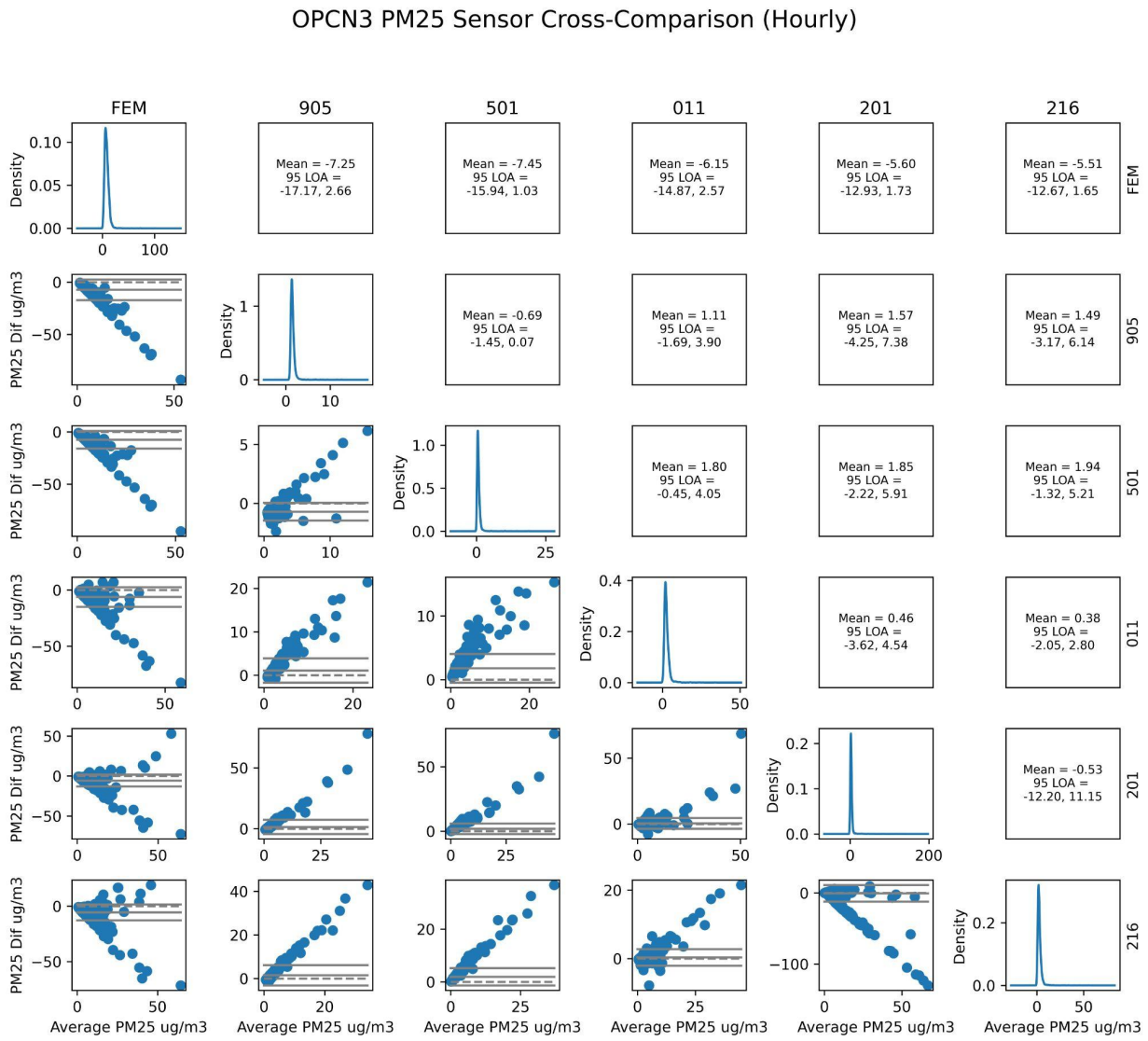


Figure S46: Summer 2025 (June 2025 to October 2025) Bland-Altman plots for comparisons of hourly FEM and raw hourly averaged OPC-N3 $PM_{2.5}$ measurements. The y-axis shows the difference between comparison measurements (column sensor minus row sensor), and the x-axis shows the average. Measurements with RH > 80% dropped. The dotted gray line represents the x-axis (y = 0). The central solid gray line represents the mean difference (bias), and the outer solid gray lines represent the 95% limits of agreement (LOA).

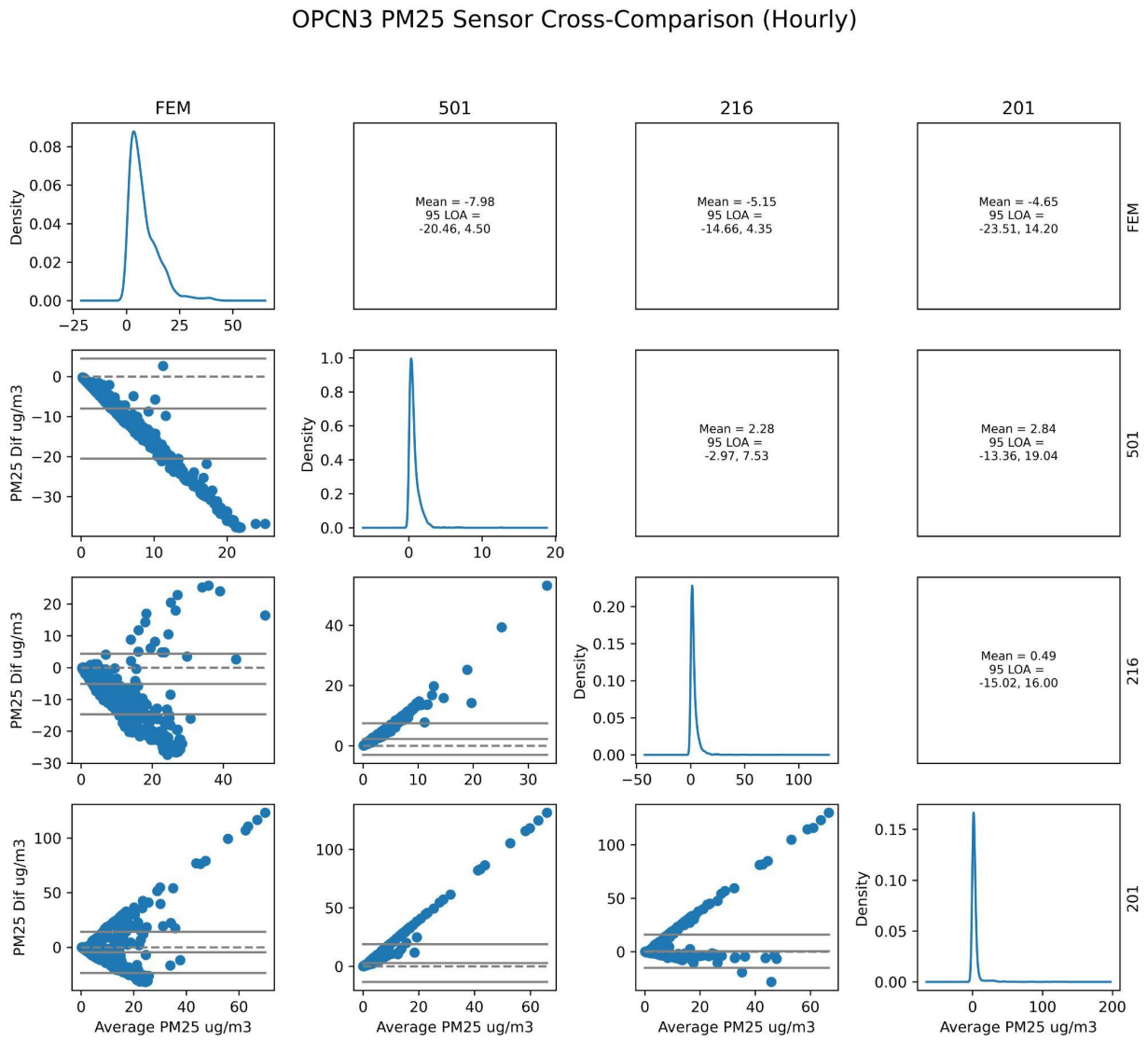


Figure S47: Winter 2025 (November 2025 to February 2026) Bland-Altman plots for comparisons of hourly FEM and raw hourly averaged OPC-N3 $PM_{2.5}$ measurements. The y-axis shows the difference between comparison measurements (column sensor minus row sensor), and the x-axis shows the average. Measurements with RH > 80% dropped. The dotted gray line represents the x-axis (y = 0). The central solid gray line represents the mean difference (bias), and the outer solid gray lines represent the 95% limits of agreement (LOA).

Seasonal PMS5003T $PM_{2.5}$ Bland-Altman plots

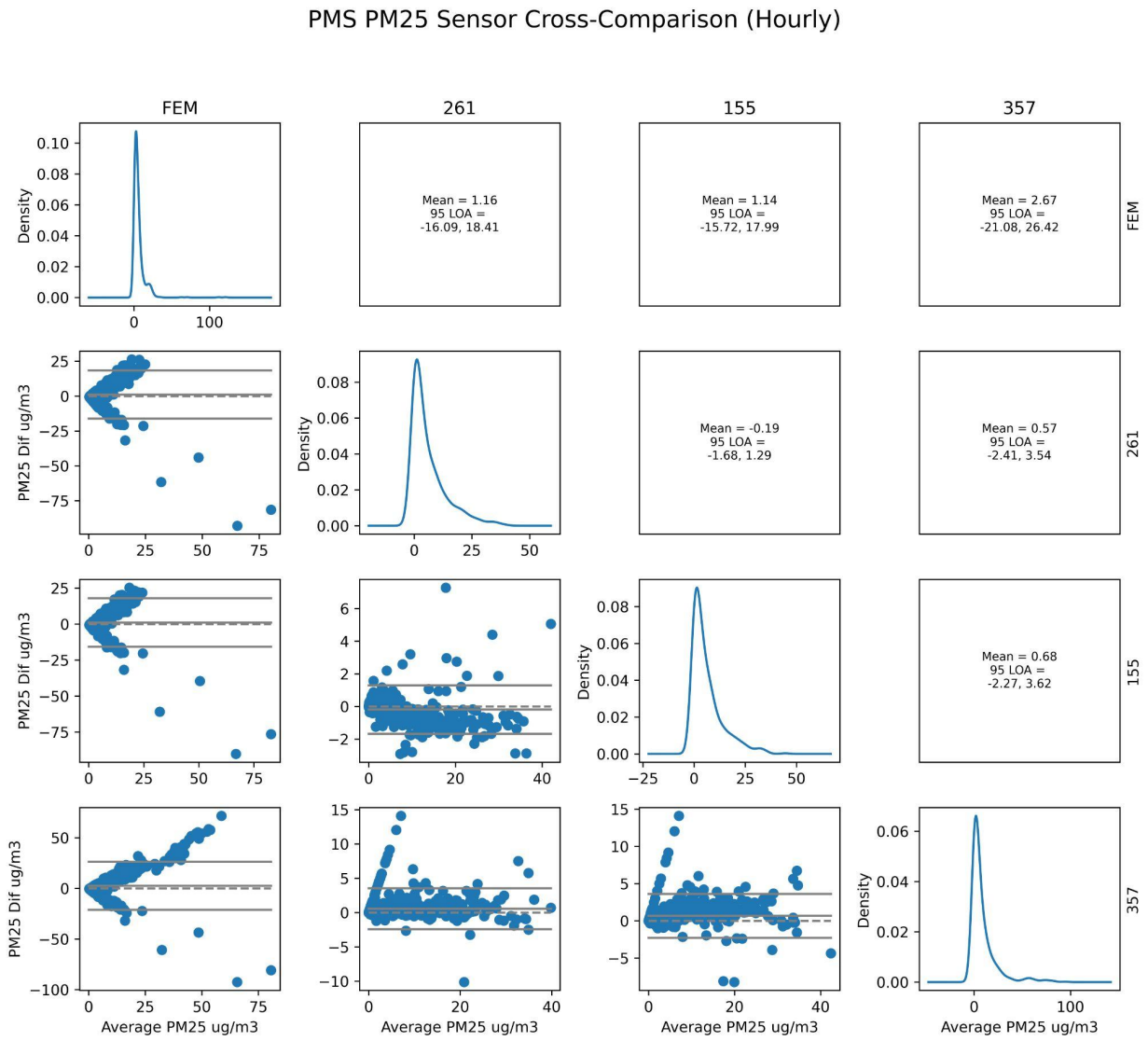


Figure S48: Winter 2023 (January to February 2024) Bland-Altman plots for comparisons of hourly FEM and raw hourly averaged PMS5003T $PM_{2.5}$ measurements. The y-axis shows the difference between comparison measurements (column sensor minus row sensor), and the x-axis shows the average. The dotted gray line represents the x-axis (y = 0). The central solid gray line represents the mean difference (bias), and the outer solid gray lines represent the 95% limits of agreement (LOA).

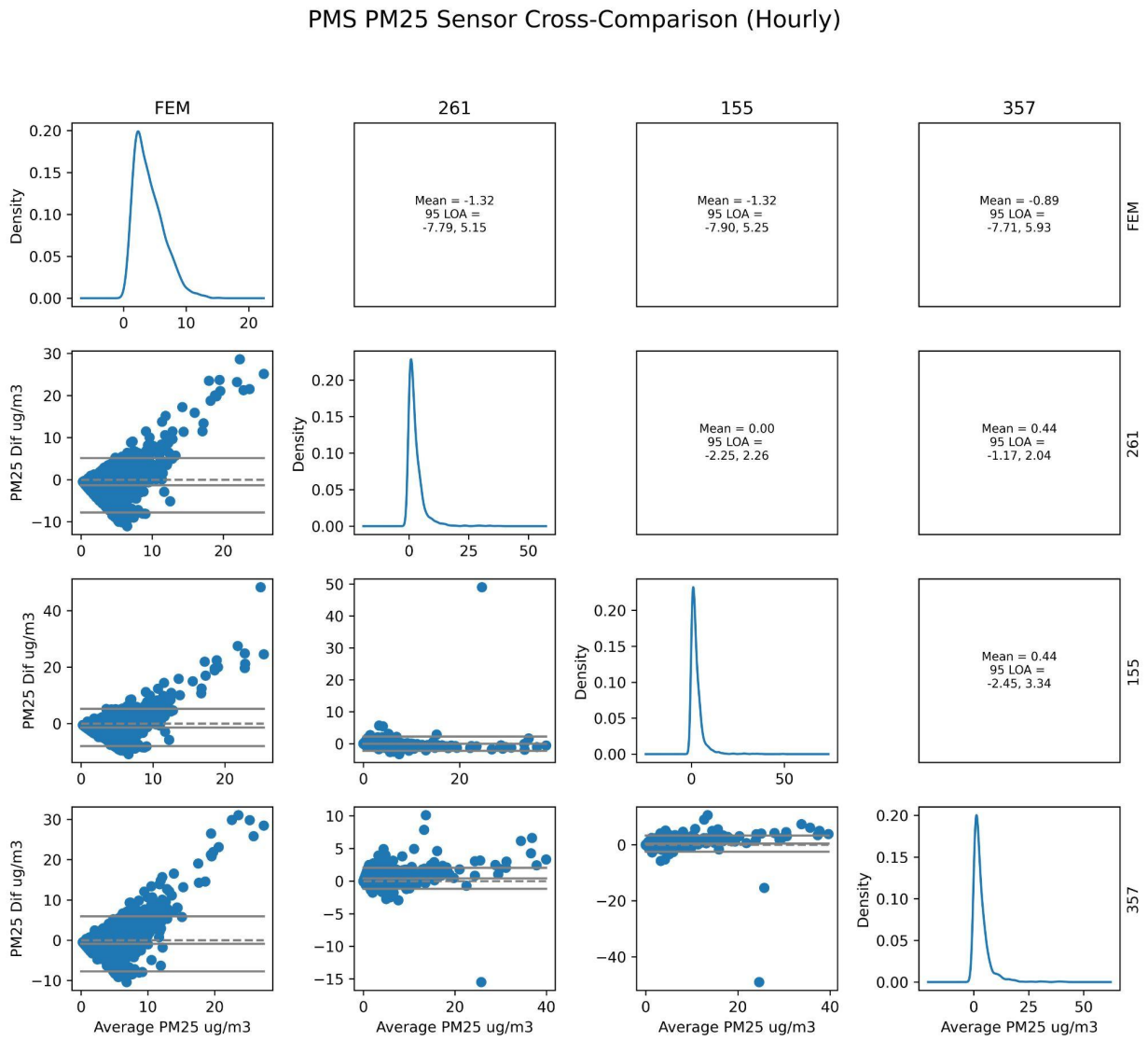


Figure S49: Spring 2024 (March 2024 to May 2024) Bland-Altman plots for comparisons of hourly FEM and raw hourly averaged PMS5003T $PM_{2.5}$ measurements. The y-axis shows the difference between comparison measurements (column sensor minus row sensor), and the x-axis shows the average. The dotted gray line represents the x-axis (y = 0). The central solid gray line represents the mean difference (bias), and the outer solid gray lines represent the 95% limits of agreement (LOA).

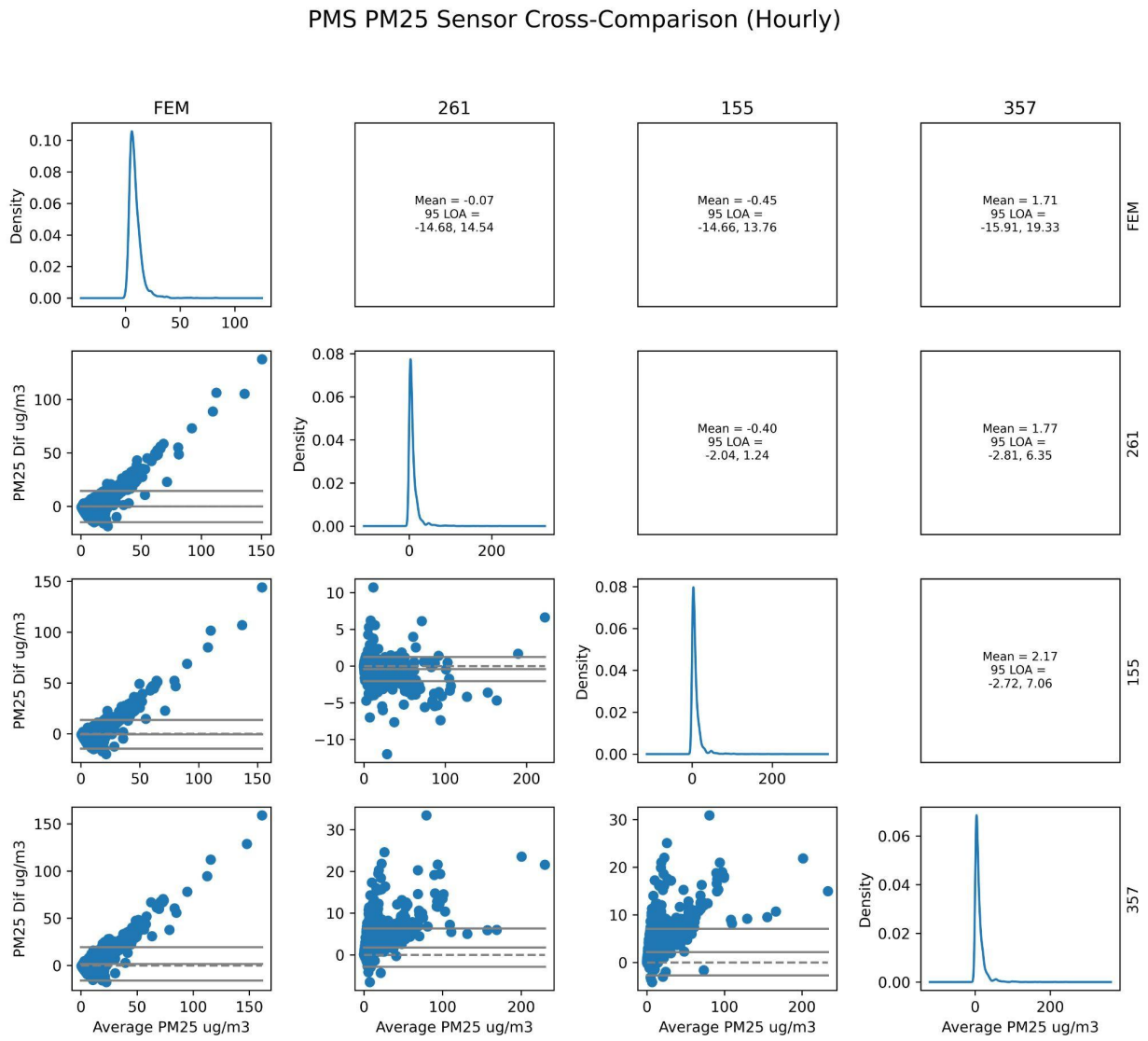


Figure S50: Summer 2024 (June 2024 to October 2024) Bland-Altman plots for comparisons of hourly FEM and raw hourly averaged PMS5003T $PM_{2.5}$ measurements. The y-axis shows the difference between comparison measurements (column sensor minus row sensor), and the x-axis shows the average. The dotted gray line represents the x-axis (y = 0). The central solid gray line represents the mean difference (bias), and the outer solid gray lines represent the 95% limits of agreement (LOA).

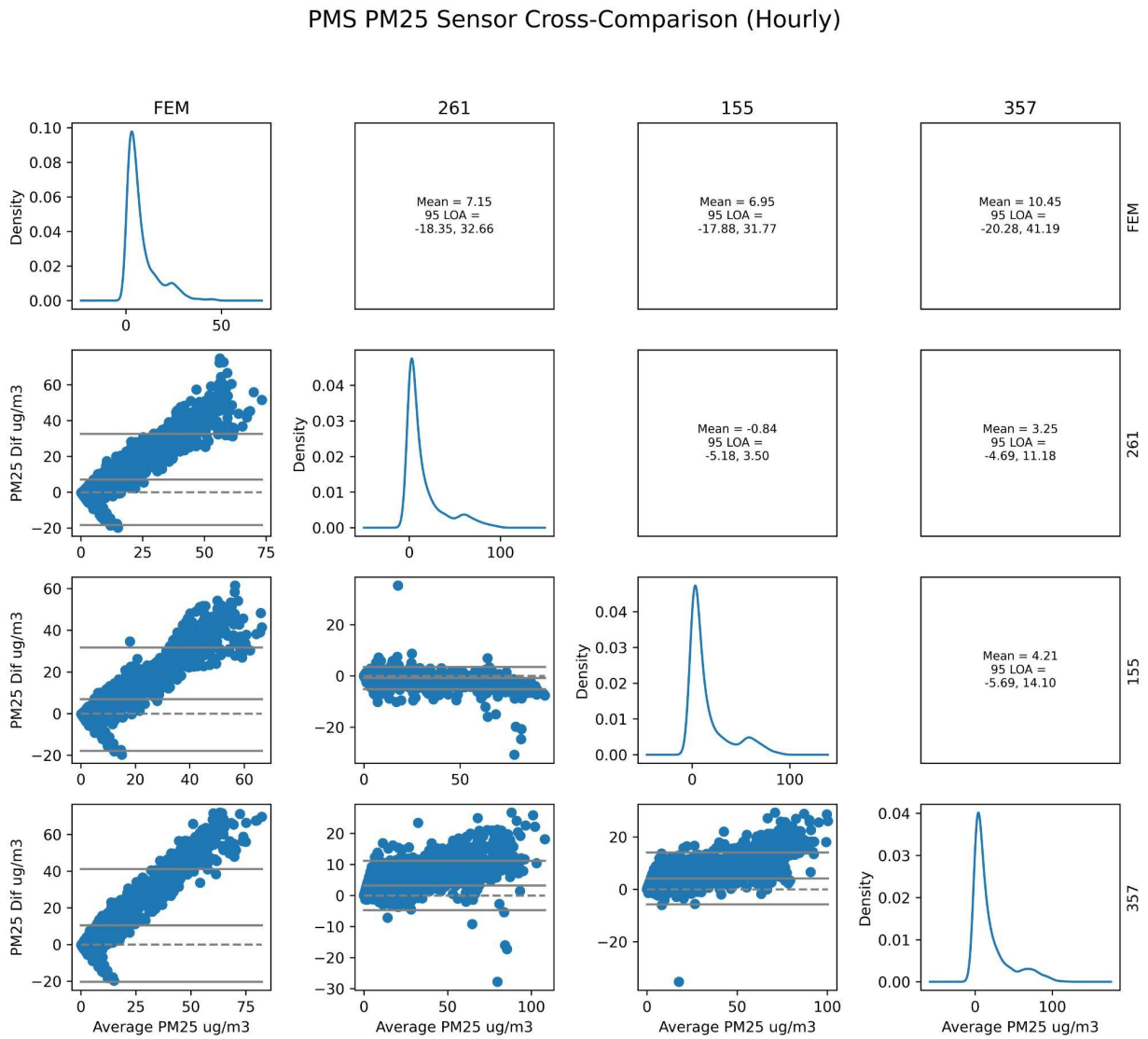


Figure S51: Winter 2024 (November 2024 to February 2025) Bland-Altman plots for comparisons of hourly FEM and raw hourly averaged PMS5003T $PM_{2.5}$ measurements. The y-axis shows the difference between comparison measurements (column sensor minus row sensor), and the x-axis shows the average. The dotted gray line represents the x-axis (y = 0). The central solid gray line represents the mean difference (bias), and the outer solid gray lines represent the 95% limits of agreement (LOA).

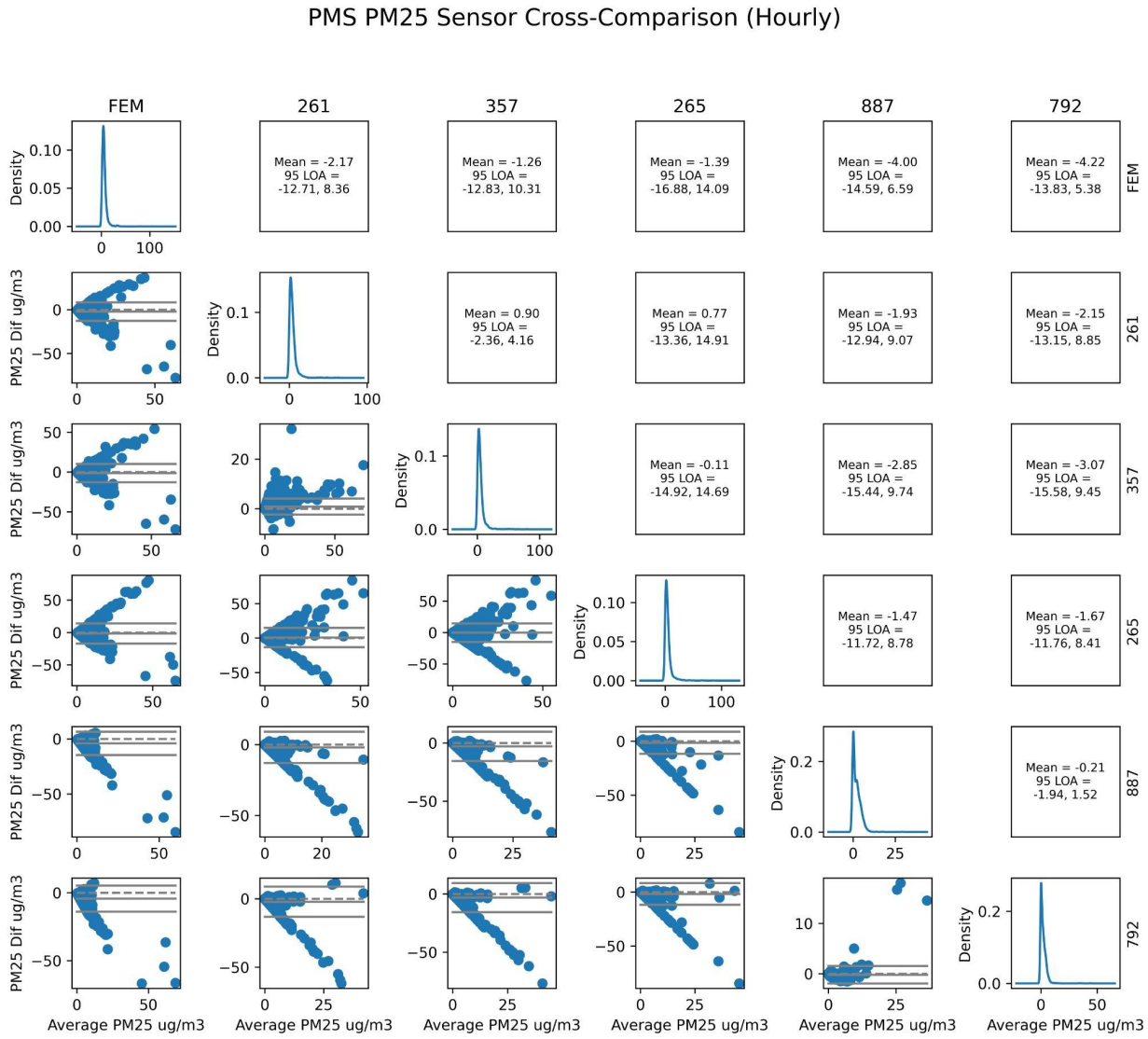


Figure S52: Spring 2025 (March 2025 to May 2025) Bland-Altman plots for comparisons of hourly FEM and raw hourly averaged PMS5003T $PM_{2.5}$ measurements. The y-axis shows the difference between comparison measurements (column sensor minus row sensor), and the x-axis shows the average. The dotted gray line represents the x-axis (y = 0). The central solid gray line represents the mean difference (bias), and the outer solid gray lines represent the 95% limits of agreement (LOA).

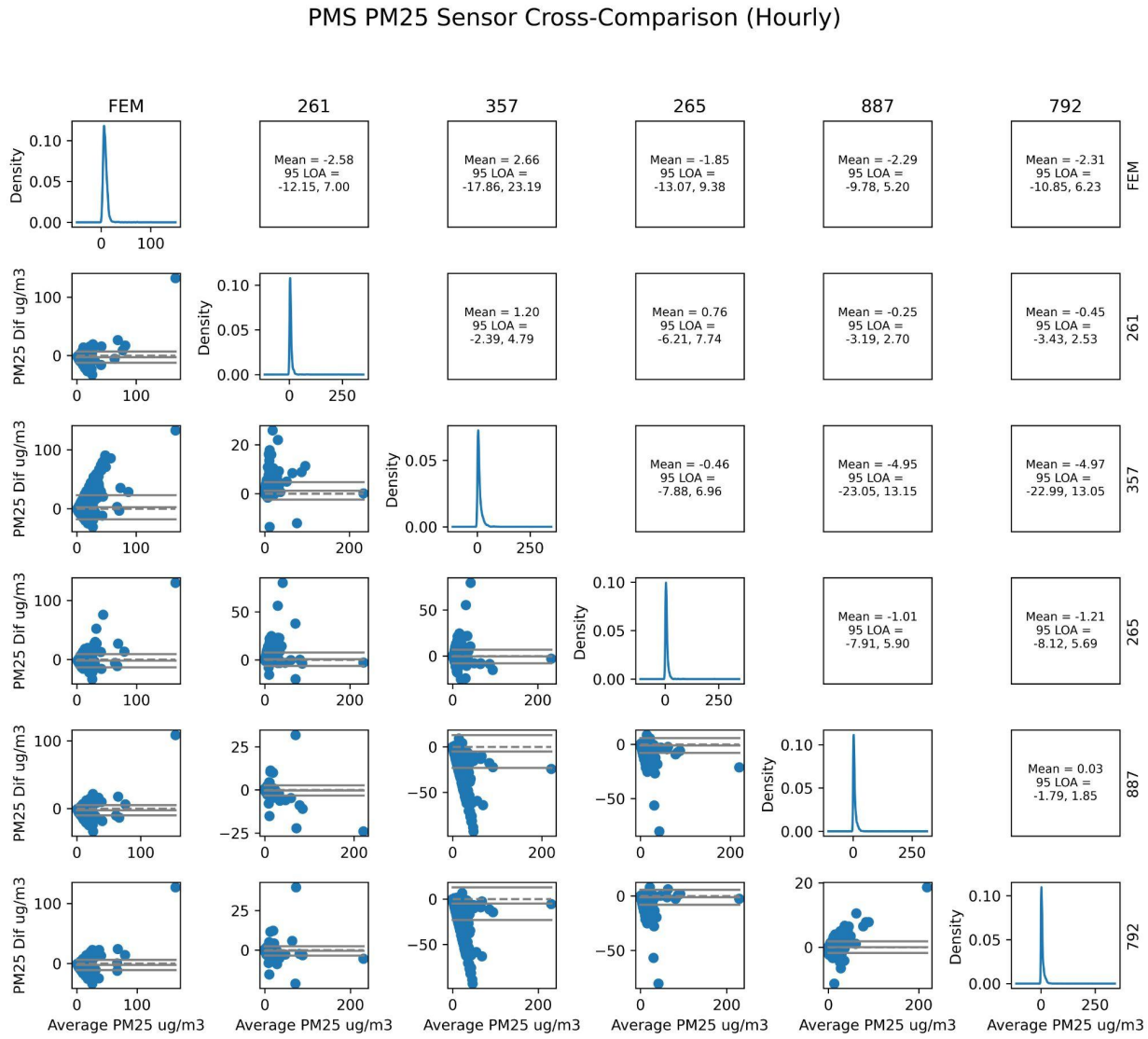


Figure S53: Summer 2025 (June 2025 to October 2025) Bland-Altman plots for comparisons of hourly FEM and raw hourly averaged PMS5003T $PM_{2.5}$ measurements. The y-axis shows the difference between comparison measurements (column sensor minus row sensor), and the x-axis shows the average. The dotted gray line represents the x-axis (y = 0). The central solid gray line represents the mean difference (bias), and the outer solid gray lines represent the 95% limits of agreement (LOA).

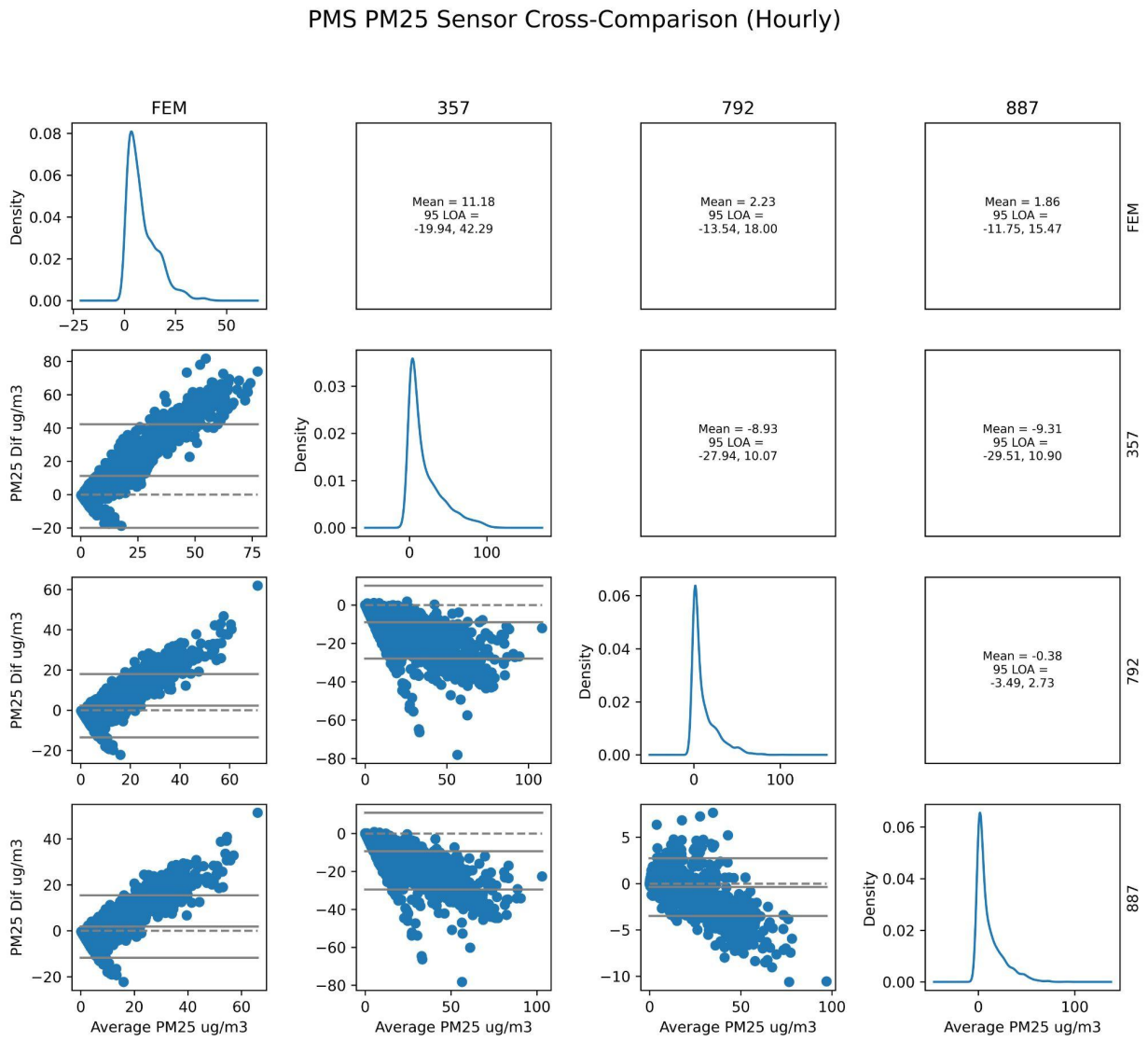


Figure S54: Winter 2025 (November 2025 to February 2026) Bland-Altman plots for comparisons of hourly FEM and raw hourly averaged PMS5003T $PM_{2.5}$ measurements. The y-axis shows the difference between comparison measurements (column sensor minus row sensor), and the x-axis shows the average. The dotted gray line represents the x-axis (y = 0). The central solid gray line represents the mean difference (bias), and the outer solid gray lines represent the 95% limits of agreement (LOA).

OPC-N3 size selectivity after mirror replacement: Monodisperse particle generator results

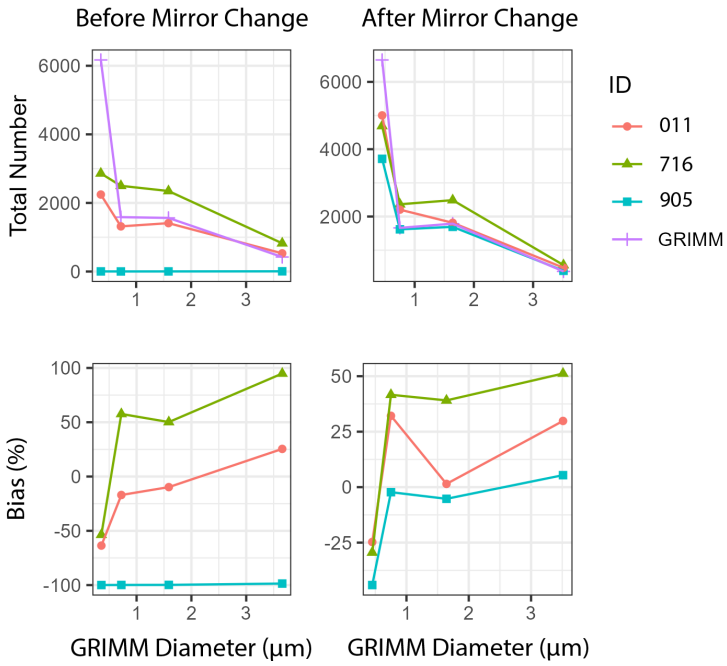


Figure S55: Total number and bias comparison between the OPC-N3 sensors and the GRIMM before (left column) and after (right column) replacing the mirror in the OPC-N3 sensors.

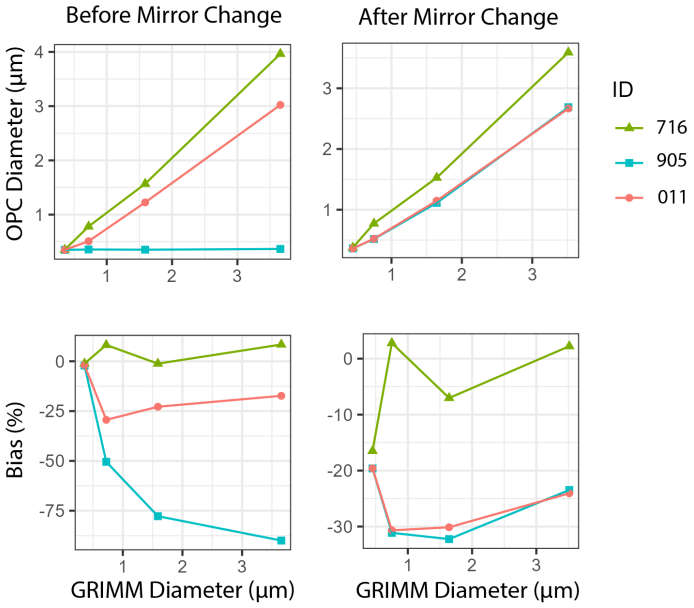


Figure S56: OPC-N3 versus GRIMM diameter and bias comparison for the OPC-N3 sensors before (left column) and after (right column) replacing the mirror.

Autocorrelation plots for OPC-N3 $PM_{2.5}$-to-PMS5003T $PM_{2.5}$ ratio



Figure S57: Autocorrelation functions (ACFs) for hourly and daily averaged OPC-N3 $PM_{2.5}$-to-PMS5003T $PM_{2.5}$ ratios for AirU Pro Unit 1 across each season.

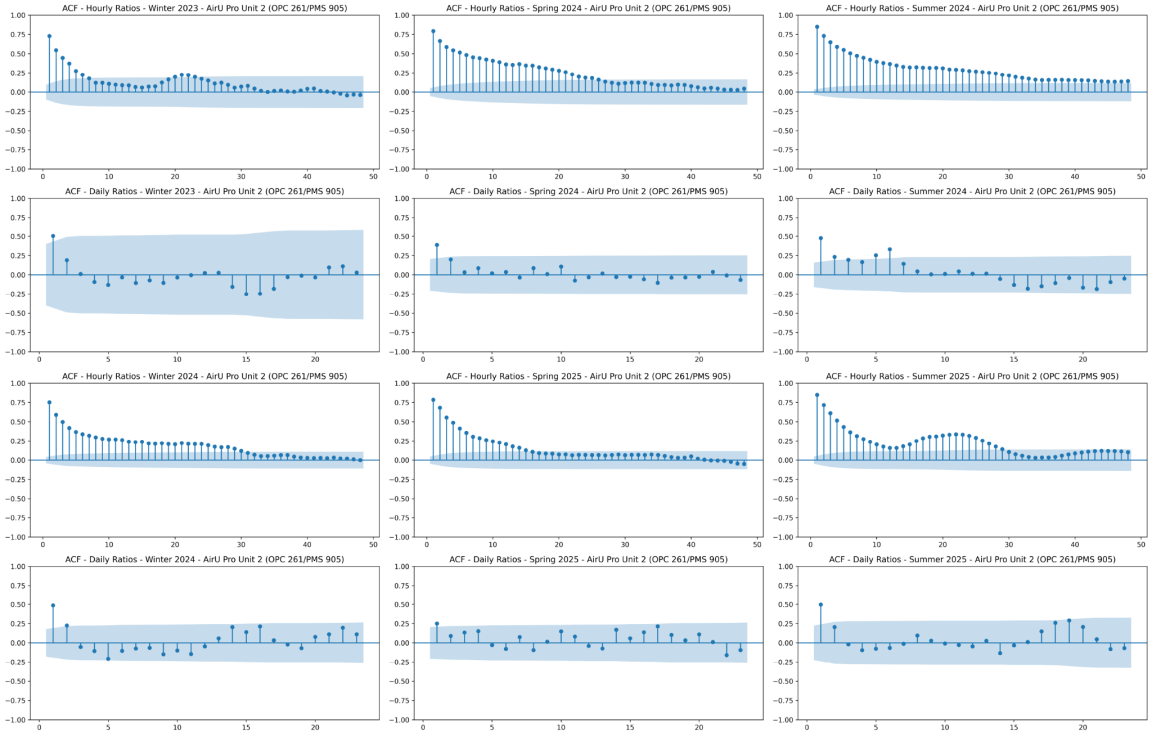


Figure S58: Autocorrelation functions (ACFs) for hourly and daily averaged OPC-N3 $PM_{2.5}$-to-PMS5003T $PM_{2.5}$ ratios for AirU Pro Unit 2 across each season.

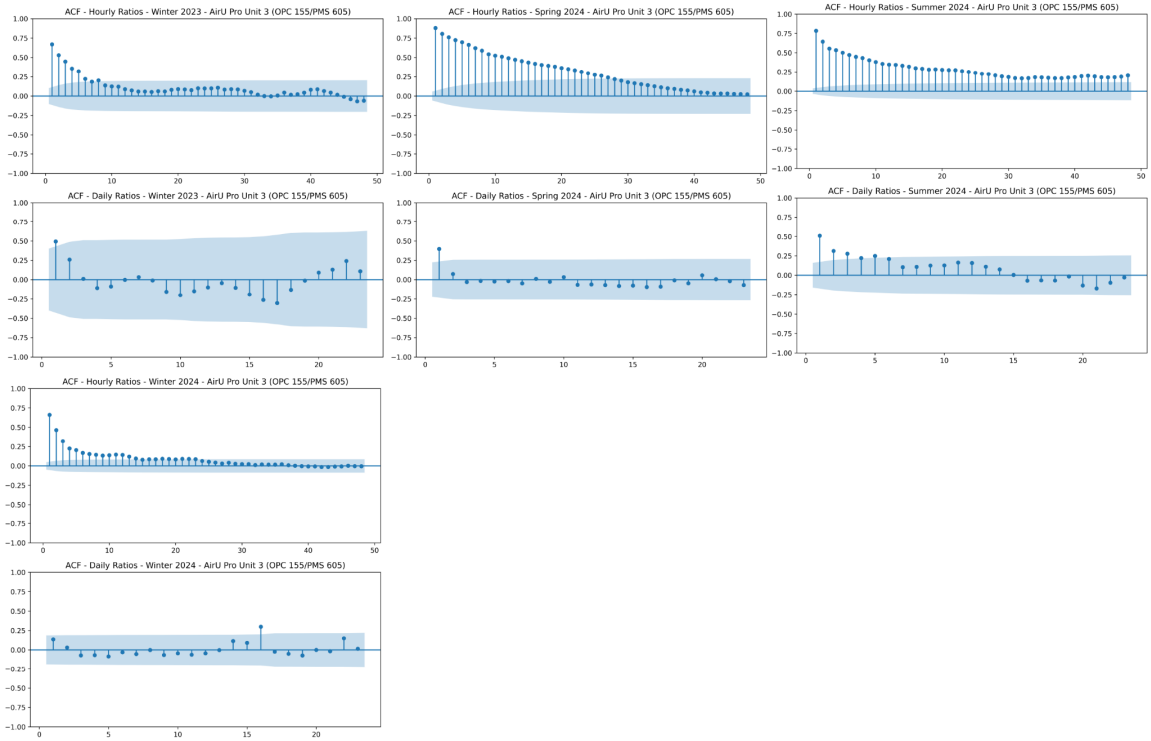


Figure S59: Autocorrelation functions (ACFs) for hourly and daily averaged OPC-N3 $PM_{2.5}$-to-PMS5003T $PM_{2.5}$ ratios for AirU Pro Unit 3 across each season.

S.2: Additional tables

Methods tables

Table S1: FMAG conditions used to generate monodisperse particles.

DOS Conc in IPA (V/V)	Frequency (kHz)	ΔP (psi)	Injection Flow rate Q (mL/hr)	Dilution flow at FMAG (LPM)	Additional dilution (LPM)	Suction removal (LPM)	Diameter from GRIMM (μm)
1.00E-06	150	1.7	2.2	15	14	0	0.357
1.00E-05	70	1	3	15	14	0	0.722
1.00E-04	80	0.9	6	15	14	0	1.59
1.00E-03	70	1	6.5	15	16	8	3.66

Correction model summary tables

Table S2: Utah Division of Air Quality (DAQ) Utah Technical Center (UTTC) hourly $PM_{2.5}$, PM_{10}, temperature (T), relative humidity (RH), and $PM_{2.5}/PM_{10}$ ratio descriptive statistics for each season.

UTTC DAQ Station	PM2.5 (ug/m3)[a]									PM10 (ug/m3)[a]								
Seasonal Stats	Mean	SD	Median	Min	Q05	Q25	Q75	Q95	Max	Mean	SD	Median	Min	Q05	Q25	Q75	Q95	Max
2023 Winter (Nov 2023 - Feb 2024)	6.08	8.49	3.6	0.4	0.8	1.80	6.98	20.3	121	21.35	31.76	13	0	2	6	24	58	369
2024 Spring (Mar 2024 - May 2024)	4.37	2.45	3.9	0.5	1.3	2.5	5.8	9	17	15.91	14.82	12	0	2	7	20	41	224
2024 Summer (Jun 2024 - Oct 2024)	9.00	6.09	7.6	0.7	3.0	5.28	11.1	19.1	83.4	28.29	19.23	24	0	8	17	34	59.8	222
2024 Winter (Nov 2024 - Feb 2025)	8.14	8.09	5.1	0.2	0.98	2.7	10.5	25.9	47.5	24.78	24.23	18	0	2	9	34.3	64	256
2025 Spring (Mar 2025 - May 2025)	6.08	5.68	5.1	0.5	1.4	3.2	7.3	13.2	102.2	24.84	41.77	16	0	3	8	29	64.5	789
2025 Summer (Jun 2025 - Oct 2025)	8.06	4.66	7.4	0.7	2.9	5.3	10	14.6	100.2	27.29	23.11	23	0	6	15	34	60	419
2025 Winter (Nov 2025 - Feb 2026)	9.04	7.46	6.8	0.3	1.0	3.3	13.2	23.7	43.6	27.81	29.72	21	0	3	12	36	64	437
UTTC DAQ Station	T (C)[b]									RH (%)[b]								
Seasonal Stats	Mean	SD	Median	Min	Q05	Q25	Q75	Q95	Max	Mean	SD	Median	Min	Q05	Q25	Q75	Q95	Max
2023 Winter (Nov 2023 - Feb 2024)	3.13	4.63	2.73	-9.57	-3.9	0.1	5.9	11.6	16.6	66.8	20.1	69	17	30	52	85	94	97
2024 Spring (Mar 2024 - May 2024)	11.5	6.78	11.0	-3.53	1.4	6.7	16.1	23.7	31.4	44.8	21.3	41	7	17	28	58	87	97
2024 Summer (Jun 2024 - Oct 2024)	23.9	7.52	24.6	2.16	10	19.2	29.3	35.3	40.4	30.4	16.2	27	5	10	18	39	63	93
2024 Winter (Nov 2024 - Feb 2025)	2.64	4.98	2.13	-9.83	-4.6	-0.8	5.4	12.3	20.1	61.5	20.0	63	8	28	46	76	94	99
2025 Spring (Mar 2025 - May 2025)	13.0	7.32	12.4	-3.49	1.7	7.6	17.9	26.5	31.3	41.9	21.7	37	5	13	25	54.5	85	100
2025 Summer (Jun 2025 - Oct 2025)	22.6	7.56	23.7	-0.47	8.1	18.3	28.2	33.2	38.8	34.6	19.5	31	3	11	20	45	74	100
2025 Winter (Nov 2025 - Feb 2026)	5.73	5.57	5.46	-16.9	-2.7	1.5	9.5	15.5	21.8	62.3	18.1	62	16	31	49	76	92	100
UTTC DAQ Station	PM2.5/PM10 Ratio[a]																	
Seasonal Stats	Mean	SD	Median	Min	Max	count < 0.4	count > 1	count > 1 flagged										
2023 Winter (Nov 2023 - Feb 2024)	0.379	0.343	0.304	0.046	3.40	499	28	24										
2024 Spring (Mar 2024 - May 2024)	0.388	0.286	0.320	0.035	3.40	1396	64	56										
2024 Summer (Jun 2024 - Oct 2024)	0.352	0.156	0.330	0.039	2.07	2472	14	6										
2024 Winter (Nov 2024 - Feb 2025)	0.398	0.284	0.350	0.031	4.00	1511	64	49										
2025 Spring (Mar 2025 - May 2025)	0.370	0.275	0.318	0.039	4.00	1398												
2025 Summer (Jun 2025 - Oct 2025)	0.370	0.271	0.322	0.021	4.60	2437												
2025 Winter (Nov 2025 - Feb 2026)	0.379	0.262	0.354	0.003	5.10	1590												

[a]PM data from AirNow.

[b]T and RH data from MesoWest.

Table S3: Colocated PMS5003T RH seasonal regression correction model, Eq. (3), results after outliers are removed.

UTTC Colocation	PMS5003T RH Regression								
Season	# Hours in Season	# Hourly Measurements	# after outliers removed (% removed)	# Sensors	b0	b1	R2	RMSE	NRMSE
2023 Winter (Nov 2023 - Feb 2024)[a]	1512	6991	6715 (4%)	10	3.63	1.15	0.880	7.63	0.129
2024 Spring (Mar 2024 - May 2024)	2184	20738	19960 (4%)	10	-2.76	1.22	0.928	5.69	0.128
2024 Summer (Jun 2024 - Oct 2024)	3696	21420	20806 (3%)	10	-3.38	1.15	0.899	4.54	0.164
2024 Winter (Nov 2024 - Feb 2025)	2856	7513	7311 (3%)	3	0.08	1.22	0.883	6.81	0.111
2025 Spring (Mar 2025 - May 2025)	2184	7882	7639 (3%)	5	-3.62	1.23	0.919	5.94	0.149
2025 Summer (Jun 2025 - Oct 2025)	3696	18305	17573 (4%)	7	-2.48	1.23	0.891	6.20	0.185
2025 Winter (Nov 2025 - Feb 2026)	2856	14261	14015 (2%)	5	11.0	1.10	0.727	9.35	0.151

[a]Sensors deployed February 2024

Table S4: Colocated PMS5003T $PM_{2.5}$ seasonal regression correction model, Eq. (4), results after outliers are removed. Abbreviations: number of measurements before outliers are removed (N), number of measurements after outliers are removed (Nout), root mean square error (RMSE), and normalized RMSE (NRMSE).

Regression	2023 Winter (Nov 2023 - Feb 2024)[a] # Hours in Season: 2952							2024 Spring (Mar 2024 - May 2024) # Hours in Season: 2184							2024 Summer (Jun 2024 - Oct 2024) # Hours in Season: 3696						
PMS5003T PM2.5	N	Nout (% removed)	b0	b1	R2	RMSE	NRMSE	N	Nout (% removed)	b0	b1	R2	RMSE	NRMSE	N	Nout (% removed)	b0	b1	R2	RMSE	NRMSE
261	652	582 (11%)	1.805	0.329	0.772	1.24	0.335	2175	2119 (3%)	3.264	0.354	0.304	1.85	0.441	3678	3564 (3%)	4.844	0.437	0.838	2.13	0.248
155	616	543 (12%)	1.737	0.356	0.76	1.24	0.337	2154	2105 (2%)	3.284	0.347	0.291	1.88	0.447	3644	3537 (3%)	4.957	0.445	0.843	2.13	0.247
357	820	731 (11%)	1.819	0.299	0.876	1.50	0.340	2127	2066 (3%)	3.096	0.346	0.323	1.81	0.434	3669	3547 (3%)	4.674	0.382	0.818	2.24	0.261
265																					
887																					
792																					
Regression	2024 Winter (Nov 2024 - Feb 2025) # Hours in Season: 2856							2025 Spring (Mar 2025 - May 2025) # Hours in Season: 2184							2025 Summer (Jun 2025 - Oct 2025) # Hours in Season: 3696						
PMS5003T PM2.5	N	Nout (% removed)	b0	b1	R2	RMSE	NRMSE	N	Nout (% removed)	b0	b1	R2	RMSE	NRMSE	N	Nout (% removed)	b0	b1	R2	RMSE	NRMSE
261	2641	2466 (7%)	2.138	0.372	0.928	1.92	0.267	2171	2014 (7%)	3.396	0.498	0.381	2.10	0.411	1842	1794 (3%)	5.112	0.545	0.638	2.05	0.247
155	2178	2002 (8%)	2.126	0.391	0.942	1.81	0.243														
357	2698	2532 (6%)	1.804	0.325	0.929	1.93	0.263	2173	2021 (7%)	3.521	0.372	0.306	2.24	0.438	3681	3561 (3%)	6.118	0.169	0.227	2.96	0.380
265								1991	1880 (6%)	4.898	0.088	0.032	2.66	0.501	1848	1774 (4%)	5.185	0.495	0.559	2.17	0.263
887								776	729 (6%)	2.52	1.093	0.502	1.96	0.337	3691	3574 (3%)	4.491	0.577	0.702	1.90	0.247
792								774	726 (6%)	2.077	1.446	0.701	2.14	0.364	3689	3580 (3%)	4.844	0.519	0.667	2.01	0.261
Regression	2025 Winter (Nov 2025 - Feb 2026) # Hours in Season: 2856																				
PMS5003T PM2.5	N	Nout (% removed)	b0	b1	R2	RMSE	NRMSE														
261																					
155																					
357	2836	2748 (3%)	2.826	0.303	0.871	2.55	0.291														
265																					
887	2840	2771 (2%)	3.159	0.531	0.906	2.22	0.253														
792	2840	2777 (2%)	3.456	0.485	0.894	2.37	0.269														

[a]Sensors deployed February 2024

Table S5: Colocated OPC-N3 PM_{10} seasonal multiple linear regression correction model, Eq. (5), results after outliers are removed. Abbreviations: number of measurements before outliers are removed (N), number of measurements after outliers are removed (Nout), root mean square error (RMSE), and normalized RMSE (NRMSE).

Regression	2023 Winter (Nov 2023 - Feb 2024)[a] # Hours in Season: 2952								2024 Spring (Mar 2024 - May 2024) # Hours in Season: 2184								2024 Summer (Jun 2024 - Oct 2024) # Hours in Season: 3696							
OPC-N3 PM10	N	Nout (% removed)	b0	b1	bRH	R2	RMSE	NRMSE	N	Nout (% removed)	b0	b1	bRH	R2	RMSE	NRMSE	N	Nout (% removed)	b0	b1	bRH	R2	RMSE	NRMSE
905	628	599 (5%)	20.8	1.44	-0.395	0.809	8.61	0.527	2104	2006 (5%)	13.2	1.27	-0.237	0.65	5.84	0.418	3656	3418 (7%)	10.4	2.26	-0.195	0.76	6.70	0.260
605	592	565 (5%)	23.6	1.33	-0.352	0.821	8.69	0.521	1750	1666 (5%)	14.0	1.47	-0.224	0.77	4.88	0.357	3620	3463 (4%)	16.1	2.06	-0.274	0.75	7.03	0.269
501	795	761 (4%)	28.9	1.37	-0.416	0.826	8.08	0.447	1732	1637 (5%)	12.6	1.37	-0.195	0.76	4.81	0.362	3647	3470 (5%)	14.3	1.96	-0.198	0.71	7.48	0.288
011																								
201																								
216																								
Regression	2024 Winter (Nov 2024 - Feb 2025) # Hours in Season: 2856								2025 Spring (Mar 2025 - May 2025) # Hours in Season: 2184								2025 Summer (Jun 2025 - Oct 2025) # Hours in Season: 3696							
OPC-N3 PM10	N	Nout (% removed)	b0	b1	bRH	R2	RMSE	NRMSE	N	Nout (% removed)	b0	b1	bRH	R2	RMSE	NRMSE	N	Nout (% removed)	b0	b1	bRH	R2	RMSE	NRMSE
905	2587	2482 (4%)	33.2	0.0024	-0.199	0.054	15.8	0.746	2077	1966 (5%)	21.6	5.55	-0.522	0.53	11.4	0.558	1836	1752 (5%)	-0.65	13.6	-0.213	0.79	8.21	0.287
605	2125	2042 (4%)	34.3	0.0035	-0.220	0.062	15.8	0.743																
501	2644	2536 (4%)	32.0	0.0015	-0.163	0.026	17.0	0.767	2081	1994 (4%)	24.3	4.85	-0.336	0.83	9.66	0.467	3664	3509 (4%)	13.9	7.74	-0.124	0.69	8.31	0.336
011									1897	1833 (3%)	18.2	2.55	-0.341	0.81	8.26	0.393	1842	1718 (7%)	9.38	2.50	-0.129	0.78	7.74	0.274
201									773	736 (5%)	19.1	0.871	-0.236	0.93	8.59	0.451	3674	3505 (5%)	30.4	0.070	-0.204	0.12	12.4	0.515
216									771	732 (5%)	16.3	1.33	-0.225	0.65	8.17	0.454	3672	3515 (4%)	13.8	1.81	-0.159	0.82	7.72	0.309
Regression	2025 Winter (Nov 2025 - Feb 2026) # Hours in Season: 2856																							
OPC-N3 PM10	N	Nout (% removed)	b0	b1	bRH	R2	RMSE	NRMSE																
905																								
605																								
501	2572	2509 (2%)	33.9	-0.0037	-0.133	0.021	16.4	0.652																
011																								
201	2843	2757 (3%)	30.9	-0.0016	-0.102	0.012	16.4	0.672																
216	2843	2751 (3%)	32.4	0.0305	-0.135	0.023	16.3	0.669																

[a]Sensors deployed February 2024

Table S6: Colocated OPC-N3 PM_{10} seasonal multiple linear regression correction mode, Eq. (5), results with RH > 80% dropped and after outliers are removed. Abbreviations: number of measurements before outliers are removed (N), number of measurements after outliers are removed (Nout), root mean square error (RMSE), and normalized RMSE (NRMSE).

Regression (>80% RH dropped)	2023 Winter (Nov 2023 - Feb 2024)[a] # Hours in Season: 2952								2024 Spring (Mar 2024 - May 2024) # Hours in Season: 2184								2024 Summer (Jun 2024 - Oct 2024) # Hours in Season: 3696							
OPC-N3 PM10	N	Nout (% removed)	b0	b1	bRH	R2	RMSE	NRMSE	N	Nout (% removed)	b0	b1	bRH	R2	RMSE	NRMSE	N	Nout (% removed)	b0	b1	bRH	R2	RMSE	NRMSE
905	505	472 (7%)	12.6	1.73	-0.27	0.891	5.43	0.324	1949	1843 (5%)	10.3	1.57	-0.23	0.73	5.35	0.362	3655	3417 (7%)	10.4	2.26	-0.20	0.76	6.71	0.260
605	471	442 (6%)	12.0	1.69	-0.16	0.955	5.05	0.282	1609	1517 (6%)	11.4	1.78	-0.21	0.83	4.44	0.306	3620	3463 (4%)	16.1	2.06	-0.27	0.75	7.03	0.269
501	603	566 (6%)	19.7	1.56	-0.27	0.926	6.03	0.302	1566	1450 (7%)	10.2	1.63	-0.18	0.81	4.26	0.302	3646	3469 (5%)	14.3	1.96	-0.20	0.71	7.49	0.288
011																								
201																								
216																								
Regression (>80% RH dropped)	2024 Winter (Nov 2024 - Feb 2025) # Hours in Season: 2856								2025 Spring (Mar 2025 - May 2025) # Hours in Season: 2184								2025 Summer (Jun 2025 - Oct 2025) # Hours in Season: 3696							
OPC-N3 PM10	N	Nout (% removed)	b0	b1	bRH	R2	RMSE	NRMSE	N	Nout (% removed)	b0	b1	bRH	R2	RMSE	NRMSE	N	Nout (% removed)	b0	b1	bRH	R2	RMSE	NRMSE
905	2088	2010 (4%)	20.1	2.51	-0.30	0.530	10.9	0.494	1947	1826 (6%)	14.7	8.07	-0.55	0.761	9.85	0.444	1837	1748 (5%)	-0.76	13.6	-0.21	0.79	8.19	0.287
605	1767	1691 (4%)	27.8	1.19	-0.28	0.505	11.8	0.528																
501	2189	2106 (4%)	24.0	3.14	-0.22	0.482	11.6	0.524	1957	1851 (5%)	16.4	7.29	-0.26	0.848	6.99	0.334	3546	3390 (4%)	12.9	7.82	-0.09	0.69	8.29	0.328
011									1836	1761 (4%)	15.9	2.68	-0.30	0.832	7.47	0.357	1843	1715 (7%)	9.48	2.51	-0.13	0.78	7.74	0.274
201									746	713 (4%)	19.4	0.87	-0.24	0.921	9.01	0.454	3551	3380 (5%)	29.2	0.07	-0.16	0.07	12.6	0.508
216									751	715 (5%)	16.2	1.35	-0.22	0.636	8.44	0.454	3555	3403 (4%)	13.2	1.82	-0.14	0.82	7.82	0.304
Regression (>80% RH dropped)	2025 Winter (Nov 2025 - Feb 2026) # Hours in Season: 2856																							
OPC-N3 PM10	N	Nout (% removed)	b0	b1	bRH	R2	RMSE	NRMSE																
905																								
605																								
501	1980	1904 (4%)	23.4	11.7	-0.28	0.777	7.97	0.315																
011																								
201	2235	2126 (5%)	33.5	0.16	-0.19	0.054	15.3	0.635																
216	2325	2223 (4%)	20.9	1.81	-0.19	0.799	8.72	0.353																

[a]Sensors deployed February 2024

Table S7: Colocated OPC-N3 PM_{10} seasonal κ-Köhler correction model, Eq. (6), results after outliers are removed. Abbreviations: number of measurements before outliers are removed (N), number of measurements after outliers are removed (Nout), root mean square error (RMSE), and normalized RMSE (NRMSE).

K-Kohler	2023 Winter (Nov 2023 - Feb 2024)[a] # Hours in Season: 2952							2024 Spring (Mar 2024 - May 2024) # Hours in Season: 2184							2024 Summer (Jun 2024 - Oct 2024) # Hours in Season: 3696						
OPC-N3 PM10	N	Nout (% removed)	b	K	R2	RMSE	NRMSE	N	Nout (% removed)	b	K	R2	RMSE	NRMSE	N	Nout (% removed)	b	K	R2	RMSE	NRMSE
905	628	591 (6%)	2.89	1.43	0.930	5.68	0.019	2104	1966 (7%)	2.67	1.38	0.77	5.10	0.034	3656	3416 (7%)	3.31	0.846	0.768	6.96	0.031
605	592	558 (6%)	2.55	0.850	0.908	6.85	0.019	1750	1621 (7%)	3.30	1.31	0.834	4.32	0.036	3620	3426 (5%)	4.68	2.54	0.768	7.33	0.033
501	795	728 (8%)	2.32	0.434	0.896	6.86	0.019	1732	1589 (8%)	2.63	0.785	0.84	4.32	0.033	3647	3438 (6%)	3.73	1.38	0.711	8.16	0.037
011																					
201																					
216																					
K-Kohler	2024 Winter (Nov 2024 - Feb 2025) # Hours in Season: 2856							2025 Spring (Mar 2025 - May 2025) # Hours in Season: 2184							2025 Summer (Jun 2025 - Oct 2025) # Hours in Season: 3696						
OPC-N3 PM10	N	Nout (% removed)	b	K	R2	RMSE	NRMSE	N	Nout (% removed)	b	K	R2	RMSE	NRMSE	N	Nout (% removed)	b	K	R2	RMSE	NRMSE
905	2587	2488 (4%)	6.90E+06	2.00E+07	-1.12	24.6	0.324	2077	1903 (8%)	14.2	3.39	0.77	8.87	0.039	1836	1737 (5%)	6.00	-1.035	-0.07	19.9	0.048
605	2125	2042 (4%)	2.72E+06	1.38E+07	-1.21	26.8	0.205														
501	2644	2549 (4%)	2.76E+06	1.21E+07	-1.41	26.4	0.347	2081	1913 (8%)	18.2	3.08	0.83	7.71	0.020	3664	3472 (5%)	12.7	0.295	0.667	9.05	0.049
011								1897	1787 (6%)	5.33	1.93	0.84	7.52	0.020	1842	1711 (7%)	2.69	-0.465	0.790	9.03	0.029
201								773	733 (5%)	2.89	1.35	0.85	7.71	0.020	3674	3479 (5%)	0.514	-0.108	-2.33	23.9	0.362
216								771	727 (6%)	3.32	1.25	0.750	7.34	0.037	3672	3460 (6%)	2.68	0.141	0.723	8.10	0.044
K-Kohler	2025 Winter (Nov 2025 - Feb 2026) # Hours in Season: 2856																				
OPC-N3 PM10	N	Nout (% removed)	b	K	R2	RMSE	NRMSE														
905																					
605																					
501	2572	2486 (3%)	84.4	9.49	-0.470	20.1	0.254														
011																					
201	2843	2708 (5%)	4.30	3.40	-1.13	24.5	0.215														
216	2843	2716 (4%)	3.94	1.13	0.219	15.9	0.050														

[a]Sensors deployed February 2024

Table S8: Colocated OPC-N3 PM_{10} seasonal κ-Köhler correction model, Eq. (6), results with RH > 80% dropped and after outliers are removed. Abbreviations: number of measurements before outliers are removed (N), number of measurements after outliers are removed (Nout), root mean square error (RMSE), and normalized RMSE (NRMSE).

K-Kohler (>80% RH dropped)	2023 Winter (Nov 2023 - Feb 2024)[a] # Hours in Season: 2952							2024 Spring (Mar 2024 - May 2024) # Hours in Season: 2184							2024 Summer (Jun 2024 - Oct 2024) # Hours in Season: 3696						
OPC-N3 PM10	N	Nout (% removed)	b	K	R2	RMSE	NRMSE	N	Nout (% removed)	b	K	R2	RMSE	NRMSE	N	Nout (% removed)	b	K	R2	RMSE	NRMSE
905	505	471 (7%)	2.54	0.925	0.920	5.58	0.019	1948	1825 (6%)	2.52	1.14	0.76	5.25	0.035	3654	3415 (7%)	3.31	0.849	0.768	6.96	0.031
605	471	431 (8%)	2.01	0.112	0.943	5.69	0.015	1608	1493 (7%)	3.04	0.998	0.840	4.39	0.034	3620	3426 (5%)	4.68	2.54	0.768	7.33	0.033
501	603	530 (12%)	2.11	0.134	0.905	6.05	0.016	1565	1440 (8%)	2.58	0.714	0.83	4.48	0.034	3646	3437 (6%)	3.73	1.38	0.711	8.16	0.037
011																					
201																					
216																					
K-Kohler (>80% RH dropped)	2024 Winter (Nov 2024 - Feb 2025) # Hours in Season: 2856							2025 Spring (Mar 2025 - May 2025) # Hours in Season: 2184							2025 Summer (Jun 2025 - Oct 2025) # Hours in Season: 3696						
OPC-N3 PM10	N	Nout (% removed)	b	K	R2	RMSE	NRMSE	N	Nout (% removed)	b	K	R2	RMSE	NRMSE	N	Nout (% removed)	b	K	R2	RMSE	NRMSE
905	2086	1998 (4%)	5.24	0.893	0.749	10.2	0.040	1943	1790 (8%)	14.4	3.63	0.76	9.15	0.04	1833	1723	12.0	0.102	0.788	8.88	0.021
605	1765	1692 (6%)	2.91	0.528	0.528	12.6	0.057														
501	2187	2099 (4%)	7.97	0.581	0.505	12.3	0.056	1956	1813 (7%)	17.5	2.65	0.83	7.69	0.020	3541	3360	12.5	0.239	0.653	9.22	0.050
011								1834	1709 (7%)	5.25	1.57	0.88	6.75	0.018	1839	1699	3.32	0.395	0.809	8.12	0.031
201								746	707 (5%)	2.90	1.35	0.85	7.87	0.020	3546	3355	0.560	-0.387	-2.32	23.6	0.358
216								750	688 (8%)	3.34	1.25	0.79	6.55	0.033	3550	3365	2.85	0.306	0.708	8.03	0.044
K-Kohler (>80% RH dropped)	2025 Winter (Nov 2025 - Feb 2026) # Hours in Season: 2856																				
OPC-N3 PM10	N	Nout (% removed)	b	K	R2	RMSE	NRMSE														
905																					
605																					
501	1978	1887 (5%)	23.0	0.499	0.773	8.24	0.059														
011																					
201	2232	2101 (6%)	2.55	0.562	-0.519	20.6	0.087														
216	2322	2213 (5%)	2.60	0.024	0.795	9.70	0.024														

[a]Sensors deployed February 2024

Cross-correlation summary tables

Table S9: Summary of seasonal scatter plot matrices for OPC-N3 $PM_{2.5}$ showing the average ± standard deviation of R^2 and slope for groups of new and old sensors. Figures S20-S26 show seasonal cross-correlation matrix results for each sensor.

OPC PM2.5 vs FEM PM2.5	Old OPC vs FEM		New OPC vs FEM			
Season	R2	Slope	R2	Slope		
Winter 2023	0.76 ± 0.08	1.64 ± 0.18				
Spring 2024	0.39 ± 0.18	0.39 ± 0.07				
Summer 2024	0.62 ± 0.03	0.24 ± 0.01				
Winter 2024	0.57 ± 0.02	0.31 ± 0.16				
Spring 2025	0.56 ± 0.16	0.25 ± 0.07	0.63 ± 0.01	0.99 ± 0.34		
Summer 2025	0.31 ± 0.01	0.08 ± 0.01	0.38 ± 0.03	0.30 ± 0.07		
Winter 2025	0.55	0.08	0.29 ± 0.32	0.32 ± 0.14		
OPC PM2.5 vs OPC PM2.5	Old OPC vs Old OPC		New OPC vs New OPC		New OPC vs Old OPC	
Season	R2	Slope	R2	Slope	R2	Slope
Winter 2023	0.99 ± 0.01	0.93 ± 0.09				
Spring 2024	0.63 ± 0.25	0.88 ± 0.05				
Summer 2024	0.84 ± 0.07	0.96 ± 0.05				
Winter 2024	0.89 ± 0.06	1.44 ± 0.90				
Spring 2025	0.76	0.70	0.96 ± 0.04	0.74 ± 0.45	0.77 ± 0.15	0.26 ± 0.12
Summer 2025	0.89	0.65	0.60 ± 0.38	0.66 ± 0.20	0.84 ± 0.08	0.27 ± 0.10
Winter 2025			0.18	0.28	0.46 ± 0.54	0.12 ± 0.12

Table S10: Summary of seasonal scatter plot matrices for PMS5003T $PM_{2.5}$ showing the average ± standard deviation of R^2 and slope for groups of new and old sensors. Figures S27-S33 show seasonal cross-correlation matrix results for each sensor.

PMS PM2.5 vs FEM PM2.5	Old PMS vs FEM		New PMS vs FEM			
Season	R2	Slope	R2	Slope		
Winter 2023	0.18 ± 0.05	0.50 ± 0.25				
Spring 2024	0.28 ± 0.02	0.88 ± 0.05				
Summer 2024	0.80 ± 0.01	1.92 ± 0.13				
Winter 2024	0.88 ± 0.01	2.41 ± 0.23				
Spring 2025	0.22 ± 0.02	0.42 ± 0.03	0.24 ± 0.20	0.24 ± 0.05		
Summer 2025	0.43 ± 0.31	1.18 ± 0.05	0.62 ± 0.06	1.18 ± 0.04		
Winter 2025	0.78	2.42	0.86 ± 0.01	1.64 ± 0.09		
PMS PM2.5 vs PMS PM2.5	Old PMS vs Old PMS		New PMS vs New PMS		New PMS vs Old PMS	
Season	R2	Slope	R2	Slope	R2	Slope
Winter 2023	0.97 ± 0.02	0.98 ± 0.05				
Spring 2024	0.91 ± 0.05	0.92 ± 0.05				
Summer 2024	0.99 ± 0.01	0.92 ± 0.09				
Winter 2024	0.98 ± 0.01	0.92 ± 0.12				
Spring 2025	0.92	0.82	0.41 ± 0.42	0.89 ± 0.06	0.08 ± 0.01	0.52 ± 0.25
Summer 2025	0.96	0.92	0.89 ± 0.09	1.01 ± 0.09	0.72 ± 0.27	1.00 ± 0.10
Winter 2025			0.99	1.09	0.87 ± 0.01	1.43 ± 0.08

Bland-Altman summary tables

Table S11: Summary of seasonal OPC-N3 $PM_{2.5}$ Bland-Altman comparisons showing the average ± standard deviation for results based on groupings of new and old sensors. Figures S41-S47 show seasonal Bland-Altman plots and results for each sensor. LOA - 95% limits of agreement. Bias and LOA units are $\mu g\ m^{-3}$.

OPC PM2.5 vs FEM PM2.5	Old OPC vs FEM				New OPC vs FEM			
Season	Bias	LOA Low	LOA High	LOA Span	Bias	LOA Low	LOA High	LOA Span
Winter 2023	-0.06 ± 1.69	-20.34 ± 3.88	20.21 ± 1.97	40.55 ± 5.15				
Spring 2024	-1.55 ± 1.21	-5.23 ± 0.58	2.14 ± 1.85	7.37 ± 1.28				
Summer 2024	-6.15 ± 0.57	-15.50 ± 0.72	3.20 ± 0.43	18.69 ± 0.29				
Winter 2024	-4.43 ± 1.71	-15.95 ± 2.38	7.08 ± 1.43	23.03 ± 1.94				
Spring 2025	-4.63 ± 1.11	-13.49 ± 0.26	4.24 ± 1.96	17.72 ± 1.70	-3.87 ± 0.27	-15.36 ± 4.35	7.63 ± 4.11	22.99 ± 8.44
Summer 2025	-7.35 ± 0.14	-16.56 ± 0.87	1.85 ± 1.15	18.40 ± 2.02	-5.75 ± 0.35	-13.49 ± 1.20	1.98 ± 0.51	15.47 ± 1.71
Winter 2025	-7.98	-20.46	4.50	24.96	-4.90 ± 0.35	-19.09 ± 6.26	9.28 ± 6.97	28.36 ± 13.22
OPC PM2.5 vs OPC PM2.5	Old OPC vs Old OPC				New OPC vs New OPC			
Season	Bias	LOA Low	LOA High	LOA Span	Bias	LOA Low	LOA High	LOA Span
Winter 2023	-1.48 ± 1.33	-5.66 ± 3.44	2.70 ± 0.81	8.36 ± 4.24				
Spring 2024	-1.31 ± 1.22	-3.25 ± 2.17	0.64 ± 0.27	3.89 ± 1.90				
Summer 2024	-0.65 ± 0.56	-2.10 ± 0.92	0.80 ± 0.20	2.90 ± 0.72				
Winter 2024	-2.28 ± 1.00	-6.54 ± 1.70	1.98 ± 2.51	8.52 ± 3.79				
Spring 2025	-1.58	-3.67	0.52	4.19	-0.07 ± 0.29	-8.75 ± 4.04	8.61 ± 4.61	17.36 ± 8.65
Summer 2025	-0.69	-1.45	0.07	1.52	0.10 ± 0.55	-5.96 ± 5.46	6.16 ± 4.41	12.12 ± 9.87
Winter 2025					0.49	-15.02	16.00	31.02
OPC PM2.5 vs OPC PM2.5	New OPC vs Old OPC							
Season	Bias	LOA Low	LOA High	LOA Span				
Winter 2023								
Spring 2024								
Summer 2024								
Winter 2024								
Spring 2025	0.90 ± 0.80	-12.36 ± 6.50	14.17 ± 6.22	26.52 ± 12.63				
Summer 2025	1.63 ± 0.31	-2.18 ± 1.36	5.43 ± 1.33	7.62 ± 2.62				
Winter 2025	2.56 ± 0.40	-8.17 ± 7.35	13.29 ± 8.14	21.45 ± 15.49				

Table S12: Summary of seasonal PMS5003T $PM_{2.5}$ Bland-Altman comparisons showing the average ± standard deviation for results based on groupings of new and old sensors. Figures S48-S54 show seasonal Bland-Altman plots and results for each sensor. LOA - 95% limits of agreement. Bias and LOA units are $\mu g\ m^{-3}$.

PMS PM2.5 vs FEM PM2.5	Old PMS vs FEM				New PMS vs FEM			
Season	Bias	LOA Low	LOA High	LOA Span	Bias	LOA Low	LOA High	LOA Span
Winter 2023	1.66 ± 0.88	-17.63 ± 2.99	20.94 ± 4.75	38.57 ± 7.74				
Spring 2024	-1.18 ± 0.25	-7.80 ± 0.10	5.44 ± 0.42	13.24 ± 0.36				
Summer 2024	0.40 ± 1.15	-15.08 ± 0.72	15.88 ± 3.02	30.96 ± 3.73				
Winter 2024	8.18 ± 1.97	-18.84 ± 1.27	35.21 ± 5.20	54.04 ± 6.47				
Spring 2025	-1.72 ± 0.64	-12.77 ± 0.08	9.34 ± 1.38	22.11 ± 1.46	-3.20 ± 1.57	-15.10 ± 1.59	8.69 ± 4.72	23.79 ± 6.30
Summer 2025	0.04 ± 3.71	-15.01 ± 4.04	15.10 ± 11.45	30.10 ± 15.49	-2.15 ± 0.26	-11.23 ± 1.68	6.94 ± 2.18	18.17 ± 3.85
Winter 2025	11.18	-19.94	42.29	62.23	2.05 ± 0.26	-12.65 ± 1.27	16.74 ± 1.79	29.38 ± 3.05
PMS PM2.5 vs PMS PM2.5	Old PMS vs Old PMS				New PMS vs New PMS			
Season	Bias	LOA Low	LOA High	LOA Span	Bias	LOA Low	LOA High	LOA Span
Winter 2023	0.35 ± 0.47	-2.12 ± 0.39	2.82 ± 1.32	4.94 ± 1.70				
Spring 2024	0.29 ± 0.25	-1.96 ± 0.69	2.55 ± 0.70	4.50 ± 1.29				
Summer 2024	1.18 ± 1.38	-2.52 ± 0.42	4.88 ± 3.18	7.41 ± 3.59				
Winter 2024	2.21 ± 2.68	-5.19 ± 0.50	9.59 ± 5.48	14.78 ± 5.63				
Spring 2025	0.90	-2.36	4.16	6.52	-1.12 ± 0.79	-8.47 ± 5.66	6.24 ± 4.09	14.71 ± 9.74
Summer 2025	1.20	-2.39	4.79	7.18	-0.73 ± 0.67	-5.94 ± 3.60	4.48 ± 2.28	10.42 ± 5.87
Winter 2025					-0.38	-3.49	2.73	6.22
PMS PM2.5 vs PMS PM2.5	New PMS vs Old PMS							
Season	Bias	LOA Low	LOA High	LOA Span				
Winter 2023								
Spring 2024								
Summer 2024								
Winter 2024								
Spring 2025	-1.56 ± 1.55	-14.23 ± 1.21	11.12 ± 2.87	25.35 ± 3.14				
Summer 2025	-1.72 ± 2.55	-11.13 ± 9.38	7.69 ± 4.70	18.81 ± 13.93				
Winter 2025	-9.12 ± 0.27	-28.73 ± 1.11	10.49 ± 0.59	39.21 ± 1.70				

OPC-N3-to-PMS5003T $PM_{2.5}$ ratio results

Table S13: Seasonal descriptive statistics for daily averaged OPC-N3 $PM_{2.5}$-to-PMS5003T $PM_{2.5}$ ratios for each AirU Pro unit. Measurements only include samples with RH ≤ 80%, PMS5003T $PM_{2.5}$ ≥ 1 µg m^{-3}, and OPC-N3 $PM_{2.5}$ ≥ 1 µg m^{-3}. N is the number of samples, SD is the standard deviation, Q25 is the 25th percentile, and Q75 is the 75th percentile.

Unit (OPC #/PMS #)	Season	N (daily)	mean	SD	min	Q25	median	Q75	max
1 (501/357)	Winter 2023	32	0.696	0.585	0.181	0.352	0.477	0.841	3.10
1 (501/357)	Spring 2024	77	1.066	1.157	0.246	0.475	0.809	1.072	8.13
1 (501/357)	Summer 2024	152	0.464	0.382	0.090	0.201	0.353	0.570	2.84
1 (501/357)	Winter 2024	111	0.403	0.594	0.041	0.082	0.147	0.431	3.31
1 (501/357)	Spring 2025	61	0.478	0.688	0.051	0.152	0.218	0.445	3.51
1 (501/357)	Summer 2025	104	0.199	0.170	0.014	0.070	0.161	0.266	0.90
1 (501/357)	Winter 2025	75	0.127	0.171	0.026	0.039	0.056	0.118	0.81
2 (905/261)	Winter 2023	24	1.401	0.847	0.434	0.794	1.175	1.817	4.04
2 (905/261)	Spring 2024	91	2.004	1.309	0.742	1.284	1.721	2.393	8.55
2 (905/261)	Summer 2024	152	0.736	0.457	0.135	0.395	0.635	0.928	2.91
2 (905/261)	Winter 2024	120	1.165	1.058	0.149	0.407	0.889	1.567	6.79
2 (905/261)	Spring 2025	91	0.881	0.557	0.145	0.489	0.705	1.073	2.84
2 (905/261)	Summer 2025	77	0.384	0.173	0.103	0.250	0.377	0.459	0.84
3 (605/155)	Winter 2023	24	0.671	0.369	0.196	0.375	0.559	0.892	1.46
3 (605/155)	Spring 2024	77	1.124	1.125	0.289	0.526	0.880	1.176	7.25
3 (605/155)	Summer 2024	151	0.556	0.388	0.118	0.261	0.447	0.731	2.52
3 (605/155)	Winter 2024	110	1.011	2.119	0.144	0.268	0.431	0.840	20.06
4 (011/265)	Spring 2025	82	0.823	0.493	0.190	0.491	0.679	0.931	2.55
4 (011/265)	Summer 2025	77	0.559	0.295	0.192	0.335	0.495	0.691	1.80
5 (201/887)	Spring 2025	33	1.128	1.460	0.400	0.625	0.752	1.016	8.89
5 (201/887)	Summer 2025	152	0.662	0.487	0.137	0.386	0.535	0.777	4.53
5 (201/887)	Winter 2025	113	1.126	2.620	0.148	0.235	0.353	0.748	20.20
6 (216/792)	Spring 2025	33	1.110	1.068	0.397	0.658	0.766	1.041	6.24
6 (216/792)	Summer 2025	152	0.734	0.525	0.119	0.424	0.623	0.926	4.81
6 (216/792)	Winter 2025	114	1.099	2.328	0.173	0.320	0.427	0.752	15.16

Table S14: Statistical comparisons of daily averaged OPC-N3 $PM_{2.5}$-to-PMS5003T $PM_{2.5}$ ratios for the same season across successive years. Measurements only include samples with RH ≤ 80%, PMS5003T $PM_{2.5} \geq 1$ µg m^{-3}, and OPC-N3 $PM_{2.5} \geq 1$ µg m^{-3}.

Unit (OPC #/ PMS #)	Comparison	Test	p-value	effect size[b]
1 (501/357)	Winter 2023-2025*	Kruskal–Wallis[a]	7.07×10^{-17}	0.337
1 (501/357)	Spring 2024 vs Spring 2025	Mann–Whitney U	8.27×10^{-12}	0.679
1 (501/357)	Summer 2024 vs Summer 2025	Mann–Whitney U	1.25×10^{-14}	0.568
2 (905/261)	Winter 2023 vs Winter 2024	Mann–Whitney U	0.061	0.243
2 (905/261)	Spring 2024 vs Spring 2025	Mann–Whitney U	7.43×10^{-18}	0.739
2 (905/261)	Summer 2024 vs Summer 2025	Mann–Whitney U	4.57×10^{-11}	0.533
3 (605/155)	Winter 2023 vs Winter 2024	Mann–Whitney U	0.195	0.170
Unit (OPC #/ PMS #)	[a]Post hoc pairwise comparisons	Test	p-value	
1 (501/357)	Winter 2023 vs Winter 2024	Dunn Bonferroni	1.30×10^{-4}	
1 (501/357)	Winter 2023 vs Winter 2025	Dunn Bonferroni	1.16×10^{-15}	
1 (501/357)	Winter 2024 vs Winter 2025	Dunn Bonferroni	5.40×10^{-9}	

[a]When the Kruskal–Wallis test identifies a statistically significant difference among winter seasons, we perform pairwise Dunn's tests with a Bonferroni correction.

[b]We quantify effect size using epsilon-squared (ε^2) for the Kruskal–Wallis test and Cliff's delta (δ) for the Mann–Whitney U test.

S.3: Investigate OPC-N3 reject counts to screen high PM_{10} measurements

OPC-N3 sensors report exceptionally high PM_{10} concentrations (on the order of 1000s µg m^{-3}) under high-humidity conditions (> 80%; Fig. S60a). During these periods, the OPC-N3-to-FEM PM10 ratio exceeds 200 (Fig. S60b). Although OPC-N3 sensors are known to overestimate PM under elevated humidity, the most extreme values coincide with high reject count (rc) metrics (Fig. S60). Table S15 summarizes the four rc metrics, including definitions and typical ranges. In this section, we first identify threshold combinations based on rc metrics to screen for high OPC-N3 PM_{10} measurements from April 2024 to January 2025. We then apply these thresholds to data from March 2025 to February 2026 to evaluate the effectiveness of this screening approach.

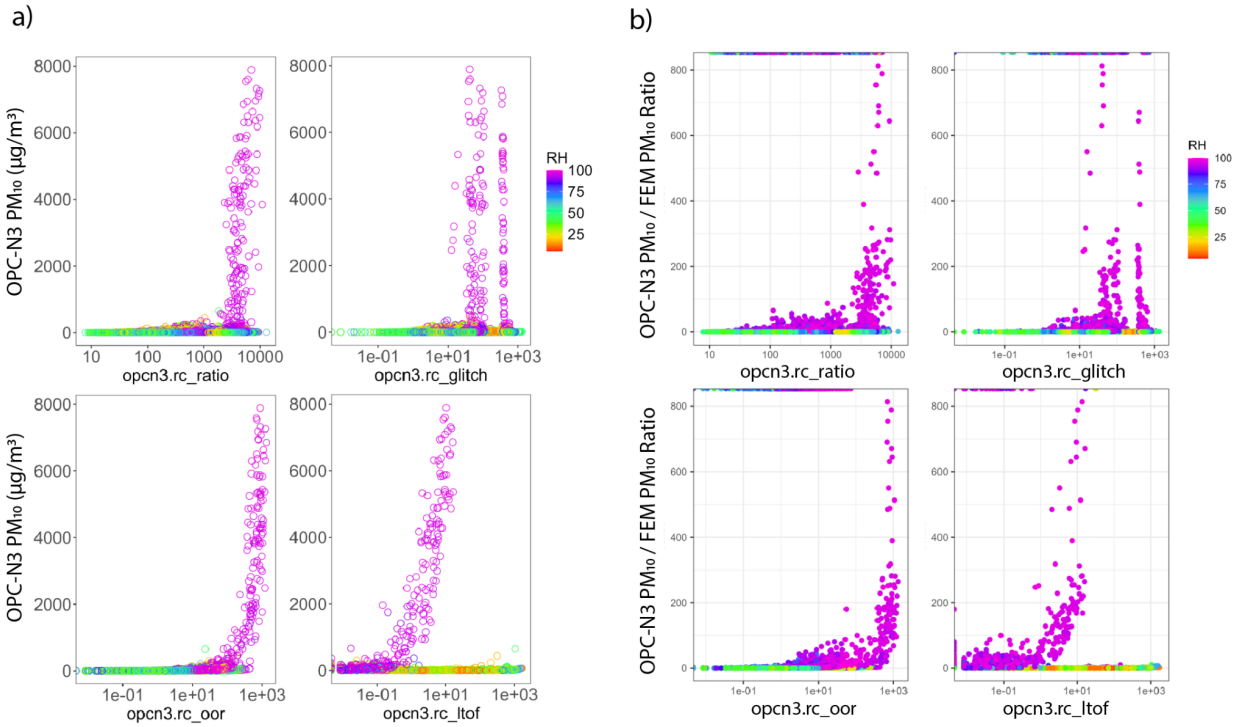


Figure S60: Raw OPC-N3 PM_{10} measurement versus the reject count metrics (rc_ratio, rc_glitch, rc_oor, rc_ltof) with scatter points colored by Utah Division of Air Quality (DAQ) relative humidity (a) from April 2024 to January 2025. OPC-N3 to FEM PM_{10} ratio versus the reject count metrics with the scatter points colored by DAQ relative humidity (b).

Table S15: OPC-N3 reject count parameters, descriptions, and values compiled from the OPC-N3 user manual and follow-up email correspondence with Alphasense.

Reject count (rc)	Diagnostic information description	Typical values
ratio	Potential particle signals deemed incorrectly positioned between the inner and outer photodiodes for correct measurement.	Not defined
glitch	An indication of electronic noise. Low values indicate low noise.	< 100
out of range (oor)	A count of particle signals that were rejected as being unsuitable for the gain setting at the time of measurement	Not defined
long time of flight (ltof)	An indication of turbulent flow inside the unit. Low is better.	< 10

Among the rc metrics, rc_oor shows the strongest relationship with OPC-N3 PM_{10} during April 2024–January 2025 (i.e., all extreme PM_{10} values correspond to rc_oor > 100; Fig. S60a). However, rc_oor > 100 also includes measurements that are not anomalously high. To retain these observations, we incorporate rc_ratio and rc_ltof as additional filters. Specifically, we apply the combined criteria rc_oor > 100, rc_ltof > 0, and rc_ratio > 2000 to remove extreme OPC-N3 PM_{10} values (Fig. S61).

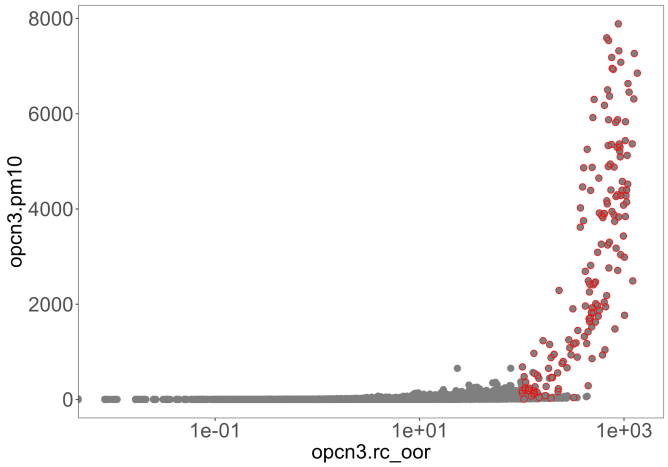


Figure S61: Red represents the raw OPC-N3 PM_{10} measurements rejected using rc_oor > 100 & rc_ltof > 0 & rc_ratio > 2000 from measurements spanning April 2024 to January 2025.

We evaluate this rc-based screening method using data from March 2025 to February 2026. Figure S62 shows similar associations between elevated OPC-N3 PM_{10} and rc metrics during this period. However, applying the rc thresholds (Fig. S63) removes a substantial number of lower PM_{10} observations. Although the rc-based screening shows some promise, a simple relative humidity threshold is simpler and effectively improves OPC-N3 correction model performance (see the main manuscript). Consequently, we do not pursue further use of rc metrics for screening OPC-N3 measurements.

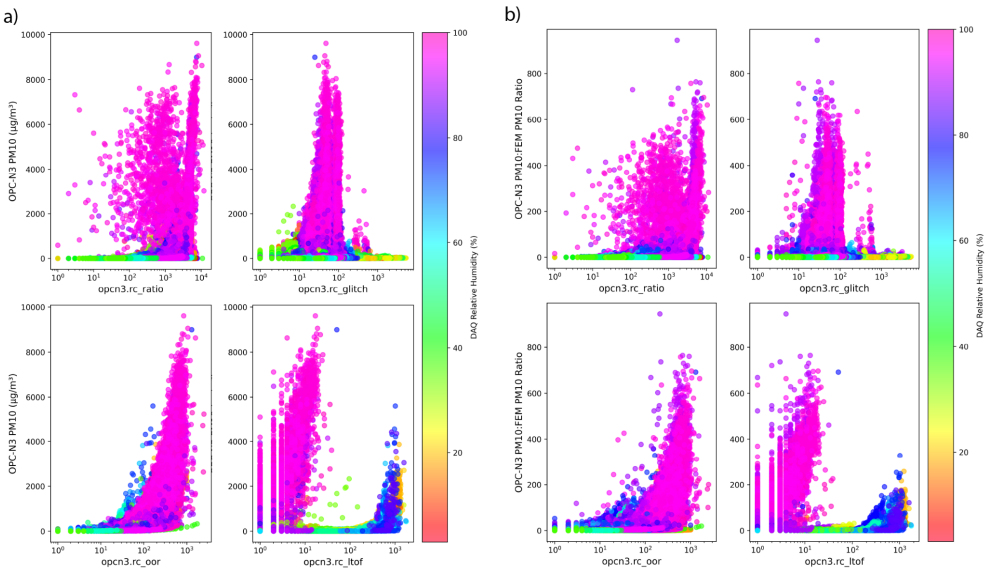


Figure S62: Raw OPC-N3 PM_{10} measurement versus the reject count metrics (rc_ratio, rc_glitch, rc_oor, rc_ltof) with scatter points colored by Utah Division of Air Quality (DAQ) relative humidity (a) from March 2025 to February 2026. OPC-N3 to FEM PM_{10} ratio versus the reject count metrics with the scatter points colored by DAQ relative humidity (b).

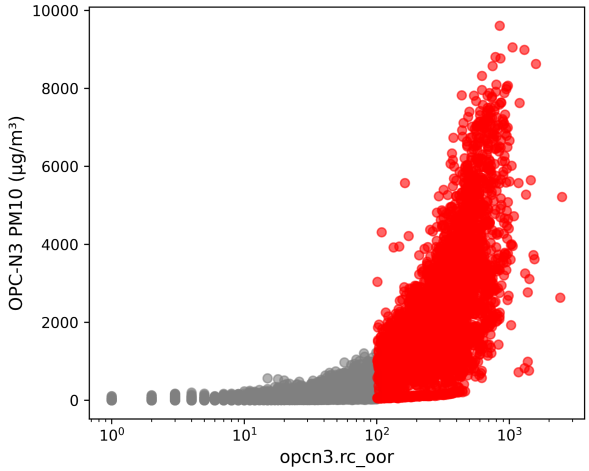


Figure S63: Red represents the raw OPC-N3 PM_{10} measurements rejected using rc_oor > 100 & rc_ltof > 0 & rc_ratio > 2000 from measurements spanning March 2025 to February 2026.

S.4: OPC-N3 sample flow rate and laser status

In addition to rc metrics, the OPC-N3 reports sample flow rate and laser status. According to the manufacturer, the instrument derives sample flow rate from time-of-flight measurements, while laser status reflects the current drawn by the laser; ideal laser status values range from 550 to 650.

Because the OPC-N3 estimates sample flow rate using time-of-flight measurements, elevated rc_ltof may indicate issues with flow estimation. In this study, OPC-N3 unit 905 exhibits variability in rc_ltof (Fig. S64). However, this variability does not correspond consistently with either high or low sample flow rates, as high rc_ltof values occur across a range of flow conditions. Additionally, laser status remains within the manufacturer-specified range for all sensors (Fig. S65), although it varies by sensor and increases with relative humidity.

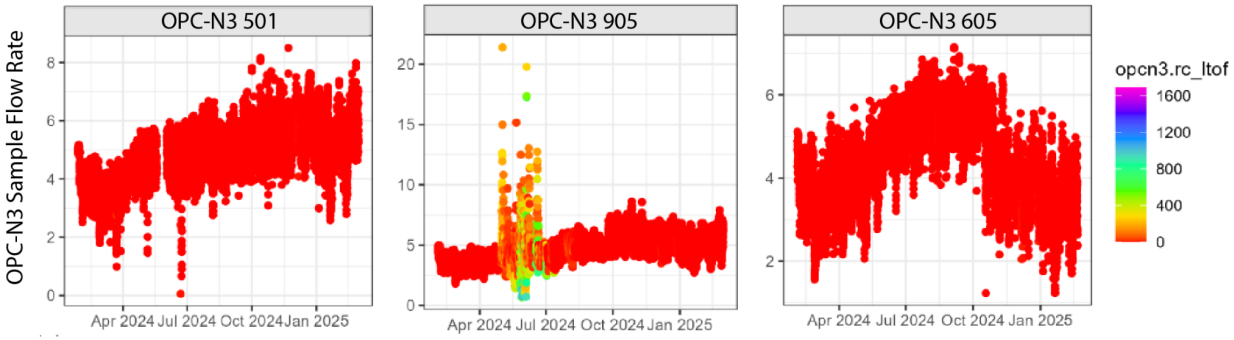


Figure S64: OPC-N3 sample flow rate timeseries with scatter points colored by the reject count long time of flight (rc_ltof) metric from April 2024 to January 2025.

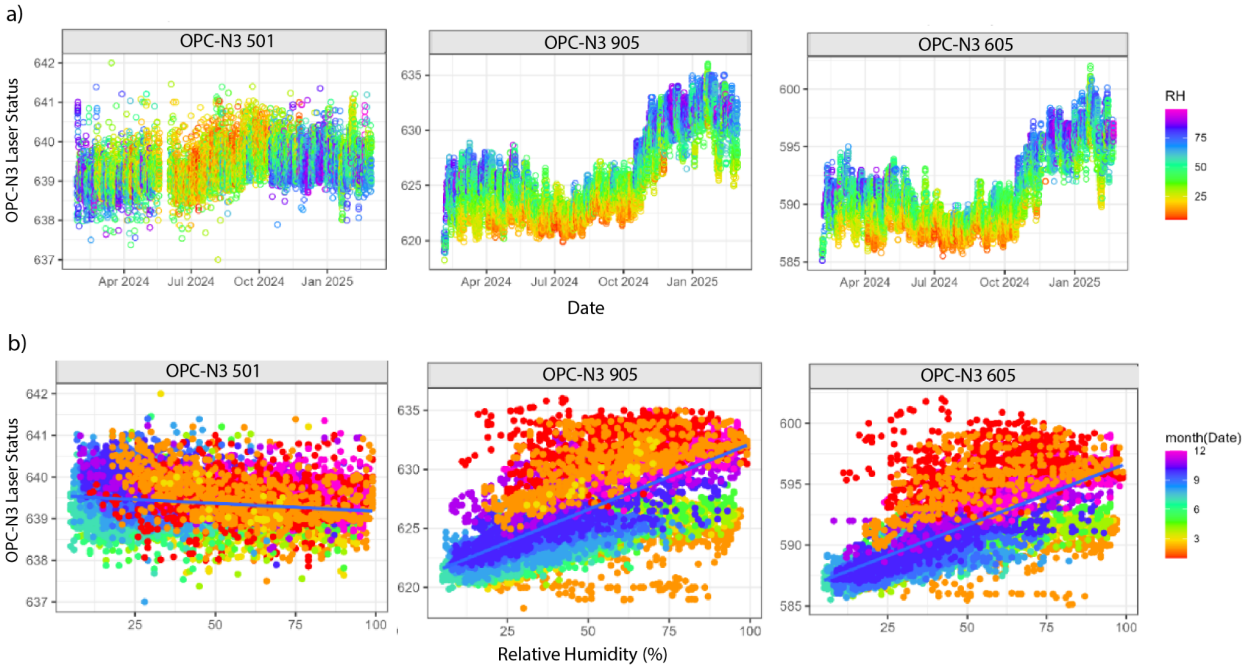


Figure S65: OPC-N3 laser status versus time (a) with scatter points colored by Utah Division of Air Quality relative humidity and OPC-N3 laser status versus relative humidity (b) with scatter points colored by date from April 2024 to January 2025.

Figure S66 presents a 3-day rolling average of sample flow rate and laser status from April 2024 to October 2024. OPC-N3 units 905 and 501 show similar trends in sample flow rate, both peaking in early October, whereas OPC-N3 unit 605 peaks in July and declines through October. For laser status, OPC-N3 units 905 and 605 follow similar trends, each varying by at least 8 units, while OPC-N3 unit 501 shows a different pattern with minimal variation (< 1 unit) compared to 905 and 605. Overall, we did not find strong evidence that sample flow rate or laser status reliably indicates OPC-N3 degradation.

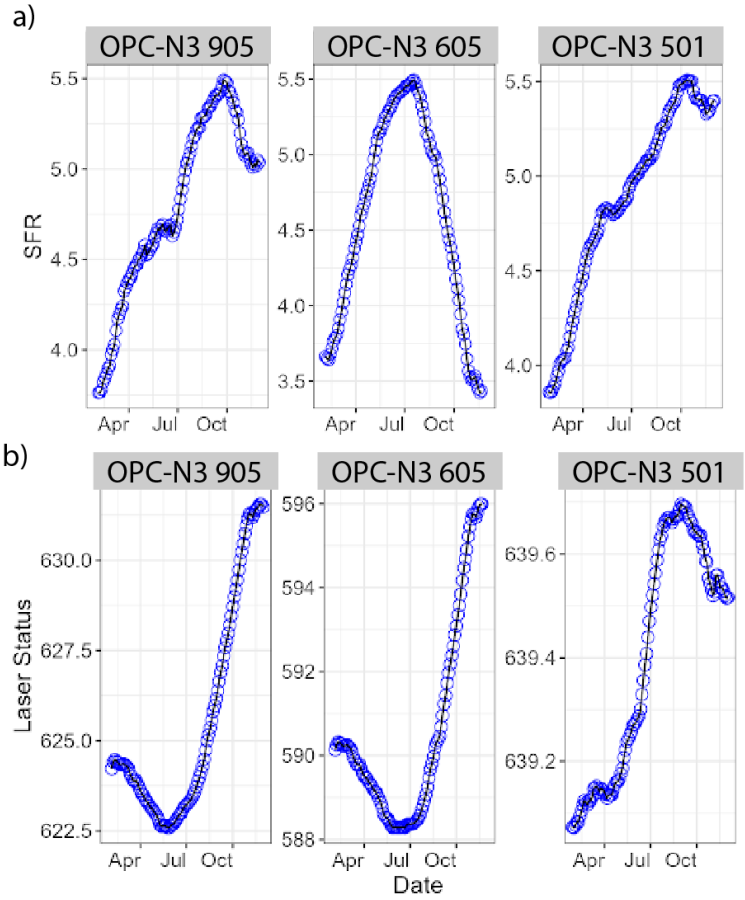


Figure S66: Rolling average values (3-day step) of the OPC-N3 sample flow rate (SFR) and laser status from April 2024 to October 2024.

S.5: Laptop/Alphasense software OPC-N3 colocation results & OPC-N3 power analysis

Laptop and Alphasense software OPC-N3 colocation

Between September 23 and November 29, 2025 (~2 months), we colocated two never-deployed OPC-N3 sensors—177400219 (219) and 177400220 (220)—at the Division of Air Quality's Utah Technical Center (UTTC) station. We connect both sensors to a laptop USB 2.0 port and collect data using Alphasense software. Earlier, on August 19, 2025, we deployed two additional new OPC-N3 sensors—177090717 (717) and 177090720 (720)—on Tellus AirU Pro boards (TELLUS Networked Sensor Solutions, Inc., Salt Lake City, Utah) at the same site. Additionally, three of the Tellus board OPC-N3 sensors were already operating at the UTTC station: sensors 201 and 216 (each with ~5 months of field deployment as of September 23, 2025) and sensor 501 (~20 months in the field) (see the main manuscript for more details on these sensors).

The goal of colocating the laptop-connected sensors is to evaluate whether the Tellus AirU Pro board influences OPC-N3 measurements. To isolate instrumentation effects, we only compare the laptop sensors (219 and 220) with the four newer Tellus board OPC-N3 sensors that have shorter deployment histories: 717 and 720 (~1 month in the field) and 201 and 216 (~5 months in the field).

Figure S67 presents a cross-correlation matrix of PM10 measurements. Comparisons between the laptop sensors (219 and 220) and the ~1-month Tellus board sensors (717 and 720) yield an average R^2 of 0.81 ± 0.05 and an average slope of 0.96 ± 0.09. Both groups also show similar agreement with the FEM: the laptop sensors have an average R2 of 0.42 ± 0.03 and slope of 0.32 ± 0.03, while the ~1-month Tellus sensors have an average R^2 of 0.41 ± 0.01 and slope of 0.34 ± 0.04. These results indicate that the platform—whether a Tellus board or a laptop running Alphasense software—does not materially affect OPC-N3 measurements.

Interestingly, comparisons with the ~5-month sensors (201 and 216) suggest early signs of sensor degradation. When we compare either the laptop sensors or the ~1-month Tellus board sensors with the ~5-month sensors, the relationships weaken, and slopes deviate further from unity. For the laptop-to-5-month comparison, the average R^2 is 0.46 ± 0.37 with a slope of 0.57 ± 0.08. For the ~1-month-to-5-month comparison, the average R^2 is 0.55 ± 0.40 with a slope of 0.59 ± 0.10. By comparison, the two ~5-month sensors have a slope of 0.94.

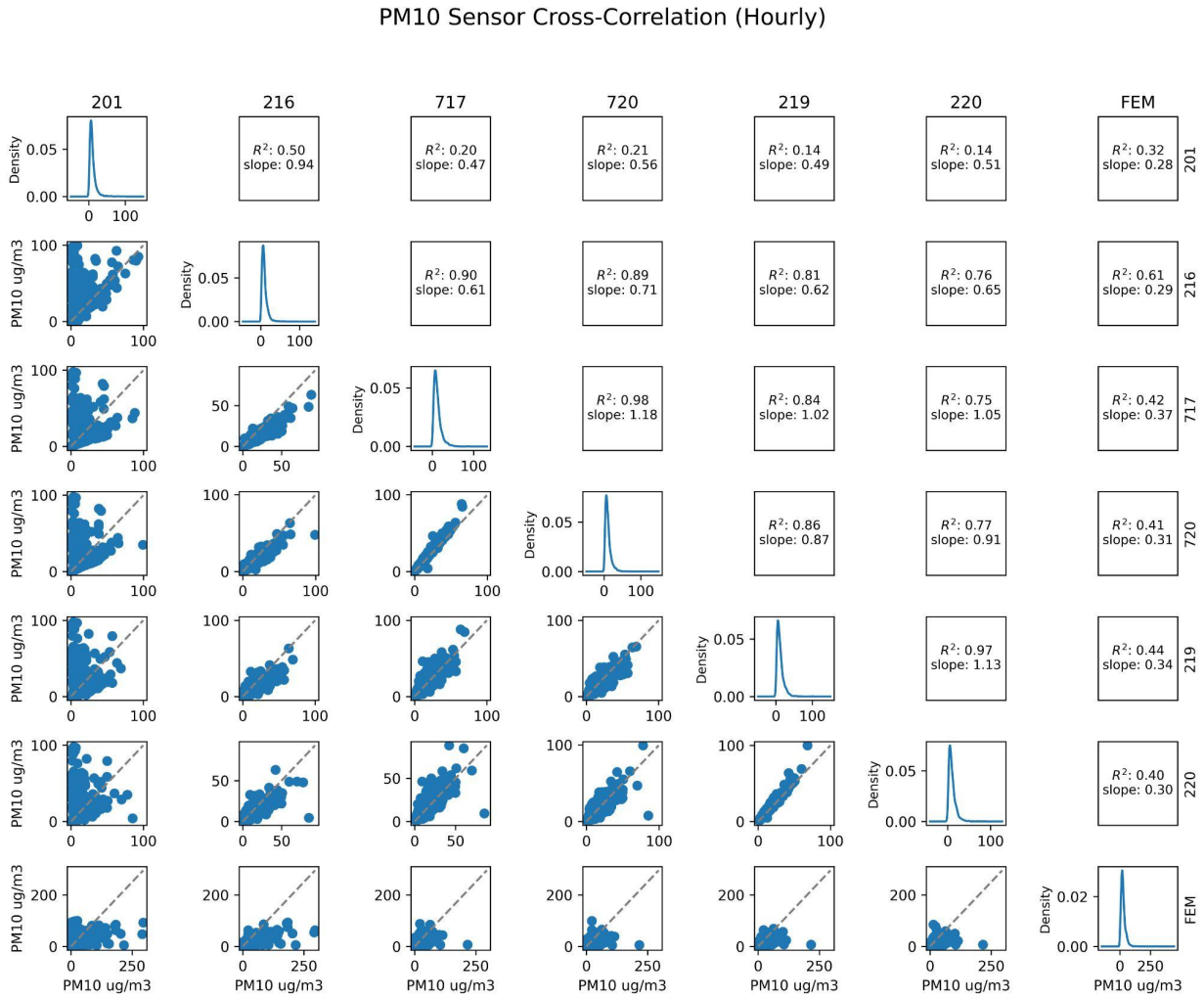


Figure S67: Hourly OPC-N3 PM_{10} concentration cross-correlation of the FEM, laptop OPC-N3 sensors using Alphasense software (219 and 220), and Tellus board OPC-N3 sensors (201, 216, 717, and 720) at UTTC from September 23, 2025, to November 29, 2025.

Power analysis

In this section, we evaluate whether the power supply or circuit affects OPC-N3 measurements. The Alphasense OPC-N3 user manual specifies an operating voltage of 4.8–5.2 VDC and a current draw of 180 mA in measurement mode (with a < 5000 mW, 1 ms startup transient).

We laboratory-calibrate three OPC-N3 sensors—177560703 (703; never deployed), 177400219 (219; deployed for ~2 months as part of the laptop colocation), and 177400220 (220; deployed for ~2 months as part of the laptop colocation)—using the Arizona road dust and DustTrak setup (Fig. S1). During calibration, each sensor operates on a different power source: OPC-N3 703 uses the Tellus AirU Pro board (TELLUS Networked Sensor Solutions, Inc., Salt Lake City, Utah), OPC-N3 219 uses a Raspberry Pi 15W USB-C power supply (5.1 V, 3 A), and OPC-N3 220 uses a laptop USB 2.0 port (5 V, 0.5 A). Each OPC-N3 logs data to its internal SD card at ~1.4 s intervals, and we retrieve the data using Alphasense software after the test. The DustTrak, fitted with a PM_{10} impactor, records

measurements at 15 s intervals. We conduct a four-point ramp calibration at approximately 0, 200, 500, and 700 μg m^{-3}.

Figure S68 presents a time series of raw PM_{10} and Bin 0 counts for the calibration. Tables S16 and S17 summarize the descriptive statistics for each concentration step across the three sensors. Although the 95% confidence intervals of the means do not overlap across sensors at each step, the mean ± one standard deviation ranges do overlap. Taken together, these results indicate that differences in power supply do not meaningfully affect OPC-N3 measurements under these conditions.

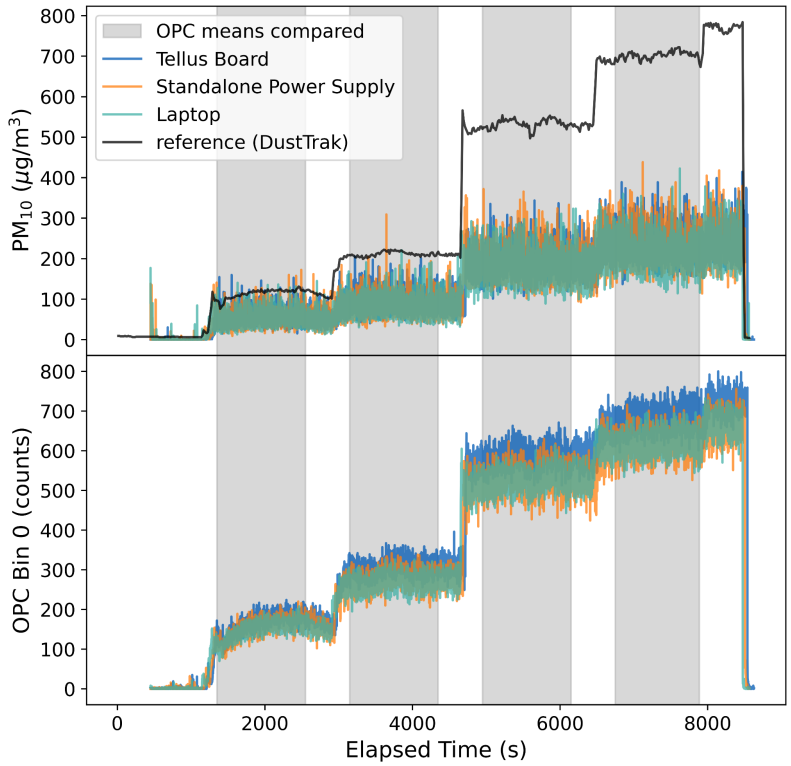


Figure S68: OPC-N3 power comparison time series for PM_{10} measurements (top) and bin 0 counts (bottom).

Table S16: OPC-N3 power comparison descriptive statistics for PM_{10}. Bolded confidence intervals (CI) are overlapping. Acronyms - number of measurements (N), standard deviation (std).

data	metric (unit)	start (s)	end (s)	N	mean	std	95% CI low	95% CI high
Tellus Board	PM10 (ug/m3)	1350	2550	859	56.9	21.7	55.4	58.3
Power Supply	PM10 (ug/m3)	1350	2550	859	51.9	21.6	**50.5**	**53.4**
Laptop	PM10 (ug/m3)	1350	2550	859	49.3	20.2	**48.0**	**50.7**
Tellus Board	PM10 (ug/m3)	3150	4350	858	92.5	26.3	90.8	94.3
Power Supply	PM10 (ug/m3)	3150	4350	858	84.9	27.2	83.1	86.7
Laptop	PM10 (ug/m3)	3150	4350	858	81.3	25.3	79.6	83.0
Tellus Board	PM10 (ug/m3)	4950	6150	859	193.1	36.4	190.6	195.5
Power Supply	PM10 (ug/m3)	4950	6150	859	187.0	40.9	184.2	189.7
Laptop	PM10 (ug/m3)	4950	6150	859	175.6	37.9	173.1	178.2
Tellus Board	PM10 (ug/m3)	6750	7890	815	236.7	39.7	234.0	239.4
Power Supply	PM10 (ug/m3)	6750	7890	815	229.0	43.0	226.0	231.9
Laptop	PM10 (ug/m3)	6750	7890	815	211.6	38.4	208.9	214.2

Table S17: OPC power comparison descriptive statistics for Bin0 counts. Bolded confidence intervals (CI) are overlapping. Acronyms - number of measurements (N), standard deviation (std).

data	metric (unit)	start (s)	end (s)	N	mean	std	95% CI low	95% CI high
Tellus Board	Bin0 (counts)	1350	2550	859	165.4	26.0	163.7	167.2
Power Supply	Bin0 (counts)	1350	2550	859	152.8	25.4	151.1	154.5
Laptop	Bin0 (counts)	1350	2550	859	147.6	23.0	146.1	149.2
Tellus Board	Bin0 (counts)	3150	4350	858	306.2	20.4	304.8	307.6
Power Supply	Bin0 (counts)	3150	4350	858	276.3	22.7	274.8	277.8
Laptop	Bin0 (counts)	3150	4350	858	266.1	19.7	264.8	267.5
Tellus Board	Bin0 (counts)	4950	6150	859	583.8	26.9	582.0	585.6
Power Supply	Bin0 (counts)	4950	6150	859	531.7	31.7	529.6	533.9
Laptop	Bin0 (counts)	4950	6150	859	523.8	26.2	522.0	525.5
Tellus Board	Bin0 (counts)	6750	7890	815	681.3	28.6	679.3	683.2
Power Supply	Bin0 (counts)	6750	7890	815	622.8	31.5	**620.7**	**625.0**
Laptop	Bin0 (counts)	6750	7890	815	620.3	27.4	**618.5**	**622.2**

S.6: Laboratory precision test variability using never-deployed OPC-N3 sensors

Laboratory precision testing of OPC-N3 sensors with Arizona road dust, using the DustTrak as a reference, exhibits inherent variability. Multiple factors contribute to this variability, including particles settling in the atomizer suspension during testing (even with a magnetic stir bar), fluctuations in pressure or flow rate, and repeated teardown and reassembly of equipment to accommodate other experiments in the gas hood.

To quantify this variability, we calibrate five never-deployed OPC-N3 sensors—177290106 (106), 177292814 (814), 177312813 (813), 177560709 (709), and 177311320 (320)—using a four-point linear calibration at PM_{10} concentrations of approximately 0, 200, 500, and 700 $\mu g\ m^{-3}$. Figure S69 presents a representative parity plot from one test batch. We test each sensor at least five times; however, OPC-N3 106 records only four valid tests due to a data-acquisition failure during one run. We define the regression as $PM10_{DT} = b1 * PM10_{OPC} + b_0$, where $PM10_{DT}$ represents minute-averaged DustTrak PM_{10} measurements ($\mu g\ m^{-3}$), and $PM10_{OPC}$ represents minute-averaged OPC-N3 PM_{10} measurements ($\mu g\ m^{-3}$). For field deployment, sensors must meet two precision criteria: (1) within each test batch, all slopes must fall within ±30% of the batch-average slope; and (2) across batches, the coefficient of variation of the slope must be less than 30%.

Figure S70 shows box plots of slopes and intercepts for each sensor, and Table S18 summarizes R^2, RMSE, normalized RMSE, slope, and intercept. We exclude one test for sensor 320 due to an operational or equipment error. All remaining calibration slopes meet the per-batch precision criterion except one: a slope of 2.71 for OPC-N3 814. Despite this outlier, OPC-N3 814 meets the overall requirement because four of its five tests pass. Across all sensors, the average slope is 1.56 ± 0.32, with passing slopes ranging from 1.20 to 2.09.

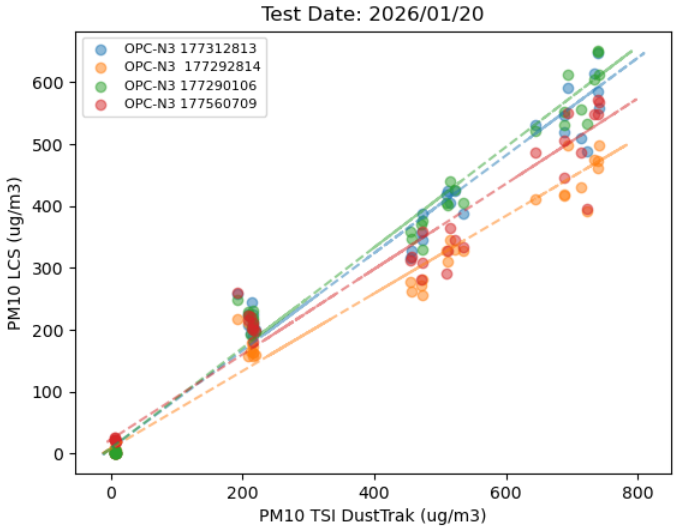


Figure S69: Parity plot for one test batch of never-deployed ("new") OPC-N3 sensors versus the DustTrak for a 4-point linear calibration using Arizona road dust particles.

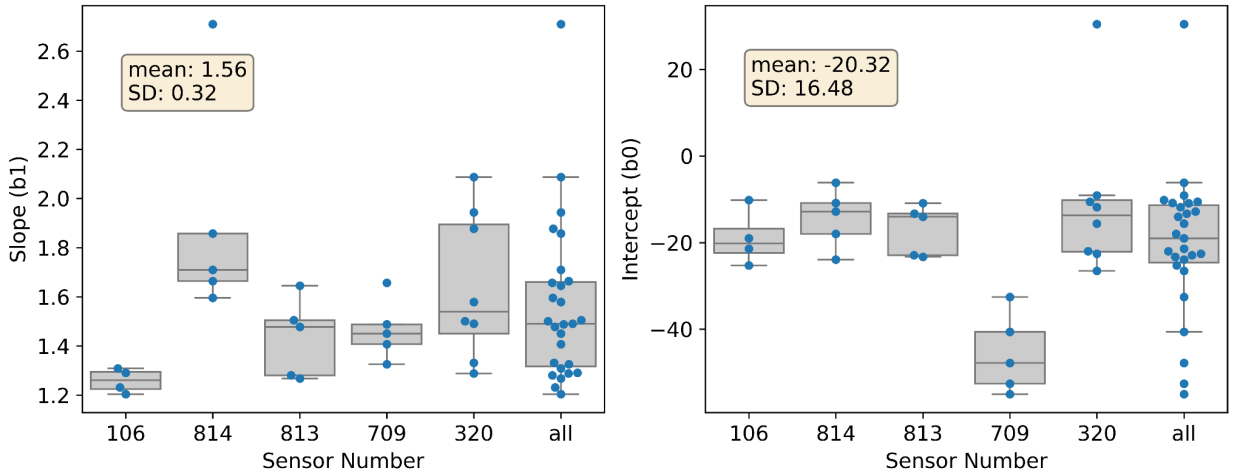


Figure S70: Never-deployed ("new") OPC-N3 sensor slope (left) and intercept (right) variability for laboratory calibration using Arizona road dust against a DustTrak. The outlier slope for sensor 814 failed the per-batch precision test criteria, requiring all slopes within ±30% of the average.

Table S18: Regression results from never-deployed OPC-N3 sensors. The sensor number is the last 3 digits of the OPC-N3 serial number.

Batch	Sensor Number	b1	b0	R2	RMSE	NRMSE (%)
1	106	1.20	-25.29	0.977	41.95	12%
3	106	1.31	-21.41	0.977	43.60	12%
4	106	1.29	-19.02	0.969	45.31	13%
5	106	1.23	-10.18	0.979	38.57	11%
1	814	1.71	-23.94	0.974	43.87	12%
2	814	1.86	-10.83	0.982	34.45	10%
3	814	2.71	-6.17	0.987	32.33	9%
4	814	1.66	-17.99	0.974	41.96	12%
5	814	1.60	-12.85	0.969	47.34	13%
1	813	1.50	-23.31	0.973	44.24	12%
2	813	1.65	-13.32	0.984	32.99	9%
3	813	1.48	-22.93	0.980	40.89	11%
4	813	1.28	-14.06	0.975	40.84	12%
5	813	1.27	-10.90	0.971	46.05	13%
1	709	1.49	-52.62	0.983	36.02	10%
2	709	1.66	-55.00	0.985	31.90	9%
3	709	1.33	-47.84	0.983	37.32	10%
4	709	1.41	-40.61	0.977	39.45	11%
5	709	1.45	-32.57	0.948	61.28	17%
1	320	1.94	-26.53	0.978	38.30	12%
2	320	1.33	30.47	0.596	121.77	55%
3	320	2.09	-11.83	0.873	54.91	30%
4	320	1.58	-22.00	0.967	2237.74	661%
5	320	1.88	-15.61	0.992	692.86	218%
6[a]	320	-45778.95	275.30	0.002	44999.10	16424%
7	320	1.29	-22.56	0.976	40.69	12%
8	320	1.49	-10.55	0.982	35.84	11%
9	320	1.50	-9.13	0.990	28.52	8%

[a]Batch 6 for sensor 320 was dropped from these results because we believe some sort of operator or experimental error contributed to the poor performance.

S.7: OPC-N3 mirror replacement standard operating procedure

Introduction

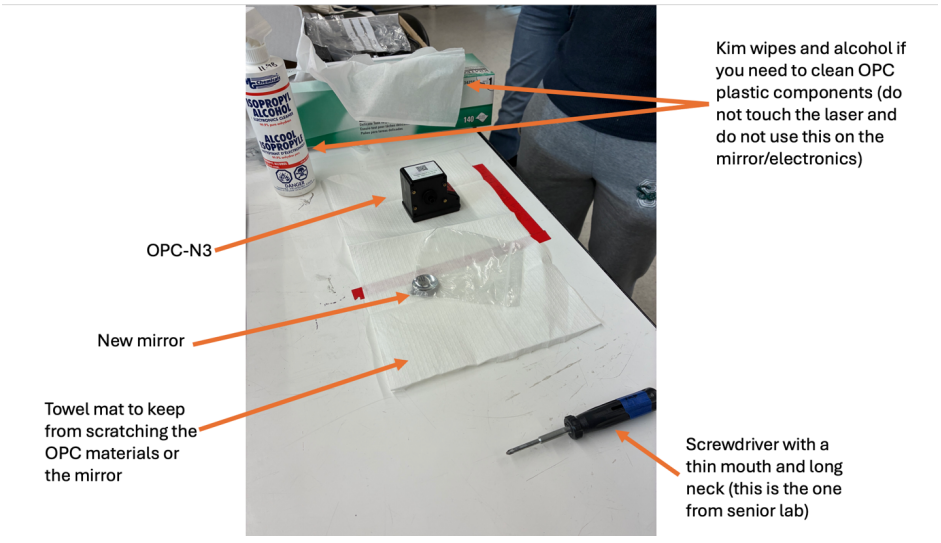
The OPC-N3 uses a mirror to focus scattered light onto a photodiode. Over time, especially during field use, this mirror can corrode. A corroded mirror reduces the instrument's ability to detect particles, so restoring proper performance requires replacing it with a new mirror.

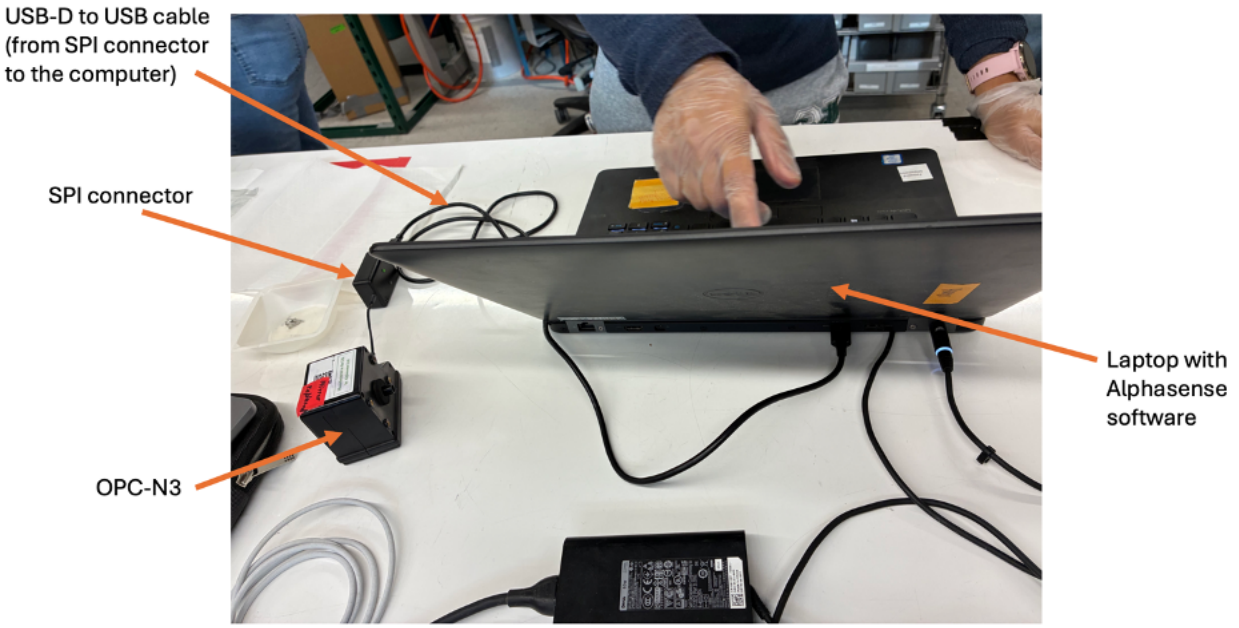
The most critical step during replacement is ensuring correct mirror alignment. If the mirror is misaligned, the focal point will not fall on the photodiode, and the OPC will register zero particle counts.

NOTICE: THIS PROCEDURE WILL VOID THE OPC'S WARRANTY.

Materials needed

1. OPC-N3
2. New/replacement OPC mirror
3. Kim wipes (to gently clean the inside of the OPC chamber)
4. Screwdriver (thin enough to unscrew the screws holding the OPC housing together)
5. Box cutter (to cut the OPC housing stickers)
6. Cotton swab (used to align the mirror and reduce the risk of stretching surfaces)
7. Gloves
8. PPE as required
9. Laptop with Alphasense software download
10. OPC SPI connector and USB-D to USB cable



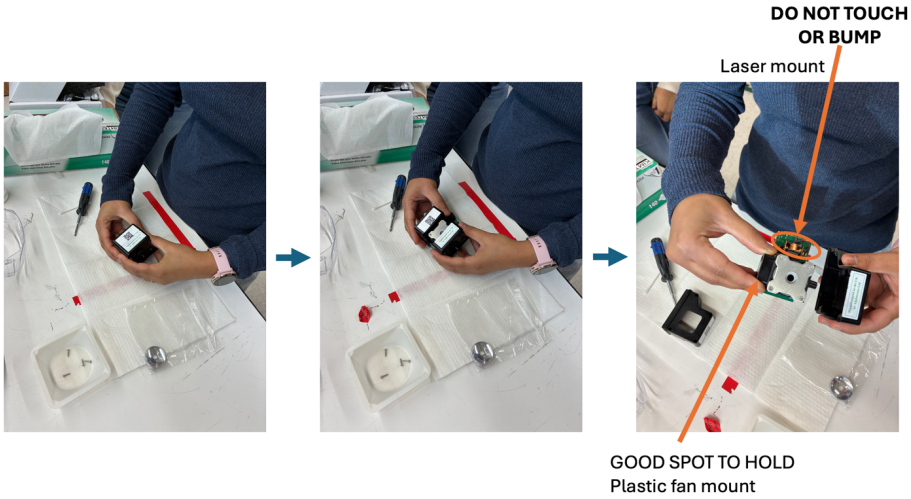


Mirror change procedure

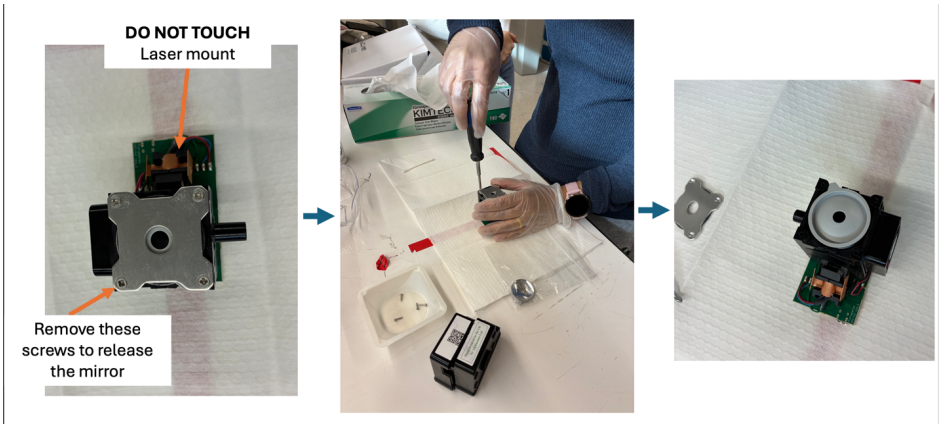
1. Disconnect any OPC cables (power and/or data transmission).
2. Before unscrewing, use the box cutter to cut the OPC stickers along the partition lines.



3. Unscrew the four OPC screws gently. Put the screws in a container to prevent losing them.
4. Gently open the OPC along the partition line. The housing will come apart easily, and nothing is attached to the casing (so do this slowly to avoid dropping the internals). All internal components of the OPC will come out together as one piece.
5. Remove the OPC internal component assembly (recommend holding onto the fan's plastic casing). **Avoid touching the side with the laser mount (the part with the bronze color).**



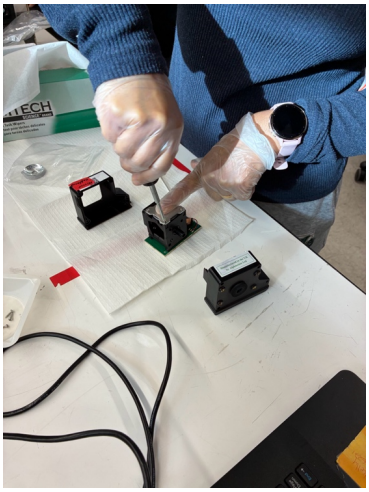
6. Holding the internal component assembly on the non-laser side, gently loosen the 4 screws of the metal plate/padding that hold the mirror in place, and set the metal plate/padding aside. Save the metal plate/padding screws in the screw container (these screws have different lengths than the OPC housing screws).
7. Remove the old/corroded mirror (if needed, save the old/corroded mirror in a Ziplock bag and label it with the OPC serial number).



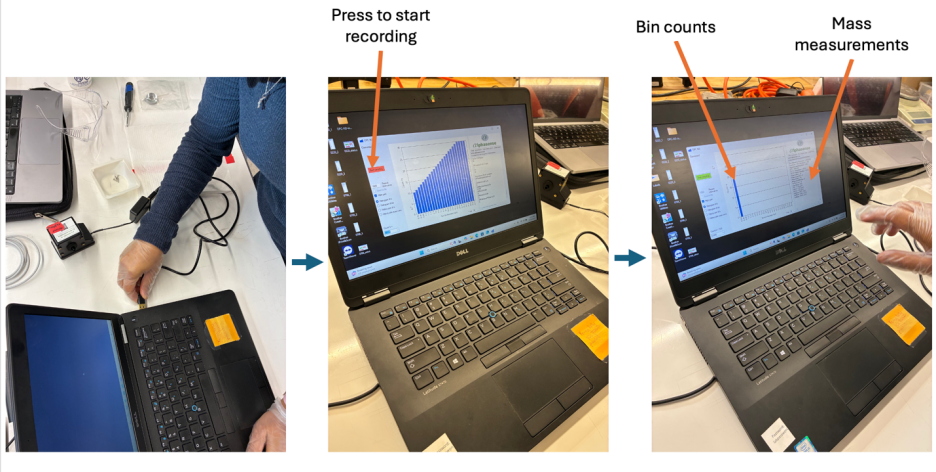
8. If needed, gently wipe the inside of the OPC chamber with a Kim wipe to clean it before placing the new mirror. CAREFUL not to bump the various components.
9. Put the new mirror in the top and replace the metal plate/padding. Do not touch the mirror's reflective surface with your hands (wear gloves) or scratch the mirror with the swab (or other tools).
10. Partially screw the metal plate/padding into place, but ensure there is still room for the mirror to move.
11. Align the mirror using the cotton swab so the hole in the mirror is directly above the photodiode. Additionally, the hole in the metal plate/padding and the hole in the mirror should be concentric.



12. Once you are satisfied with the alignment, press the metal plate/padding from the center to hold it in place and prevent components from shifting while you tighten the screws. Continue applying gentle pressure on the padding as you tighten the screws.



13. Put the internal structure back into housing (CAREFUL NOT TO BUMP THE LASER MOUNT WHILE SLIDING THE COMPONENT ASSEMBLY INTO THE HOUSING).
14. Before screwing the housing back together, do a quick test by connecting the OPC to the laptop running Alphasense software using the SPI connector and a USB-to-USB cable.
15. Check if any particles are being measured in the OPC bins (very rough check). If the OPC shows zero particle counts in Bin 0, the mirror alignment is probably off and needs to be adjusted (in room air, you should see some particles in Bin 0).
    a. To adjust the mirror alignment, disconnect any cables from the OPC (power and/or data) and unscrew the metal plate/padding screws a little bit and move the mirror with the cotton swab.
    b. Once you are satisfied with the alignment, press the metal plate/padding from the center to hold it in place and prevent components from shifting while you tighten the screws. Continue applying gentle pressure on the padding as you tighten the screws.
    c. Repeat the quick particle check in Bin 0. Repeat until you are satisfied with the initial alignment



16. Replace the OPC housing screws.

Alignment check procedure

1. Conduct a laboratory calibration of the OPC with the replaced mirror(s) with at least 1-2 new/never-deployed OPCs.
2. Re-align the mirror by repeating steps in the Mirror Change Procedure as needed.
3. Once you are satisfied with the new mirror's alignment and preliminary laboratory calibration results, repeat the laboratory calibration 5 times. We suggest that the OPC must meet the per-batch precision criteria at least 4 out of 5 times to be considered "good" and redeployed in the field.
    a. In our laboratory, per-batch precision criteria: OPC slopes must be within ±30% of the batch-average slope.

S.8: Mirror replacement repeatability tests

After replacing the mirrors in OPC-N3 sensors 177111905 (905; 18 months in the field), 177112011 (011; 5 months in the field), and 177520716 (716; never deployed), and verifying size selectivity using the FMAG and GRIMM (see the main manuscript), we evaluate the robustness of the mirror replacement standard operating procedure (SOP) by repeatedly calibrating the sensors using the Arizona road dust setup and comparing results to the DustTrak. Between calibration runs, we perform a mock mirror replacement following the SOP, in which we remove and reinstall the same mirror. We include a never-deployed OPC-N3 sensor, 177311320 (320), as a control; we do not open this sensor or subject it to mock mirror changes.

Three people each conduct three calibration runs, performing a mock mirror replacement between runs (removing and reinserting the same mirror). We use a four-point linear calibration with target PM_{10} concentrations of approximately 0, 200, 500, and 700 µg m^{-3}. We define the regression as $y_{REF} = b1 * x_{LCS} + b_0$, where y_{REF} is the minute-averaged DustTrak PM10 concentration (µg m^{-3}) and x_{LCS} is the minute-averaged OPC-N3 PM_{10} concentration (µg m^{-3}). We place all four OPC-N3 sensors at the same terminal Y-split position (Fig. S1) for every test to minimize positional variability. Sensors that had slopes that did not fall within the per-batch slope limits (within ±30% of the mean) were dropped from the batch.

Table S19 summarizes the mirror-replacement repeatability tests by batch, and Table S20 summarizes the results by sensor. In Table S19, the top section reports the mean slope for each batch, the corresponding ±30% precision bounds, and the sensors that fail the per-batch criterion. The bottom section reports the recalculated results after removing failing sensors—typically one or two clear outliers—and identifies any sensors that still fail after this exclusion.

During testing, we inadvertently bumped the laser mount on OPC-N3 sensor 716 between Person 2 Batch 2 and Batch 3 (Table S20). After this event, sensor 716 fails all subsequent tests, and adjustments to mirror alignment do not restore performance. This result indicates laser misalignment that likely requires the manufacturer's laser realignment. OPC-N3 sensor 905 also fails all tests in this series (caveat: it does pass two tests after careful alignment in Sect. S.9, but see that section for details). In contrast, the results for OPC-N3 sensor 011 are more promising. These results demonstrate that careful mirror replacement and alignment can restore performance sufficiently for the OPC-N3 sensor to pass the Arizona road dust laboratory calibration.

Table S19: Mirror replacement repeatability (mock mirror replacement between each test) results per batch summary. The slope limits are set at ±30% of the mean.

	Person	Batch	b1 avg	b1 upper limit	b1 lower limit	Sensors that failed:
	1	1	16.87	21.94	11.81	905, 011, 320, 716
	1	2	31.48	40.92	22.04	011, 320, 716
	1	3	3.86	5.02	2.70	905, 320
	2	1	17.66	22.96	12.36	905, 011, 320
	2	2	40.90	53.17	28.63	905, 011, 320, 716
	2[a]	3[a]	-11570.46	-15041.60	-8099.32	905, 011, 320, 716
	3	1	22.55	29.32	15.79	905, 011, 320, 716
	3	2	11.92	15.50	8.34	905, 011, 320, 716
	3	3	35.27	45.85	24.69	905, 011, 320, 716
Drop sensors	Person	Batch	b1 avg	b1 upper limit	b1 lower limit	Sensors that failed:
905	1	1	2.67	3.47	1.63	none
905, 011	1	2	1.58	2.05	0.96	none
905	1	3	2.56	3.33	1.56	none
905	2	1	2.15	2.80	1.31	none
905	2	2	2.62	3.40	1.60	none
DROP ENTIRE BATCH[a]	2[a]	3[a]				
905, 011, 716[b]	3	1	1.29	1.67	0.79	none (only one sensor left)
905, 011, 716[b]	3	2	1.49	1.94	0.91	none (only one sensor left)
716[b]	3	3	2.40	3.12	1.46	905

[a]Person 2 Batch 3 was entirely dropped due to operational or experimental error.

[b]OPC-N3 716 sensor's laser mount was bumped/pressed when sliding the internal component assembly back into the housing during the mock mirror replacement between Person 2 Batch 2 and Person 2 Batch 3.

Table S20: Mirror replacement repeatability (mock mirror replacement between each test) results per sensor. Slopes in red indicate sensors that failed to meet the per-batch slope limits.

Person	Batch	sensor #	b1	b0	R2	RMSE	NRMSE (%)
1	1	905	59.49	-15.25	0.969	45.71	15%
1	2	905	30.83	72.86	0.350	154.39	69%
1	3	905	7.77	-5.64	0.833	62.82	34%
2	1	905	48.67	274.30	0.030	65134.50	20226%
2	2	905	155.76	-0.10	0.744	21964.92	6907%
2[a]	3[a]	905	-528.31	394.15	0.085	41268.59	15062%
3	1	905	67.47	61.86	0.801	118.27	35%
3	2	905	6.97	-3.03	0.982	35.89	11%
3	3	905	3.13	-0.67	0.995	19.97	6%
1	1	011	3.38	-23.47	0.986	29.97	10%
1	2	011	91.93	-10.90	0.486	137.32	61%
1	3	011	2.72	-14.01	0.871	55.21	30%
2	1	011	2.73	-19.06	0.953	3183.63	989%
2	2	011	3.28	-8.20	0.991	758.52	239%
2[a]	3[a]	011	16.92	-13.61	0.963	1656.40	605%
3	1	011	13.80	-18.06	0.952	58.21	17%
3	2	011	5.12	-9.24	0.977	41.04	12%
3	3	011	2.56	-5.24	0.990	28.21	8%
1	1	320 (control)	1.94	-26.53	0.978	38.30	12%
1	2	320 (control)	1.33	30.47	0.596	121.77	55%
1	3	320 (control)	2.09	-11.83	0.873	54.91	30%
2	1	320 (control)	1.58	-22.00	0.967	2237.74	661%
2	2	320 (control)	1.88	-15.61	0.992	692.86	218%
2[a]	3[a]	320 (control)	-45778.95	275.30	0.002	44999.10	16424%
3	1	320 (control)	1.29	-22.56	0.976	40.69	12%
3	2	320 (control)	1.49	-10.55	0.982	35.84	11%
3	3	320 (control)	1.50	-9.13	0.990	28.52	8%
1	1	716	2.68	-22.93	0.983	33.30	11%
1	2	716	1.82	37.18	0.564	126.41	57%
1	3	716	2.87	-12.25	0.894	50.11	27%
2	1	716	failed to record data				
2	2	716[b]	2.69	-14.63	0.993	639.03	201%
2[a]	3[a]	716[b]	8.49	20.83	0.975	1128.08	412%
3	1	716	7.67	-15.66	0.953	57.67	17%
3	2	716	34.10	31.81	0.857	101.36	30%
3	3	716	133.88	224.86	0.445	215.16	60%

[a]Person 2 Batch 3 was entirely dropped due to operational or experimental error.

[b]OPC-N3 716 sensor's laser mount was bumped/pressed when sliding the internal component assembly back into the housing during the mock mirror replacement between Person 2 Batch 2 and Person 2 Batch 3.

S.9: Repeated tests for the mirror alignment check after replacing the mirror

After carefully adjusting and aligning the new mirrors in OPC-N3 sensors 177112011 (011), 177520716 (716), and 177111905 (905), and completing an Arizona road dust calibration, where the OPC-N3 passes (if possible). We then repeat the calibration five times without opening the sensors or adjusting the mirrors between runs. Based on variability results for never-deployed OPC-N3 sensors (Sect. S.6), which at minimum pass 4 out of 5 repeated calibrations, we adopt the same criterion for OPC-N3 sensors after mirror replacement. Specifically, a sensor must pass at least 4 of 5 repeated Arizona road dust calibrations to qualify for field redeployment. Like the mirror repeatability tests, the OPC-N3 sensor 177311320 (320) is used as the control.

Table S21 summarizes results by batch, and Table S22 summarizes results by sensor. As expected, the OPC-N3 sensor 716 fails all tests after the laser mount was bumped during the mirror replacement repeatability tests. OPC-N3 sensor 905 passes the first two tests following careful alignment, but fails the remaining three and does not meet the overall redeployment criterion. Again, the results for OPC-N3 sensor 011 are more positive, as it passed all 5 of the repeated Arizona road dust lab calibrations.

Although the size-selectivity tests using the FMAG and GRIMM for OPC-N3 905 show that mirror replacement improves bin assignment, the Arizona road dust calibration results indicate that this improvement may be insufficient to consider the sensor suitable for field redeployment.

Table S21: Repeated tests after replacement mirrors aligned per batch summary.

	Batch	b1 mean	b1 upper limit	b1 lower limit	Sensors that failed
	1	2.75	3.58	1.93	716[a], 320
	2	2.93	3.81	2.05	716[a], 320
	3	4.07	5.29	2.85	716[a], 905
	4	4.73	6.15	3.31	716[a], 905
	5	4.91	6.38	3.44	716[a], 905
Drop sensors	Batch	b1 mean	b1 upper limit	b1 lower limit	Sensors that failed
716[a], 320	1	2.35	3.06	1.65	none
716[a], 320	2	2.51	3.26	1.75	none
716[a], 905	3	1.78	2.31	1.25	none
716[a], 905	4	2.05	2.66	1.43	none
716[a], 905	5	2.10	2.73	1.47	none

[a]OPC-N3 716 sensor's laser mount was bumped/pressed during the mirror replacement repeatablity tests. The laser is likely misaligned and cannot be corrected by adjusting the mirror.

Table S22: Repeated tests after replacement mirrors aligned per sensor summary. Slopes in red represent sensors that failed the per-batch slope limits

Batch	sensor #	b1	b0	R2	RMSE	NRMSE (%)
1	011	2.16	-0.68	0.991	16.05	10%
2	011	2.30	-5.73	0.989	26.95	8%
3	011	2.25	-19.30	0.981	37.38	11%
4	011	2.54	-16.48	0.985	34.28	10%
5	011	2.63	-9.01	0.981	36.66	11%
1	716[a]	5.09	7.51	0.971	29.20	18%
2	716[a]	5.47	9.98	0.984	32.66	9%
3	716[a]	9.79	-0.90	0.956	56.13	16%
4	716[a]	11.66	17.66	0.976	42.39	12%
5	716[a]	12.07	17.30	0.949	60.32	17%
1	320 (control)	1.21	-2.80	0.984	21.35	13%
2	320 (control)	1.25	0.19	0.994	19.86	6%
3	320 (control)	1.31	-8.99	0.990	26.31	7%
4	320 (control)	1.55	-16.44	0.988	30.71	9%
5	320 (control)	1.57	-17.65	0.988	28.84	8%
1	905	2.55	7.98	0.988	18.56	12%
2	905	2.71	-2.87	0.993	22.24	6%
3	905	2.92	-16.70	0.977	40.26	11%
4	905	3.17	-9.62	0.993	23.47	7%
5	905	3.38	-10.23	0.979	38.87	11%

[a]OPC-N3 716 sensor's laser mount was bumped/pressed during the mirror replacement repeatablity tests. The laser is likely misaligned and cannot be corrected by adjusting the mirror.